Remodelling of Mycobacterial Peptidoglycan During Cell Division and the Epigenetics of Macrophages during *M. tuberculosis* infection

By Nathan Scott Kieswetter

KSWNAT001

SUBMITTED TO THE UNIVERSITY OF CAPE TOWN

In Fulfilment of the Requirements for a Doctor of Philosophy of Clinical Science and Immunology

Faculty of Health Science, Institute for Infectious Disease and Molecular Medicine & University of Cape Town

Supervisor: A/Prof Reto Guler

Co-supervisors: Dr Mumin Ozturk and Prof Frank Brombacher

Declaration

I, **Nathan Scott Kieswetter**, hereby declare that the work on which this dissertation/thesis is based is my original work (except where acknowledgements indicate otherwise) and that neither the whole work nor any part of it has been, is being, or is to be submitted for another degree in this or any other university.

I empower the University of Cape Town to reproduce, for research, either the whole or any portion of the contents in any manner whatsoever.

Further, this thesis/dissertation has been submitted to the Turnitin module (or equivalent similarity and originality checking software) and I confirm that my supervisor has seen my report and any concerns revealed by such have been resolved with my supervisor.

Signed by candidate

PhD Candidate Signature:

Signed by candidate

Supervisor Signature:

Date: 1st September 2020

Acknowledgements

There are so many people who I would like to thank. If it takes a village to raise a child, it certainly takes a city to train a scientist. Firstly, I would like to thank my supervisors, A/Prof Reto Guler, Prof Frank Brombacher and Dr Mumin Ozturk for allowing me to further my studies and allowing me to work on several interesting projects. Specifically, I would like to take this opportunity to thank A/Prof Reto Guler for his insightful patient advice, training and ever willingness to talk about my work. His brilliant example has made me a better scientist. Further, I would also like to thank Dr Mumin Ozturk for his constant, patient mentorship, help, advice and friendship. His influence, guidance and example have affected me more than he'll ever know. Lastly, but certainly not least, I would like Professor Bavesh Kana and for all his advice and support.

I would also like to express my gratitude to my labmates from the Brombacher group. All the conversations, laughs, celebrations and commiserations have made this journey undeniably easier. In particular, I would like to thank Shelby-Sara Jones for her constant willingness to help with lab work whilst chatting about everything under the sun.

To my friends and family, there are no words to express my unending gratitude. Without their love and support along the way, I would never have gotten to this stage in my life. To my parents and s ister, I would like to say a huge thank you for their constant support and love during my academic career so far. You guys have been wonderful. A huge thank you to Daniela de Almeida and the French's for their support and love from afar– you guys have been great. I would like to say a special thank you to Dustin Fischer who has always been there for a beer and good old-fashioned rant. I can only hope that my friendship and advice have been even the smallest bit as helpful to him as he has been to me during our long trek through academia. To the Cunniffes, thank you for all your support down this long road and truly making me feel like one of the family.

Last but by no means least, I would like to thank my partner, Teagan Cunniffe, whose effortless grace, wit, humour, friendship and constant love have been the single greatest gifts I have ever received. I look forward to our adventures to come. Thank you for being there every step of the way and keeping me sane - *This dissertation is dedicated to you*.

Contents

List of Figures

List of Tables

Abbreviations

Ami – Amidase

BCG - Bacillus Calmette Guérin

BMDM – Bone-marrow-derived macrophage

CCL - Chemokine (C-C motif) ligand

CD - Cluster of Differentiation

CXCR - C-X-C chemokine receptor

DNA - Deoxyribonucleic Acid

ELISA - enzyme-linked immunosorbent assay

ESX - Early secretory antigenic target (ESAT6) protein family secretion

FCS – Fetal calf serum

G-CSF - Granulocyte colony-stimulating factor

GTC - Guanidinium thiocyanate

HIV - Human Immunodeficiency Virus

IFNγ - Interferon γ

IL- Interleukin

iNOS - inducible nitric oxide synthase

lincRNA – long intergenic non-coding RNA

lncRNA – long non-coding RNA

LTBI - Latent Tuberculosis Infection

M. smeg – *Mycobacterium smegmatis*

MCP-1 - Monocyte chemoattractant protein-1

MDM – Monocyte-derived macrophage

miRNA – microRNA

Mtb – *Mycobacterium tuberculosis*

MYD88 - Myeloid differentiation primary response gene 88

ncRNA – non-coding RNA

NOD - Nucleotide-binding oligomerization domain-containing protein

nt – nucleotides

PBMCs - Peripheral blood mononuclear cells

PBS – Phosphate buffered saline

PCR - Polymerase Chain Reaction

PG - Peptidoglycan

pH - Potential of Hydrogen

PhD - Doctor of Philosophy

piRNA – PIWI-interacting RNA

PMN - Polymorphonuclear leukocytes

ROS - Reactive Oxygen Species

scaRNA – small Cajal body-specific RNA

siRNA – small interfering RNA

snoRNA – small nucleolar RNA

snRNA – small nuclear RNA

sRNA – small non-coding RNA

TB - Tuberculosis

TFh – T follicular helper

Th1 - T helper 1

TLR - Toll-like receptor

tmRNA – transfer–messenger RNA

TNF - Tumour necrosis factor

WHO – World Health Organisation

Abstract

Tuberculosis (TB) has emerged as the world's most deleterious infectious disease. The etiological agent of TB, *Mycobacterium tuberculosis* (Mtb), has evolved the ability to evade the host immune system using several mechanisms; emphasising the need for novel treatment strategies. Peptidoglycan (PG) is an important immunomodulatory heteropolysaccharide structure that can be shed during mycobacterial infection with immunological consequences and as such, changes in PG structure are expected to have important implications on disease progression and host responses. Mycobacterial amidases have been shown to have important roles in the remodelling of PG during cell division in *M. smegmatis* and are implicated in sensitivity to antibiotic treatment. However, their roles in modulating host immunity remain unknown. Herein, we assess the immune responses to Mtb mutants defective for either one of two amidases, Ami1 and Ami4, in bone marrow-derived macrophages (BMDM) and the C57BL/6 murine models of tuberculosis. Both Ami1 and Ami4 deletion resulted in increased pro-inflammatory response in BMDM. Infection with the Mtb *Δami1* mutant in mice resulted in differential induction of pro-inflammatory cytokines and certain chemokines during the acute phase of the infection, an effect that was abrogated in chronic phase infection. The *Δami1* mutant was found to be susceptible to antibiotics in liquid growth culture but this sensitivity was negated in macrophages and reversed to a tolerant phenotype in mice. The *Δami4* mutant, by contrast, did not display differential antibiotic susceptibility and did not significantly alter cytokine and chemokine responses relative to the wildtype control in mice. These findings suggest that Ami1 and Ami4 in Mtb play a nonoverlapping role in antibiotic sensitivity and modulating host immunity during tuberculosis.

Additionally, the specific epigenetic alterations which occur during host-Mtb infection that contribute to immune evasion remain unknown. Here, we propose a method to elucidate transcriptomic changes in both human primary monocyte-derived macrophages (MDM) and the Mtb bacillus with which they were infected. In this study, we exhibit a dual-RNA-seq proof-of-concept methodology where, from a single donor, we successfully sequence host RNA from infected MDMs as well as Mtb RNA enriched from those same infected MDMs. Utilizing this optimised methodology, we aim to discover and model epigenetic and transcriptional alterations as well as their effector proteins in primary human macrophages following Mtb infection. Further, we aim to identify novel and annotated ncRNAs which are correlated with these epigenetic modifications.

Chapter One

Literature Review

1.1 Tuberculosis History and Discovery

Tuberculosis (TB) is an ancient disease which has afflicted sensitive human populations worldwide for thousands of years [1]. Modern molecular biological and sequencing techniques have implied that *Mycobacterium tuberculosis* (Mtb) was found in East Africa approximately three million years ago [2]. However, it is understood that the modern Mtb strains which affect the world today may have arisen only 20000 – 15000 years ago [3, 4]. Further, the six strains, or lineages, which are currently present in the human population worldwide are all present in East Africa today [5]. These lines of evidence imply that the establishment of humanity may have coincided with the occurrence and spread of TB from Africa to the rest of the world. In addition to the direct evidence of TB presence in ancient East Africans, TB has also been observed in Egyptian remains and art as long as ~5000 years ago [6-8]. Additional lines of evidence have shown that as humans spread out of Africa, TB was spread as far as China, India, Peru and the Americas [7].

Perhaps more famous, was the first documented identification of TB in Ancient Greece by Hippocrates. The disorder which then known by the Greeks as phthisis. Hippocrates understood TB and its clinical presentation. Further, he recognised and noted that phthisis primarily affected young adults [9]. Through the proceeding years, TB lurked within the human population claiming many victims and gained other names such as consumption, scrofula, the White Plague, the King's Evil and perhaps the most poetic; The Captain of all these Men of Death. Benjamin Marten was perhaps the first person to elude to the infectious nature of TB in his paper entitled “A new theory of Consumption” [10]. However, in 1865, a French physician named Jean-Antoine Villemin provided the first evidence of the infectious ability of TB by transferring infected liquid acquired from the diseased lungs of dead TB patients during an autopsy to a small rabbit [11]. Upon sacrificing the animal, he discovered that it was indeed infected with Mtb. Perhaps the greatest change in the way physicians and scientists understood TB was brought forward by Robert Koch [12]. In 1882, Koch presented his data to the Berlin Physiological Society providing evidence of the TB bacillus as well as detailing his famous postulates, which would later become the golden standard for the identification of infectious agents worldwide. Later in 1890, Koch presented his work on a compound that he had isolated from Mtb [13]. He claimed that this substance, tuberculin, could remove TB bacilli from a human body and thus

be the first anti-TB therapeutic to protect against TB. Ultimately, tuberculin was proved to be ineffectual against TB, however, Koch claimed that the substance may have a role in diagnostics in the future. Roberts Koch's contribution toward the field of infectious bacteriology, particularly his work on the aetiology of TB, later earned him the 1905 Nobel Prize in Medicine and Physiology. Additional knowledge of TB was later added by Clemens Freiherr von Pirquet in 1909. In that year, Pirquet published a detailed study providing evidence in which he showed that children which were exposed to tuberculin exhibited a localised immune response similar to that of active TB patients, but never progressed to TB themselves; these children he termed 'latently infected' – a term which is still in use and actively debated today [14]. The next tool in the war against TB was discovered in the 1930s where Florence Seibert developed a standardised purified protein derivative, or PPD, which provided a comparable method to better carry out the tuberculin skin test and elucidate the epidemiology and biology of TB at that time [15]. Despite the growing understanding of TB aetiology and pathogenesis, the disease still had a deleterious impact worldwide.

Improvements in diagnostics such as X-ray identification of lesions helped in the diagnosis of the disease, however, the treatment of TB consisted primarily of a healthy diet and ample sunshine; a treatment regime that was used in almost all sanitoria worldwide. However, a powerful weapon against TB was discovered in 1921 by Albert Calmette and his partner Camille Guerin who were working on a vaccine for TB at the Pasteur Institute of Lille where they strived to attenuate *Mycobacterium bovis.* This attenuated mycobacterium vaccine, called BCG, was to be the first and only commercially available vaccine to TB for almost the next 100 years [16]. The protective effect of BCG was first observed in an infant whose mother was TB positive and was given into the care of TB positive grandmother – miraculously, the child did not develop TB. In 1944, the next landmark victory against TB was made by Albert Schatz, Elizabeth Bugie, and Selman Waksman. Those authors first reported on an antibiotic compound named streptomycin which had anti-Mtb activity and was clinically verified soon after [17, 18]. Ten years later, the discovery of efficacious oral anti-TB drugs; primarily, isoniazid and rifampicin in 1952 and 1957 respectively, was the turning point in the fight against TB and marked the end of sanitoria worldwide [19].

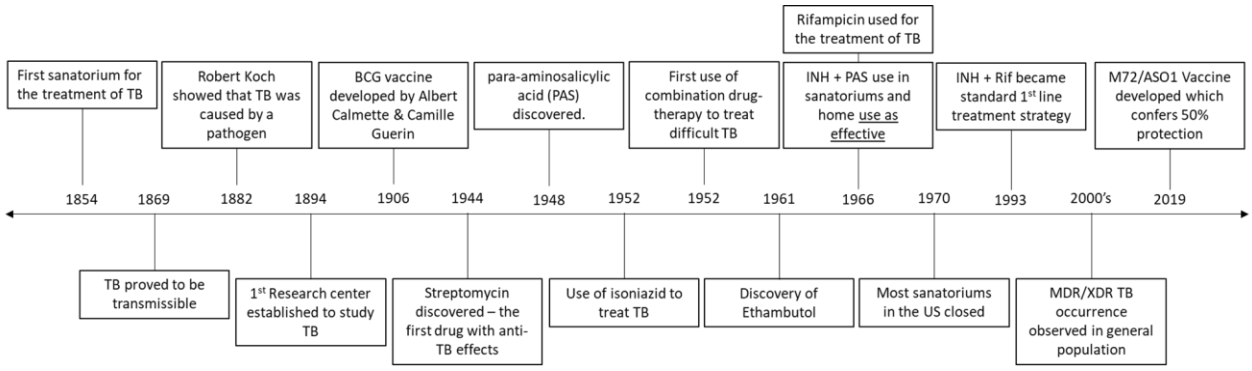

Figure 1: **TB Timeline and Implementation of Treatment Strategy**

1.2 Tuberculosis: A Modern-Day Global Health Crisis

Improvements in TB education, healthcare and drug-development have served to drastically reduce the incidence and mortality observed since the mid-19th century, where 1 in 4 people was killed by TB in America and Europe [20]. However, factors such as the emergence of HIV in the early 1970s, the global increase of other immunosuppressive diseases and the increasing incidence of drug-tolerant phenotypes have powered the modern-day spread TB [21]. It is estimated that approximately 1 in 4 people are latently infected with Mtb, the etiological agent of TB [21]. However, of this large proportion, only 10% will progress to the active disease within their lifetime [21, 22]. The loss of host-directed immune control of Mtb is a prerequisite for reactivation of latent infection or progression to TB [23]. It is well documented that immunosuppressive states such as HIV infection, diabetes, malnutrition, extreme age (both very young and very old) and tumour necrosis factor (TNF) therapies all contribute to the loss of mycobacterial control [22-24]. Further, TB may present as a spectrum of disease ranging from latent TB infection (LTBI), characterised by the presence of un-transmissible, quiescent Mtb within the host without the clinical symptoms, to active TB infection (ATBI). ATBI is characterised by abnormal chest x-rays, sputum positive cultures, coughing, chest pain, weight loss, anaemia and night sweats. The exact cellular mechanisms and factors which lead to disease pathogenesis in these physiological sensitive states, and what contributes to latent vs. active disease, are still poorly understood.

The disease's mode of transmission has played a key role in the successful dissemination of TB on a worldwide scale. The bacillus is transmitted within aerosolized droplets from a TB-infected patient's cough or sneeze. This implies that uninfected individuals are at risk of being exposed to the pathogen, and potentially become infected, simply via breathing. During 2018, there were approximately 10 million documented new cases of TB worldwide with 57% occurring in men, 32% occurring in women

and 8.6% occurring in children respectively [21]. It is reasonable to assume that these figures are underestimating the true distribution of disease due to poor diagnostic capabilities and healthcare infrastructure in countries where the prevalence of the disease is highest. In terms of disease incidence, most of the burden is experienced by the regions of Sub-Saharan Africa and South-east Asia (Fig. 2), with eight countries; South Africa, China, Pakistan, India, Nigeria, the Philippines, Bangladesh and Indonesia being accountable for up to approximately 60% of global disease burden [21].

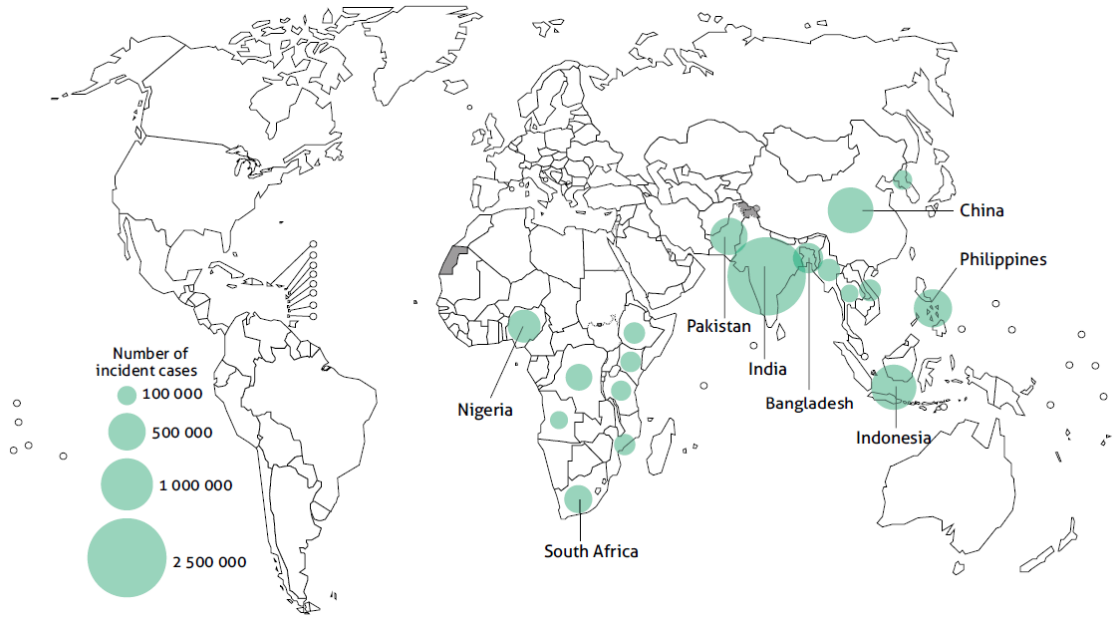

Figure 2: **Estimated TB incidence in 2018, for countries with at least 100 000 incident cases.** The global burden of TB is localised to the Sub-Saharan African and South-East Asian Regions. Adapted from the World Health Organisation Global TB Report, 2019 [21].

TB has become the world's highest infectious killer and is the main cause of mortality in HIV-infected individuals [21]. In high burden countries such as South Africa, the percentage of new and relapse cases of TB can be upwards of 50% in individuals who are HIV positive [21]. Though HIV-infected individuals are at a notably higher risk for contracting TB, the large majority (± 70%) of deaths due to TB occur in HIV-negative individuals (Fig. 3 and 4). In 2018, 1.2 million deaths due to TB were observed in HIV-negative patients relative to 250 000 deaths attributed to HIV-TB coinfection. These mortality data correlate to 27% and 60% reduction in deaths since 2000 [21].

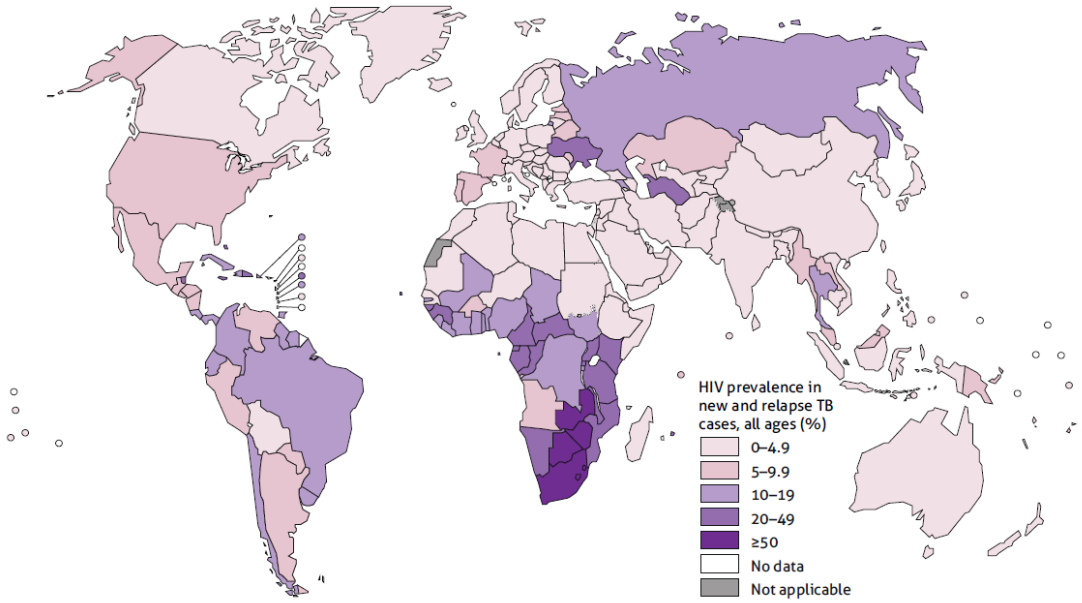

Figure 3: **Approximate HIV prevalence observed in new and reactivation cases of TB, 2018.** In high burden countries, such as South Africa, upwards of 50% of new and reactivation TB cases occur in HIV-positive patients**.** Adapted from the World Health Organisation Global TB Report, 2019 [21].

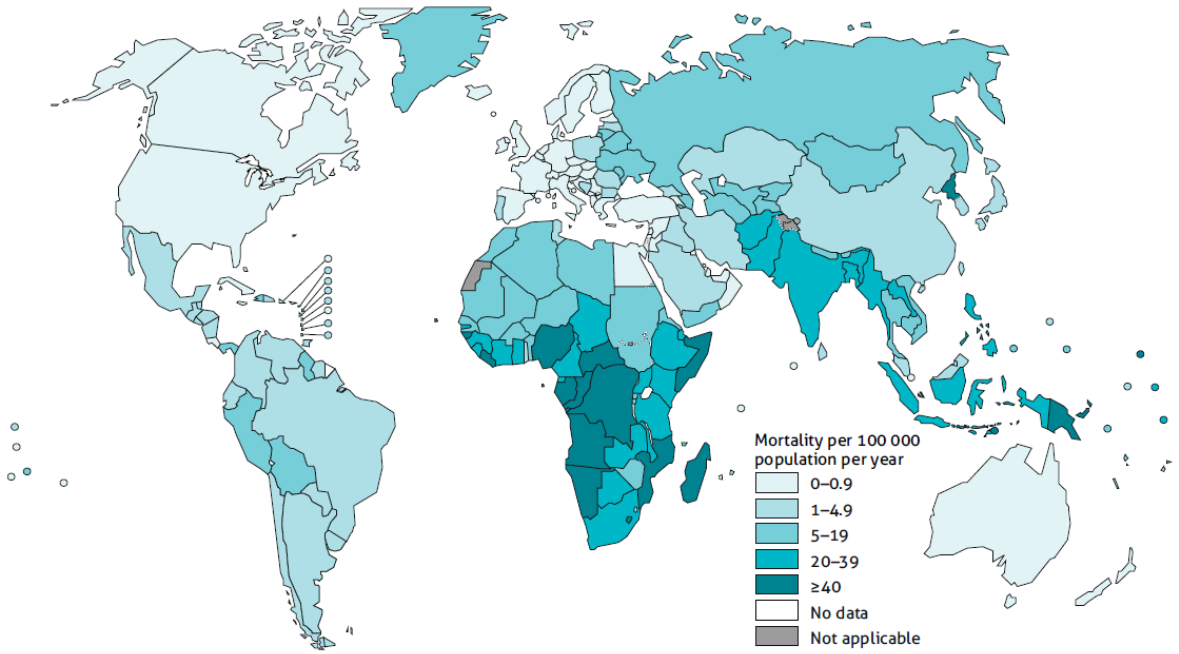

Figure 4: **Estimated deaths due to TB in HIV-negative individuals, 2018.** The global mortality of TB is localised to the Sub-Saharan African and South-East Asian Regions. Adapted from the World Health Organisation Global TB Report, 2019 [21]

The long duration of treatment (and associated poor adhesion to treatment regimens), improper dosing of antibiotic treatments and/or interrupted drug logistics in countries with poorly developed health infrastructure has led to the advent and increased spread of drug-resistant strains of Mtb (Fig. 5). These strains have far-reaching deleterious implications, particularly for immunocompromised individuals who are already at risk of TB, as well as "healthy" persons in high-burden third-world countries.

The generation and spread of treatment-resistant phenotypes of Mtb, perhaps unsurprisingly, mirrors the burden of global TB as seen in Figure 1. In 2018, it is estimated that approximately 500 000 new cases of TB (~5%) exhibited rifampicin (RIF) resistance, of which, 78% were multiple drug-resistant (MDR). The highest observed incidence of treatment-resistant TB originated in India (27%), China (14%) and the Russian Federation (9%) (Fig. 5).

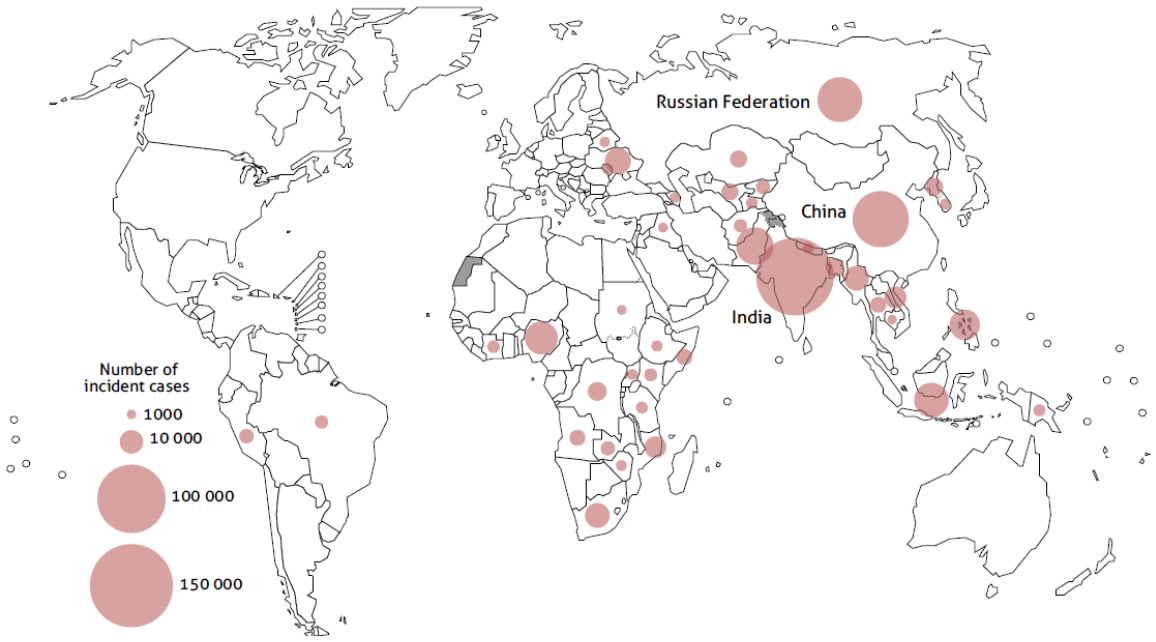

Figure 5: **Estimated incidence of drug-resistant TB in 2018.** Adapted from the World Health Organisation Global TB Report, 2019 [21]

1.3 The Lifecycle of Mtb: Infection, Immunopathology and Treatment

Mtb is a slow-growing, aerobic bacterium which historically only affects human hosts, and is not found in other species or abiotic environments [25]. The causative infectious unit of TB, Mtb, is transmitted as an aerosol within microscopic droplets when an infected individual with active disease coughs, sneezes or speaks (Fig. 6). In high burden countries, this imposes a significant problem for a high

proportion of the population, who live in high density, low-income areas and will experience an increased risk of exposure simply via breathing. In 90% of infected individuals, the host immune response can effectively control infection and prevent progression to disease. Infected individuals, where this control is evident, are termed latently infected and are unable to spread the pathogen to uninfected persons. The factors which facilitate eradication or lifelong control in latently infected individuals remains unclear. Conversely, in 10% of individuals, the adaptive immune phase fails to control Mtb infection. This loss of control ultimately leads to the reactivation of disease in people who have been previously infected, as well as facilitates the dissemination and progression to disease in new cases of infection. Again, the exact mechanisms which contribute to this loss of control are still largely unknown, however extreme age, as well as diseases and treatments which induce suppression of the host immune system, are hypothesised to play key roles. Progression to active disease results in the presentation of multiple symptoms such as chronic coughing, weight loss, fever, night sweats, blood in sputum, chills and a loss of appetite [21].

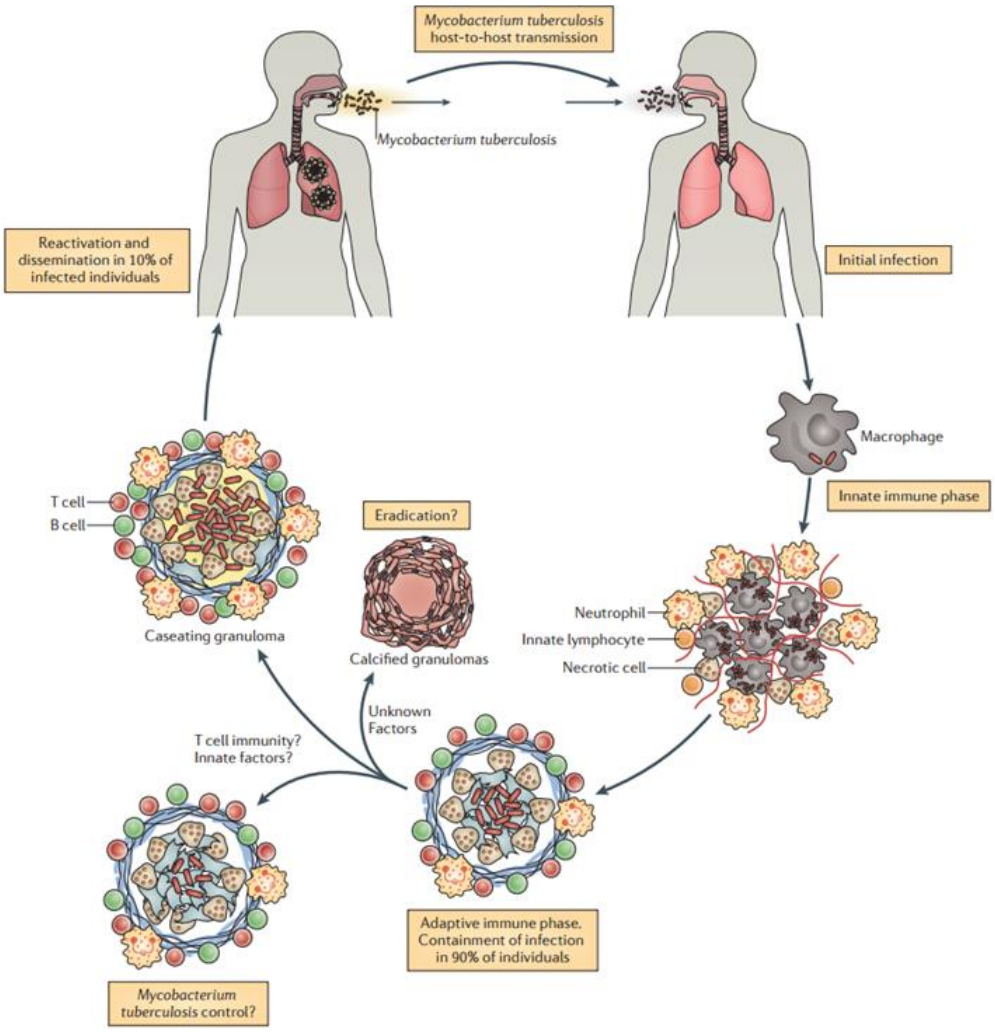

Figure 6: **Lifecycle of Transmissible TB.** Adapted from Nunes-Alves et al., 2014 [26]

During the initial infection, the Mtb bacillus is detected and phagocytosed by tissue-resident alveolar macrophages within the lung parenchyma [27]. These tissue-resident cells, the first line of defence against infection, then release several cytokines (TNFα, IFN-γ) and chemokines to initiate a coordinated immune response comprising of different cellular subtypes (Fig. 6). Neutrophils followed by peripheral monocytes which differentiate to interstitial macrophages are recruited quickly to the initial site of infection[27]. Later, dendritic cells, another subset of professional antigen-presenting cells (APC), are recruited to the site of infection and, via efferocytosis, take up dead or dying immune cells, live bacilli and bacterial antigen [28, 29]. These cells then translocate into the lymphatic system, eventually finding their way to the lymph nodes and initiating the humoral/adaptive immune response. This translocation of DCs is coordinated via IL-12p40 and the chemokine receptors CCR2 and CCR7 [30]. In the draining lymph nodes from the lung, the infected DCs stimulate the $CD4^+$ T cells via MHCII resulting in the differentiation and the clonal expansion of T_H1 type $CD4^+$ T Cells [31]. These cells primarily express and secrete high levels of interleukin 2 (IL-2) and interferon-gamma (IFN-γ) [32]. The expression of CXCR5 on these T_h1 cells allows them to locate themselves efficiently around the granuloma through the interaction of IL-23 and CXCL13 [33, 34]. These T_H1 cells, and the IFN-γ and TNFα that they secrete, are essential for a successful immune response and formation/maintenance of the granuloma [35]. Both mice and human patients which are deficient in IFN-γ are extremely sensitive to Mtb infection, have defective granuloma formation, heightened neutrophil recruitment, increased inflammation and necrosis [36-38]. Further, the cellular differentiation of $CD4^+$ T-cells to T_H1 cells is dependent on the transcription factor T-bet [39]. Mice deficient in T-bet have been observed to have diminished $CD4^+$ T cell IFN-γ responses, a high infiltration of eosinophilic macrophages, giant cells and neutrophils, and are ultimately more susceptible to Mtb infection [40]. Whilst the presence of T_H1 cells is essential to mounting an effective immune response to Mtb, the cytokine environment in which they differentiate is equally important. Previous studies have found IL-12 and IL-23 are critical to mounting efficient IFN-γ T cell responses during mycobacterial infection [34, 41]. However, patients with mutations in these genes were still able to form granulomas, indicating that while IL-12 and IL-23 are important in Mtb infection they are not as indispensable as IFN-γ. DCs are the main source of both cytokines, providing a positive feedback loop between T_h1 cells and themselves, which is ultimately regulated by endogenous IL-10 [42].

Whilst the uptake of Mtb bacilli is reasonably efficient, it is evident from the exponential growth of intracellular Mtb that macrophages alone are insufficient to control TB pathogenesis [43, 44]. This situation is changed somewhat upon the arrival of the adaptive immune response (B- and T-cells) which activates and amplifies the ability of macrophages to control Mtb growth. IFN-γ induced killing

is achieved through the secretion of ROS and inducible nitric oxide synthase [45]. The coordinated action of the innate and adaptive immune responses facilitates the formation of a mature granuloma; consisting of an inner section of macrophages and neutrophils which is surrounded by fibrotic tissue, fibroblasts, epithelial macrophages and other lymphocytes. The formation of lung granulomas is a hallmark of clinical disease and vital for the control of Mtb proliferation and infection. However, when immune control fails, granulomas are also the biological reservoir that initiates new infections from the original host. Further, certain immune cells within the granuloma are permissive to Mtb. Foamy macrophages are another common immune cell subset. Their "foamy" morphology is a consequence of a large accumulation of intracellular lipid droplets [46]. Further, phagolysosomal maturation is abrogated in these macrophages due to their general M2 phenotype. The slow maturation of the phagolysosome coupled with the ability of phagocytosed Mtb to utilise the lipid droplets as a carbon source has allowed Mtb to reside within these macrophages, creating a reservoir of infection [27, 46]. Multinucleated macrophages, formed via the fusion of multiple individual macrophages and the activation via Mtb-derived lipomannan, are another cellular subset which is thought to be permissive to Mtb pathogenesis [47]. It has been shown that these cells have a diminished ability to phagocytose Mtb bacilli but an increased ability to phagocytose apoptotic macrophages [47].

An acellular, creamy, cheese-like substance named caseum is often observed to form at the centre of many granulomas. This caseum is comprised of necrotic tissue, dead immune cells and viable, proliferating bacilli (Fig. 6) [48]. If the formation of the host granuloma and subsequent immune response is successful, the continued formation of the caseum is abrogated, with the necrotic tissue becoming progressively calcified and fibrotic. Such granulomas are considered the clinical hallmarks of a successful host immune response. However, should the immune response be unsuccessful, the caseum increases in size and becomes progressively more liquid over time. Further, the liquid caseum is laden with billions of viable, amplifying Mtb bacilli which, upon the physical breakdown of the granuloma, are released into the lung cavity. This phenomenon results in the cavitation of host lung tissue and allows for the spread of Mtb to new, uninfected hosts [48].

1.3.1 Treatment of Tuberculosis

Without treatment, TB is often fatal and can disseminate to other parts of the body apart from the lungs, such as the kidneys, spine, meninges or joints which can cause significant deleterious effects in peripheral parts of the body [49]. Fortunately, TB is readily curable with the duration of treatment lasting approximately six to nine months.

Table 1: **Anti-TB Medication throughout the years.** Adapted from Marimani et al., 2018 [50]

1st/2nd Line Treatment	Anti-TB Drugs	Discovered Anti-TB Action	Mode of Action
2nd Line	Amikacin (AMK)	1972	Interacts with the 30S ribosomal subunit inhibiting protein synthesis
	Bedaquiline	2012	Inhibits energy production by halting the activity of ATP synthase
2nd Line	Capreomycin (CAP)	1963	Associates with the 70S ribosomal subunit and prevents protein synthesis
	Clofazimine	1950	Binds to Mtb DNA leading to growth retardation
2nd Line	Cycloserine/ Terizidone (Cs /Trd)	1955	Impairs cell wall synthesis and diminishing growth by changing the role of D-alanine in the Mtb cell wall
1st Line	Ethambutol (EMB)	1961	Impairs metabolism and induces cell death by preventing synthesis of required metabolites
2nd Line	Ethionamide (ETH)	1961	Disrupts Mtb cell wall biosynthesis by inhibiting the production of mycolic acid
1st Line	Isoniazid (INH)	1952	Disrupts Mtb cell wall biosynthesis by inhibiting the production of mycolic acid
2nd Line	Levofloxacin (LVX)	1992	Disrupts DNA replication, transcription, recombination and repair by blocking the activity of DNA gyrase and topoisomerase IV
	Meropenem	1976	Induces cell death by inhibiting the synthesis of vital cell wall components
2nd Line	Moxifloxacin (MXF)	1988	Inhibits DNA replication and transcription via the association with the subunit of DNA gyrase
2nd Line	Ofloxacin (OFX)	1980	Inhibits of DNA replication, transcription, repair and recombination bacterial via the association to topoisomerase IV and DNA gyrase
2nd Line	p-aminosalicylic acid (PAS)	1948	Diminishes bacterial growth and depleted iron by the impairment of the synthesis of folic acid and mycobactin, respectively
1st Line	Pyrazinamide (PZA)	1954	Prevents translation by associating with the ribosomal protein S1 (RpsA) and diminishes fatty acid synthesis
2nd Line	Prothionamide (Pto)	1965	Disrupts Mtb cell wall biosynthesis by inhibiting the production of mycolic acid
1st Line	Rifabutin (RBT)	1975	Prevents chain initiation via the impairment of RNA polymerase
1st Line	Rifampicin (RIF)	1963	Prevents chain initiation via the impairment of RNA polymerase
1st Line	Rifapentine (RPT)	1965	Prevents chain initiation via the impairment of RNA polymerase
2nd Line	Streptomycin (STR)	1944	Inhibits protein synthesis via the association to the 30S ribosomal subunit
2nd Line	Kanamycin (KAN)	1957	Interferes with the protein synthesis by binding to the 30S subunit of the bacterial ribosome

Treatment is generally segregated into two groups: first-line and second-line drugs. First-line treatment is generally implemented for new cases of TB and includes Isoniazid (H/Inh), Rifampicin (R/Rif), Pyrazinamide (Z/Pza), Ethambutol (E/Emb) and Streptomycin (S/Stm). The second-line drugs are utilized for patients who have repeat infections, or those who are not responding to first-line treatment. It is difficult to pinpoint the exact causes which contribute toward the generation and spread of antibiotic-resistant strains of Mtb. However, poor adherence to treatment regimens, as well as improper prescription of antibiotics (incorrect regime) by doctors and clinics are widely accepted to be two of the major factors which have facilitated the selection and spread of drug-resistant strains of Mtb.

1.4 The Successes and Failures of Modern TB Vaccine Design

A universally efficacious vaccine or therapeutic intervention which is applicable and effective to all age groups is urgently needed to prevent and control TB. Efforts to develop such a therapeutic intervention or vaccine have been hampered primarily by a limited understanding of the mechanisms of protective immunity against Mtb and the mechanics of host immune invasion via the bacterium. The Bacillus Calmette-Guerin (BCG) vaccine has been used for almost a hundred years, with vaccination being dispensed in early childhood in many countries (Fig. 7 and 8) [51, 52]. The vaccine has been shown to confer varying efficacies of protection against disseminated disease in children and infants, however, BCG immunisation is unable to elicit protection to the pulmonary chronic form of the disease as the child progresses to adulthood [52].

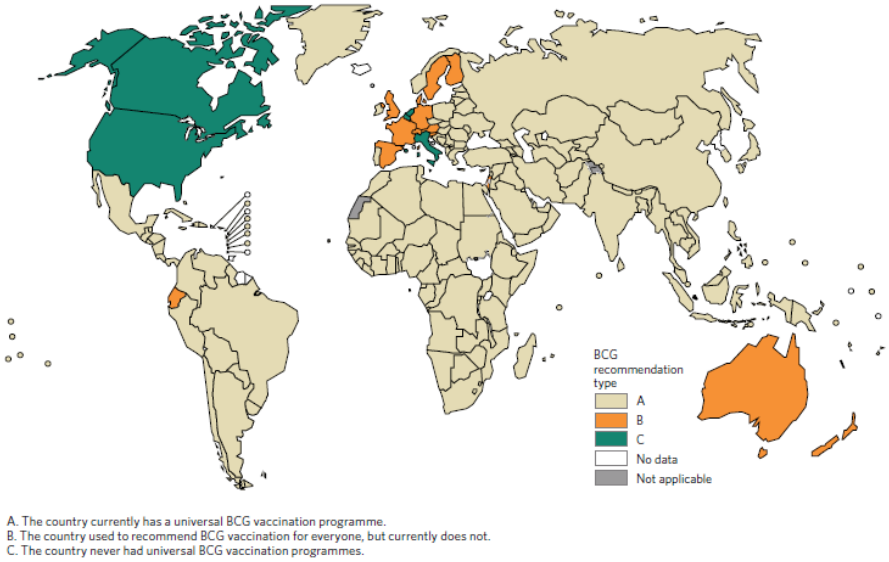

Figure 7: **Bacillus Calmette-Guerin (BCG) vaccination policy by country, 2015.** With the exception of the United States of America, most countries have/had some form of BCG vaccination program implemented at a national level. Adapted from the World Health Organisation Global TB Report, 2016 [51]

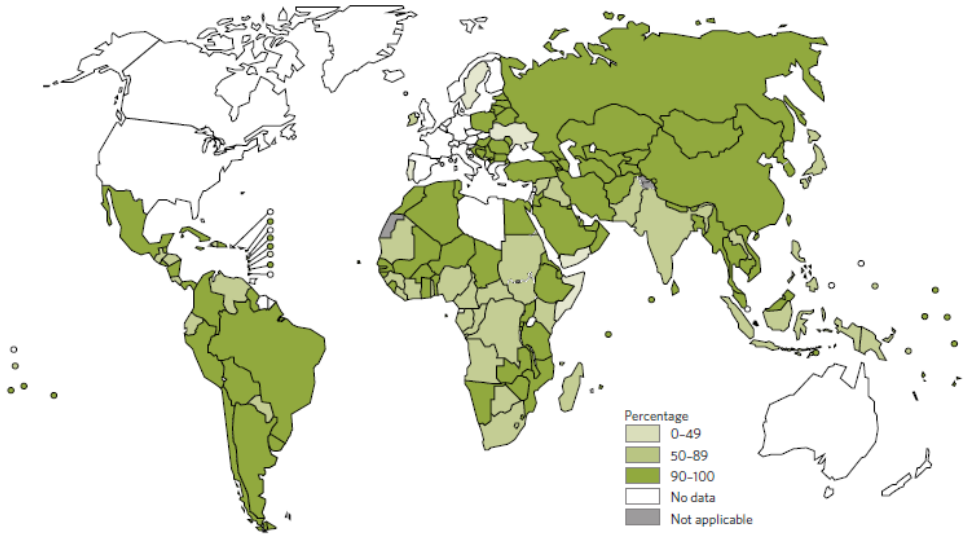

Figure 8: **Coverage of Bacillus Calmette-Guerin (BCG) vaccination, 2015.** Adapted from the World Health Organisation Global TB Report, 2016 [51]

The first new vaccine candidate since the discovery and implementation of BCG in many parts of the world almost 90-years-ago was an inoculant called MVA85A [53, 54]. The vaccine candidate was synthesised from a strain of *Vaccinia Ankara* virus which expressed antigen 85A from Mtb. Research on this vaccine candidate before clinical trials was promising, and MVA85A proceeded to clinical trials in both adults and infants. The vaccine was designed to be a booster following vaccination of BCG and was shown to have good immunogenicity in animal studies but was ultimately found to be unprotective in adults and infants regardless of satisfactory cell-mediated host immune responses (Fig. 9 and 10) [53, 54].

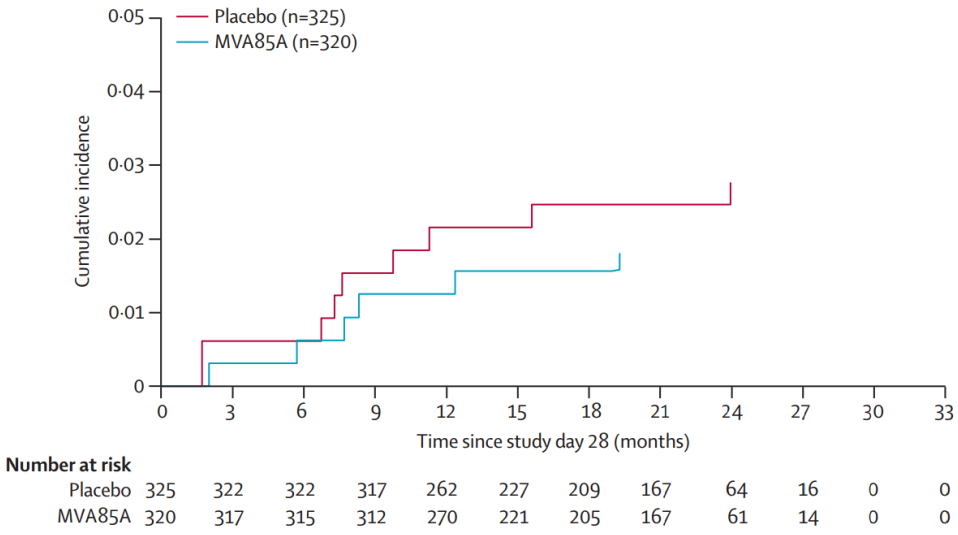

Figure 9: **Incidence of TB acquisition in adults receiving the MVA85A vaccine relative to those who received a placebo**. No significant difference was observed between those patients who received the vaccine and the placebo group. Adapted from Ndiaye et al., 2015 [53]

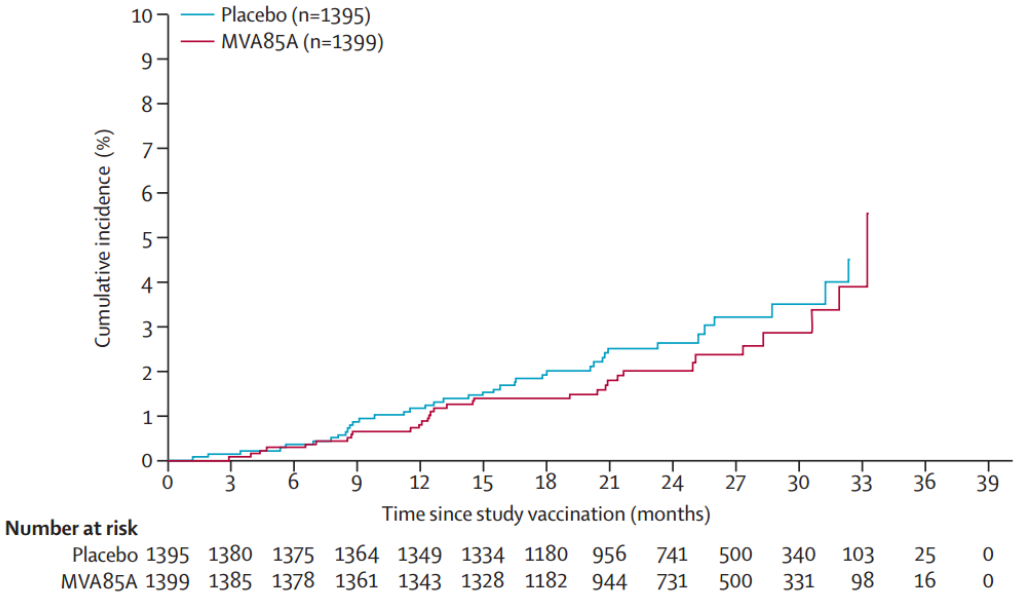

Figure 10**: Incidence of TB Acquisition in Infants receiving the MVA85A vaccine relative to those who received a placebo.** No significant difference was observed between those patients who received the vaccine and the placebo group. Adapted from Tameris et al., 2013 [54]

More recently, a large scale, multinational phase 2b clinical trial has provided evidence that a novel adjuvanted subunit vaccine (M72/AS01E) can protect around 50% of adult individuals from contracting TB (Fig. 11) [55]. Whilst this is a promising step forward, the failure to create a universally efficacious vaccine highlights the need for new effective therapies to elicit clearance of Mtb pathogen.

The discovery and characterization of novel gene targets for therapeutic intervention thus remain a key area of TB research which holds significant promise for the alleviation of TB.

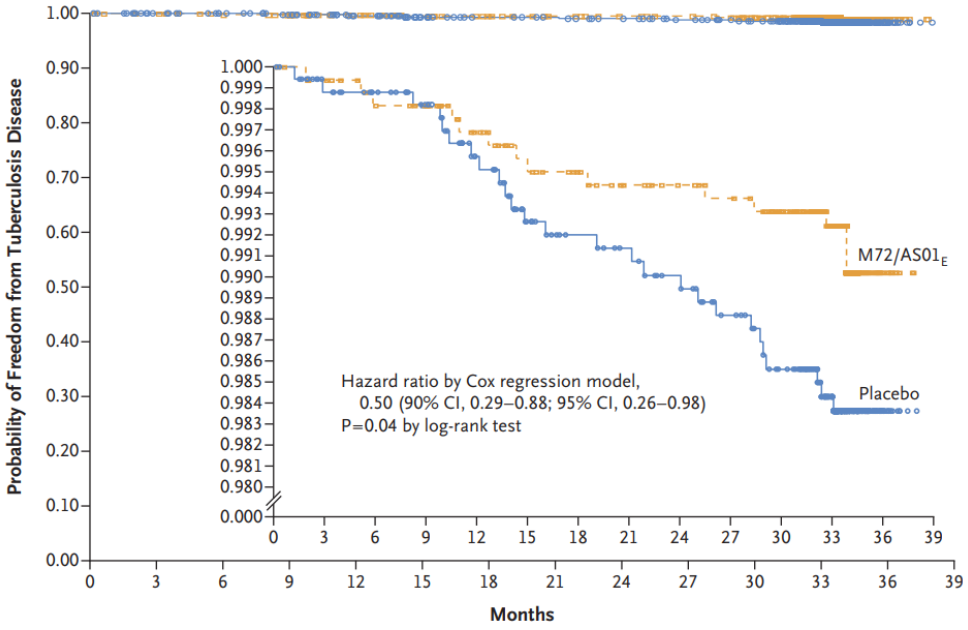

Figure 11: **Kaplan–Meier Estimate showing the effectiveness of the novel M72/ASO1$_E$ vaccine candidate.** The vaccine as shown to confer protection in approximately 50% of cases. Adapted from Tait et al., 2019 [55].

1.5 Antibiotic tolerance/resistance in *Mycobacterium tuberculosis*

As mentioned above, the occurrence of MDR- and XDR-TB are important global health issues. Drug resistance was first observed almost immediately after the introduction of the first TB drug, streptomycin [56]. Combination treatments largely solved this issue until resistant strains were observed utilising even these treatment strategies. It is now understood that the emergence of drug-resistant TB can be attributed to two phenomena. Firstly, chaotic treatment which refers to the lack of standardised TB treatment protocols, variations in the access to diagnosis and treatment, as well as socio-economic issues, contributed to the rise of these resistant strains [57]. Secondly, once drug resistance is observed or there are drug-resistant Mtb colonies present, the short-course chemotherapy strategies, namely, the "directly observed treatment, short-course" or DOTS, paradoxically exacerbated the emergence of drug-resistant phenotypes by providing sufficient drug pressure to rapidly evolve resistance to first- and second-line drugs [57]. But what are the mechanisms employed by Mtb to develop resistance to these anti-TB compounds?

The ability to sequence and compare Mtb genomes has allowed for a greater understanding of the mechanisms by which Mtb evolve drug resistance. It is now understood that Mtb possesses both intrinsic and acquired strategies for tolerance and resistance to antibiotic stress.

1.5.1 Intrinsic Attributes and Mechanisms which Contribute to Antibiotic Resistance

One of the primary aspects which hamper the ability of the antibiotic effectiveness in Mtb is the impermeability of its cell wall. This barrier is maintained by the complex, coordinated action of multiple enzymes. For example, Mur and MurB are vital enzymes involved in the biosynthesis of UDP-N-acetylmuramic acid (UDP-MurNAC) during the formation of the peptidoglycan (PG) layer of the cell wall [58]. In other bacterial species, MurA can be targeted by the antibiotic Fosfomycin, however, in Mtb, this antibiotic does not work due to the presence of a single nucleotide polymorphism (SNP) where a cysteine residue, which Fosfomycin acts upon, is mutated into aspartic acid [58]. Further, Mtb can evade the action of β-lactam antibiotics such as amoxicillin due to the presence of a secondary set of Mtb-specific transpeptidases, the L, D-transpeptidases (Ldt) [59]. Mtb also possesses another important protein mycolyltransferase complex called antigen 85 (Ag85). These proteins facilitate the formation and maintenance of the bacterial cell wall [60]. Previous studies have shown that the inhibition of Ag85 results in an altered cell wall structure and increased permeability [61, 62]. Further, Mtb Ag85 gene mutants were significantly more susceptible to anti-TB compounds [63-65]. Many other genes have been reported to be important to Mtb cell wall homeostasis and have been hypothesised to be good targets for therapeutic intervention, however, this information is outside the scope of this dissertation and will not be discussed further.

Mtb also possesses morphological attributes that confer significant resistance to antibiotic action. The Mtb plasma membrane has a significantly reduced permeability relative to other Gram-positive bacterial species. To overcome this, hydrophilic solutes utilise porins (transmembrane channel proteins) to enter the cell [66]. In *M. smegmatis*, MspA, a porin-like protein is responsible for the uptake and sensitivity of this mycobacterium to antibiotic action [67]. Further, the expression of *mspA* from *M.smegmatis* in Mtb was sufficient to induce sensitivity to β-lactams as well as the increased sensitivity to anti—TB drugs [68]. Mtb's resistance to a large range of antibiotics is often also attributed to its ability to actively expel these compounds out of the cell via its efflux pumps. In Mtb, it has been shown that the overexpression of efflux pump proteins, such as the major facilitator superfamily (MFS) efflux pumps, results in an inducible drug-resistant phenotype which is clinically similar to MDR-TB. To illustrate that this, *jefA* overexpression in Mtb was shown to confer resistance to isoniazid and ethambutol [69].

1.5.2 A Genetic Basis to Acquired Antibiotic Resistance in Mtb

Anti-TB medications function through the specific association to a target site. Conformational changes that occur at these target sites can ablate the activity of the drug being used. In Mtb, the acquisition of point mutations or SNPs which induce drug resistance is the principal strategy by which Mtb evades therapeutic stress. Such mutations have been observed for all first-line anti-TB compounds.

Resistance to INH, relative to other first-line drugs, is induced by several possible gene mutations such as *katG*, *ndh*, *ahpC*, *kasA*, and *inhA* [70]. The mechanisms of INH activity are well established. As a pro-drug, it requires enzymatic activation by the proteins transcribed from *katG*. In Mtb, mutations in *katG* and the subsequent reduction in enzymatic activity, are the main sources of INH resistance [70]. Additionally, mutations in the promoter of the *inhA* gene resulting in the upregulation of *inhA* levels have been shown to confer slight INH resistance [71]. Further, previous studies looking into INH resistance in Mtb report that 80% of cases can be explained by a combination of these two mutations [72]. Mtb has also evolved resistance to Rifampicin (RIF), the other major first-line TB drug used in conjunction with INH. It has been reported that approximately 95% of all rifampicin-resistant Mtb strains possess a mutation in the 81-bp region of RNA polymerase beta-subunit gene (*rpoB*) [73]. Pyrazinamide (PZA) is an antibiotic often incorporated into drug regimens to shorten treatment durations. Like other first-line drugs, Mtb has evolved resistance-conferring mutations in several genes. In 2016, it was reported that alterations in the *pncA* gene resulted in the inhibition of PZA activity whilst also correlating to resistance [74]. Further, additional studies showed that PZA resistance may be induced by mutations in the *rpsA*, *panD* and *clpC1* genes [75-78]. Ethambutol (EMB) is another first-line anti-TB drug which is included in combination therapies to further prevent drug resistance. Mutations in the *embB* and *ubiA* genes have been shown to confer resistance to EMB [64, 79, 80]. Resistance conferring mutations have also been reported in many second-line anti-TB drugs. The major compounds with clinical relevance have been summarised below (Table 2).

Table 2: **Common Second-line ant-TB drug and the genes which confer resistance when altered.** Adapted from Nasiri et al., 2017 [81]

Second-Line Drug	Drug Family	Resistance conferring Genes
Kanamycin, amikacin	Aminoglycosides	*rrs*
Moxifloxacin, levofloxacin, sparfloxacin	fluoroquinolones	*gyrA, gyrB*
Linezolid	Oxazolidinone	*rplC, rrl*
Bedaquiline	Diarylquinoline	*atpE*

1.6 The Cellular Envelope of *Mycobacteria Tuberculosis*: Peptidoglycan Synthesis, Remodelling and Cell Division

1.6.1 Normal Mycobacterial Cell Division

The host environment in which Mtb proliferates exerts both environmental and immunological stressors on the Mtb bacillus. Thus, Mtb has adopted several strategies to not only tolerate these stressors but to proliferate in this harsh environment and usher in TB. The strategies used to evade the host immune system are varied [82]. However, a key consideration should be given to the composition and remodelling of the mycobacterial cell wall during cell division to elucidate targets for therapeutic intervention.

As mentioned, the majority of antibiotic compounds inhibit the formation or homeostasis of the bacterial cell wall. The mycobacteria genus displays significantly different cell wall morphology relative to traditional model bacterial systems such as *Escherichia coli* (*E. coli*) and *Bacillus subtilis* (*B. subtilus*). As such, the construction and maintenance of the cell wall in mycobacteria are, unsurprisingly, under the regulation of varying proteins relative to these model systems. This is further emphasised by the observation that at least a quarter of the annotated genes in the Mtb genome are attributed to the biogenesis and regulation of the cell wall [83].

The proliferation and division of bacterial cells can be segregated into two stages, namely the elongation of the mother cell, and division of the elongated mother cell into two daughter cells during cytokinesis [84]. All bacteria which display rod-shaped morphology possess two poles present at the farthest ends of the bacillus: an old pole, which is a remnant of the mother cell, and a new pole, which is synthesised during division [84]. In model systems, the division of the elongated mother cell results in the formation of two symmetrical daughter cells. However, in mycobacteria, it has been widely

observed that the daughter cells which arise after division vary in size [85]. Two main hypotheses have been proposed to explain the asymmetrical growth of mycobacteria.

The first hypothesis states that the growth of mycobacteria is unipolar due to the slow rate of growth observed at the new pole relative to the old pole [85]. However, it is now accepted that both poles contribute to elongation, though at highly variable rates which then facilitate the generation of daughter cells of many different sizes [85, 86]. The second hypothesis suggests a model where the growth rate at the poles, both old and new, is the same for most of the cell cycle [86]. However, excessive growth is observed primarily at the old pole post-cytokinesis [86]. This asymmetrical growth facilitates daughter cells of varying sizes.

Defining the underlying mechanism which elucidates the generation of asymmetrical progeny is generally confounded by whether researchers define cell division as the separation of daughter cells or rather as cytokinesis before physical separation [85, 86]. Regardless, both models agree on several observations; firstly, that growth at the poles varies, where rapid growth is observed at the old pole, and that the variation in growth rates results in the generation of the progeny of varying sizes [2, 86]. Secondly, daughter cells that contain the old pole are generally larger and elongate faster than the daughter cells which inherited the new pole. This implies that though both daughter cells are genetically identically there is an increased frequency of phenotypical variation during each division cycle. This phenotypically heterogeneous population of daughter cells has been shown to elicit vast cell wall remodelling during infection [84]. Given these lines of evidence, it has been hypothesised that this phenotypic variation may confer a selective advantage to the pathogen in the context of a constantly changing host environment. This hypothesis has been illustrated through the observation of the increased susceptibility to antibiotic treatments in larger bacterium possessing the old pole [85]. Importantly, there is also an asymmetric distribution of cell wall subunits and components, with one of the daughter cells receiving a newly formed cell wall [84].

The proliferation and polar division of bacteria are intrinsically dependent on the biogenesis of new cell wall material. This process is relatively simpler in model bacterial organisms in comparison to mycobacteria who, apart from peptidoglycan (PG), must concurrently synthesise mycolic acids (MA) as well as arabinogalactan (AG) [84]. The elongation of mycobacteria before septation is achieved through the action of a multi-protein complex called the elongation complex (described further below). After the mother-cell has elongated, the cell divides to form two daughter cells. The exact region at which this split occurs is highly variable and is thought to further contribute to the heterogeneity of the mycobacterial population [84].

The process of division is facilitated through a large complex of many proteins, collectively called the divisome [84]. It is hypothesised that some form of cross-talk exists between the elongation complex and the divisome which coordinates the synthesis of peptidoglycan away from the poles to the mid-cell region, thus facilitating the formation of a septum where the cell will divide [87]. The formation of the septum and its subsequent hydrolysis during physical separation is coordinated by a range of structural factors that stabilise the divisome and PG synthesis/hydrolytic enzymes which form and break down the cellular septum [88, 89]. These processes are essential for the generation of new daughter cells.

Septation in both traditional model bacteria and mycobacteria is achieved through the polymerization of the self-activating GTPase FtsZ into a contractive ring-shaped structure commonly called the Z ring [90]. The site at which septation will occur, the provision of energy for the constriction of the cellular membrane during division, and the scaffold for subsequent PG remodelling enzymes are driven by this Z ring [90, 91]. Thus, the correct spatiotemporal orientation of the Z ring within a cell is essential for cell division and is highly controlled in mycobacteria. This is generally achieved through the modulation of genetic programs which impact the polymerization of the FtsZ and placement of the Z ring. For example in Mtb, Rv3660c overexpression has been shown to inhibit both FtsZ formation and the biogenesis of the septum [92]. In Mtb, the FtsZ ring is further regulated via phosphorylation. It has been shown *in vitro* that the serine/threonine protein kinase (STPK) Pkn ameliorates GTP hydrolysis via FtsZ, thus preventing its formation and subsequent ability to initiate septation [93]. Other intrinsic regulatory mechanisms have been reported, but these will not be discussed further in this dissertation.

The physical separation of the daughter cells requires the hydrolytic breakdown of the newly synthesised septum [88]. In mycobacteria, one PG hydrolase (RipA) has been documented to be essential for the hydrolysis of the septum [94]. Its deletion has been shown to induce long strains of cells with multiple undigested septa [94]. Further, this PG hydrolase has been found to interact with an additional PG hydrolase, called RpfB [95]. *In vitro* experiments have shown that the interaction of these two enzymes results in the synergistic cleavage of PG [95]. However, this cleavage is confounded by the action of PonA1, a PG synthase which competes with RpfB to bind RipA [96]. It has been hypothesised that the ratio of RpfB to PonA1 is a potential mechanism which ensures that hydrolysis of the septum only occurs after PG synthesis. By contrast, in other model species, such as *E. coli*, the hydrolysis of the septum is achieved via the action of amidases and other PG hydrolases (FtsE and FtsX), however, few studies have assessed these hydrolytic enzymes in the context of Mtb [97, 98]. More recently, the functional role of RipA in the hydrolysis of mycobacterial division septa has been better characterised [99]. Their findings indicate that this endopeptidase is indispensable for regular

septation. The exact action of these canonical PG hydrolases in the context of mycobacterial cell division remains a gap in the literature.

1.6.2 Remodelling of the Mycobacterial Cell Wall and Implications for Therapeutic Intervention

The formation of the mycobacterial cell wall, and the remodelling of the complex macromolecules of which it is comprised, is an essential process which is under strict regulatory control to facilitate normal cell division and growth, virulence, as well as resistance to antibiotics [100-102]. Such remodelling is required for the insertion of new cell wall subunits for repair or growth, the incorporation of flagella, specialised secretion apparatus, or porins which are required for normal homoeostasis and cell functioning.

The dynamic balance of cell wall biogenesis vs. degradation is an intricate process which is achieved via the coordinated action of multiple enzymes [103]. Dysregulation of this complex, dynamic process has deleterious implications for the bacterial cell and may result in the formation of non-viable progeny during binary fission. The targeted inactivation of one or several of the enzymes involved in the process of cell wall biogenesis and degradation have been successful strategies for the development of antibiotics such as penicillin [104, 105]. Common beta-lactam antibiotics have proven ineffective in the control of Mtb due to the thick mycobacterial cell wall and expression of beta-lactamase, an enzyme capable of inactivating beta-lactam antibiotics [106].

The thick cellular envelope of Mtb is comprised of three distinct layers of macromolecules moving outwards from the cell membrane (Fig. 12); first is the peptidoglycan (PG) layer which is followed by the arabinogalactan (AG) layer and then finally the mycolic acid (MA) layer [84]. These three constituents of the cell wall are encompassed by a capsule made of noncovalently linked proteins and polysaccharides [84]. The abnormally high density of lipids found in the mycobacterium cell wall makes accurate Gram staining of this species difficult at best. They are, however, able to be stained via acid-fast dyes such as Ziehl-Neelsen [89]. The cell wall, or rather the enzymes which facilitate the cell wall synthesis, have been successfully used as targets for therapeutic intervention in the past; however, the increasing number of multiple-drug-resistant (MDR) and extremely drug-resistant (XDR) strains of Mtb [51] have highlighted the need for novel drugs or host-directed therapies which can disrupt cell wall biogenesis and lead to the death of the Mtb bacillus.

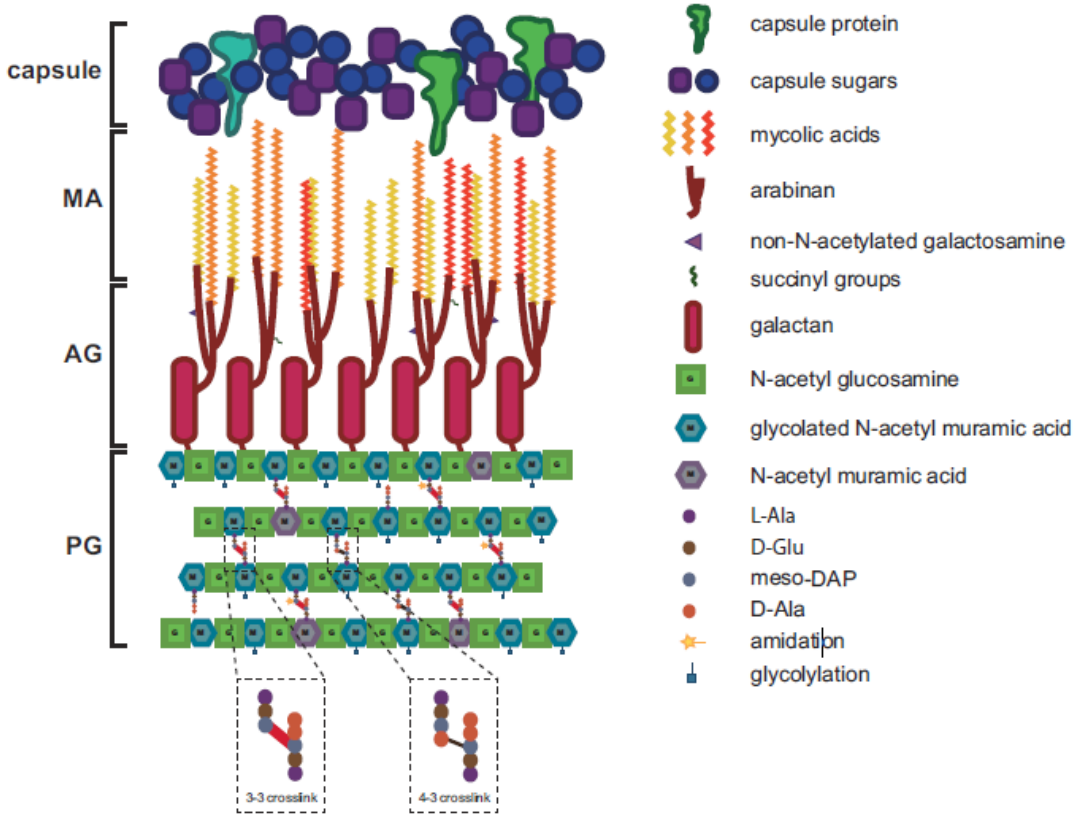

Figure 12: **Cell Wall of *Mycobacterium tuberculosis* showing the peptidoglycan (PG), arabinogalactan (AG), mycolic acid (MA) and capsule**. Adapted from Kieser and Rubin, 2014 [84].

1.6.3 Remodelling the Peptidoglycan (PG) Layer of the Bacterial Cell Wall

During bacterial fission, the peptidoglycan of the mycobacterium is biosynthesised under the coordinated control of the elongation complex and numerous PF hydrolases (Fig. 13). These enzymes facilitate the synthesis of long polymers of disaccharide N-acetyl glucosamine and N-acetyl muramic acid (NA and NAM respectively) which are linked via the inclusion of peptide bridges [84, 102]. This murein (peptidoglycan) precursor is then bound to the membrane-anchored lipid carrier, thus facilitating the creation of the peptidoglycan lipid II [107]. The precursor of peptidoglycan (PG Precursor Lipid II) is synthesised in the cytoplasm of the bacillus and is transported across the cell membrane via the action of the transmembrane protein MviN (Fig. 13) [84, 102, 108]. The peptidoglycan is polymerised via the action of penicillin-binding proteins, glycosyltransferases, L, D- and D, D-peptidases [88]. More specifically, Penicillin-binding proteins PonA1/2 functionally integrate newly synthesised subunits into the existing structure of the peptidoglycan cell wall promoting elongation and the synthesis of the septum [84]. To ensure that the synthesis of the PG occurs in the right direction (directed to the poles of the cell), the elongation complex is anchored to the correct

place by Wag31, a homologue of DivIVA as seen in E. coli, and its interaction with CwsA, a cell wall synthesis protein [109, 110]. Overexpression of the CwsA has been shown in *M. smegmatis* to increase the localisation of the Wag31 at the poles, whilst its deletion results in a decreased localisation of Wag31 [111]. Most of the low molecular weight penicillin-binding proteins regulate the peptidoglycan synthesis via acting as D, D-carboxypeptidases. This regulation of polymerization is achieved via the removal of the terminal D-Ala residues at position-5 of the pentapeptides [112]. Yet-to-be-identified enzymatic hydrolases have been hypothesised to have an integral role in the opening of the peptidoglycan mesh for the insertion of these new precursors during processes of growth, repair and cellular division [84, 102]. The hydrolytic cleavage of the covalent bonds present in the cell wall is an essential process which allows for an increase in length with no change in thickness [88]. The newly integrated PG subunits are then crosslinked via the action of transpeptidases (PBPA, PBPB, LdtA and LdtB) [84]. The cross-linking observed in Mtb is excessive relative to other well-studied model bacteria such as *Escherichia coli (E. coli)* with up to 80% of the peptidoglycan displaying atypical 3→3 peptide cross-links in contrast to the more traditional 4→3 peptide crosslink structure [84, 113]. The residues which make up the peptidoglycan layer have several modifications. Commonly, the glycolylation of N-acetylmuramic acid (NAM), as well as the amidation of the d-Glu and mesodiaminopimelic acid (mDAP) residues of the peptide side chain, have been observed and published in the literature [114, 115].

The silencing, or deletion, of specific enzymes involved in the remodelling of peptidoglycan, has been shown to have deleterious effects on the viability and pathogenicity of a bacterium. For example, in *B. subtilis,* the deletion of two endopeptidases, *cwlO* and *lytE* results in a complete loss of viability [116]. The inactivation of these enzymes can also affect the phenotype of the bacterium. As shown in a previous study within *B. subtilis*, the silencing of LytF resulted in the formation of slightly filamentous cells, whilst the double deletion of LytF with LytE exacerbated this phenotype greatly [117]. The separation of daughter cells requires the efficient cleavage of peptidoglycan. In *E. coli*, it has been shown that 13 periplasmic cell wall hydrolases can cleave almost any peptide, amide or glycoside bond [118]. This huge redundancy has led to the repeated observation that within *E. coli*, no single deletion of any cell wall hydrolase has impaired the growth and division of this bacillus [118]. The loss of function effect of amidase deficiency within model species has been well explored. This will be discussed further below.

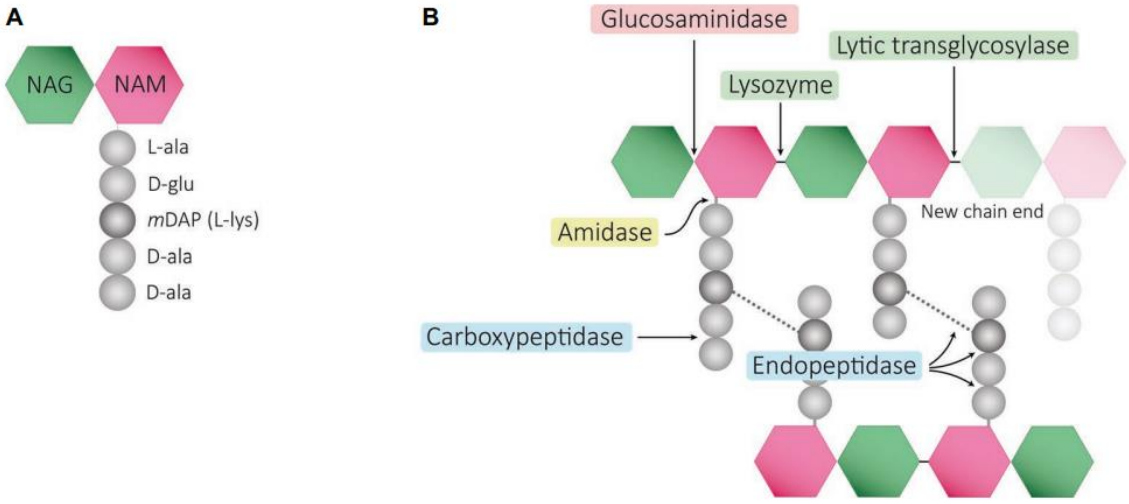

Figure 13: **Diagram illustrating bacterial peptidoglycan and the site at which PG remodelling enzymes are active. A**) Schematic representation of muropeptide. **B**) Cleavage points of PG hydrolases. Adapted from Irazoki et al., 2019 [119]

It has been reported that in one cycle of bacterial fission approximately 45% of the cell wall material is turned over [120]. Thus, the loss of cell wall material, or the mechanism whereby peptidoglycan is completely newly synthesised, would impart significant energy costs to the bacillus and may impact survival [121, 122]. To mitigate this loss, bacteria employ several strategies to recycle cell wall material, particularly PG (Fig. 14). Whilst PG only accounts for a small percentage of the bacterial cell, during nutrient starvation or excessive competition for resources the recycling of PG may allow for a single round of division before entering the stationary phase [122]. The first studies to observe differences in cell wall recycling in gram-positive/negative bacilli reported a significant loss of PG material bacilli ranging from 25 - 50% in gram-positive strains [123, 124]. In contrast, *E. coli* was found to have a PG turnover rate ranging from 0% [123] to 5% [125]. This was later substantiated and elaborated on by Goodell and others, where those authors showed that *E. coli* had turnover rates similar to gram-positive bacteria, but were able to recover a large percentage of PG [120]. The mechanisms of murein recycling have been well elucidated in gram-positive bacteria, whilst a knowledge gap still exists for gram-negative bacteria. Several enzymes and proteins have been shown to have important roles in PG recycling, of which, and in the context of this dissertation, are cell wall amidases [122, 126]. In addition to the survival benefit, the recycling of PG may also play an important role in host immune evasion. Studies have shown that both the intact PG and PG fragments are immunomodulatory [127]. Thus, the knockout of enzymes which are important to the remodelling of the cell wall may have subsequent immunomodulatory effects through impaired PG recycling.

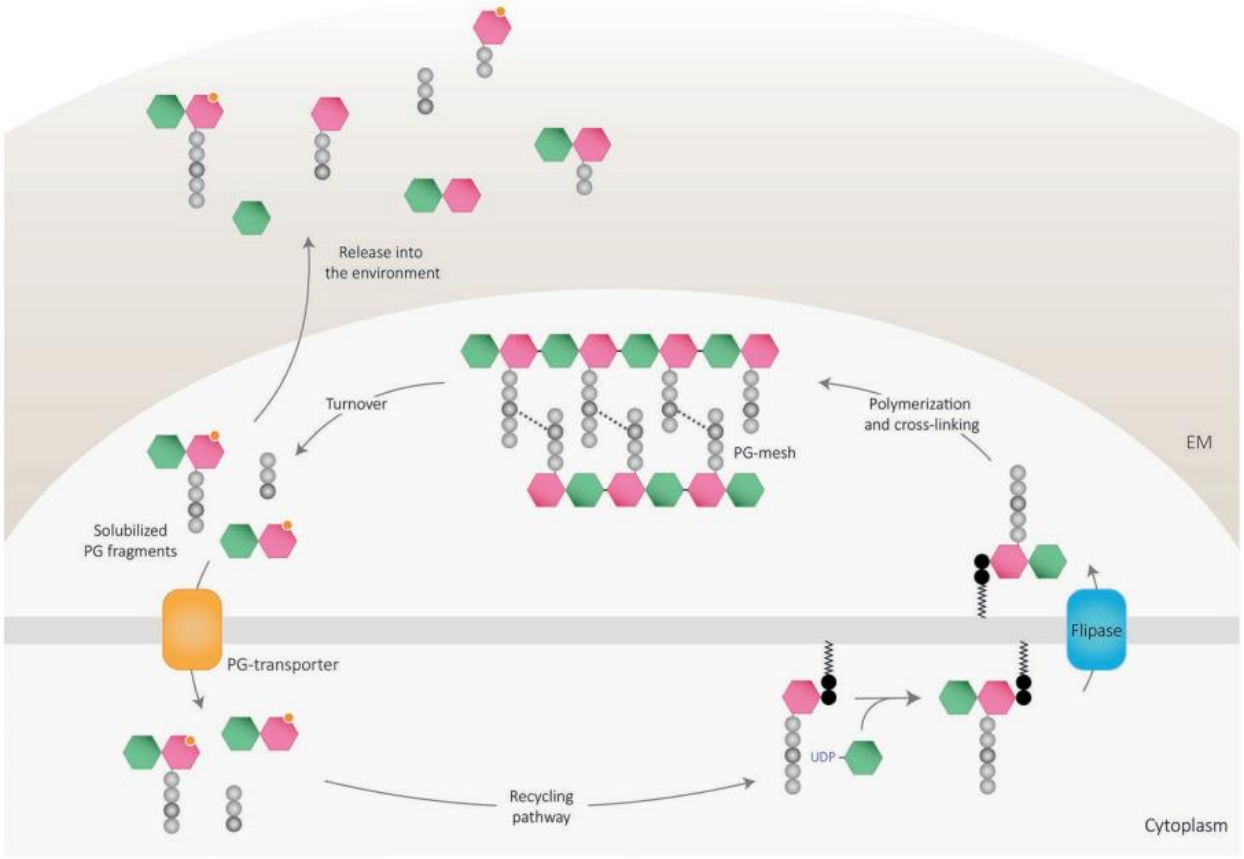

Figure 14: **Homeostatic recycling of bacterial PG.** Adapted from Irazoki et al., 2019 [119]

In the following sections, each of the classes of enzymes responsible for the remodeling of the cell wall (Fig. 13) mentioned above will be briefly discussed.

1.6.4 Peptidoglycan Glycosidases

Peptidoglycan, or cell wall glycosidases, are involved in the hydrolysis of the glycosidic bond or linkage found within the complex sugars of the bacterial cell wall. The hydrolysis of these linkages results in the formation of either a glucide hemiacetal or hemiketal [128, 129]. There are currently 135 families of glycosidase which can be separated into two categories *viz;* N-acetylglucosaminidases, and lysozymes.

N-acetylglucosaminidases, comprising of two glucosaminidase activity domain families viz; glycosyl hydrolase family 3, or GHF-3 and the glycosyl hydrolase family 73, or GHF-73, have been found to be involved in the hydrolysis of the glycosidic bond in a range of complex sugars.

Lysozymes and lytic transglycosylases (LTGs) act on the same glycosidic bond via two different actions which result in structurally different products. Lysozyme hydrolyzes the β1,4- glycosidic bond resulting

in a terminal reducing murein (MurNAc) residue which does not form a ring. Conversely, transglycosylases do not hydrolyse the same bond by cleaving it between the murein and N-Acetylglucosamine (GlcNAc) - the resulting product being a 1,6-anhydro ring which forms at the murein residue [130]. Further, Lysozymes have been divided largely into 5 main subgroups namely Bacteria- (B), Chicken (C), Fungi- (F), Goose- (Goose) and Bacteriophage lambda (P) types [131]. In bacteria, and certainly mycobacteria, lysozymes remain poorly characterized with only three domains being currently recognized, namely: glycosyl hydrolase family 22 (GHF-22), glycosyl hydrolase family 24 (GHF-24) and glycosyl hydrolase family 25 (GHF-25) [132].

1.6.5 Peptidoglycan Peptidases

Cell wall peptidases, or CWPs, are enzymes which cleave the amide bond between amino acids in the peptidoglycan of the cell wall [128]. Depending on their substrate specificity, cell wall peptidases can be categorized as either carboxy- or endopeptidases. Carboxypeptidases remove C-terminal amino acids whilst endopeptidases cleave the peptidoglycan peptide bond [132]. Three isoforms of endopeptidases have been observed: D, L-, L, D- and D, D-peptidase, which have a similar action, with different targets depending on the amide bond between L- and D- amino acids [133].

Currently, ten different domains have been published for cell wall peptidases namely: (i) cysteine histidine-dependent amidohydrolases/peptidases (CHAP), (ii) new lipoprotein C/protein of 60-kDa (NlpC/P60), (iii) peptidase M14 (PM14), (iv) peptidase M15 (PM15), (v) peptidase M23 (PM23), (vi) peptidase M74 (PM74), (vii) peptidase S11 (PS11), (viii) peptidase S13 (PS13), (ix) transpeptidase (TP), and (x) peptidase S66 (PS66) [132].

1.6.6 Peptidoglycan Amidases

1.6.6.1 Identification and Function

The peptidoglycan (PG) polymer is modified via the action of several remodelling enzymes such as transpeptidases, endopeptidases, carboxypeptidases, amidases and transglycosylases, which are all hypothesised to have key interactions in the synthesis, crosslinking and remodelling of the peptidoglycan during bacterial cell wall repair and growth [84, 88].

Amidases are enzymes which have been hypothesised to be integral to peptidoglycan degradation during cell division, peptidoglycan recycling and the homeostatic regulation of osmotic pressure via the hydrolysis of the amide bond between the glycan strand and the stem peptide in peptidoglycan layer [88]. These enzymes have been found in multiple different species from viruses to eukaryotes. Within bacteria, most identified amidases are members of the bacterial autolytic enzyme system

important in the transport of a signal peptide across the cytoplasmic membrane. In contrast to this, amidases identified in bacteriophage proteomes have been observed to act as autolysins which do not transport signal peptides, despite their ability to translocate across the cytoplasmic membrane [134, 135]. Amidases are classified based on their domain-containing proteins into either amidase_2 (PF01510) or amidase_3 (PF01520), and studies which have assessed the catalytic domain have observed a high degree of structural conservation [136]. In *E. coli*, five amidase homologues have been identified and have been allocated the names AmiA – AmiD and AmpD [137]. AmiA and AmiC vary in their transport to AmiB. Whilst the latter's translocation is facilitated via Sec machinery, AmiA and AmiC are exported via the twin-arginine protein transport (Tat) system [138]. This export system has been documented to facilitate the movement of tertiary proteins containing one or more cofactors across the cytoplasmic membrane. Within a *Bacillus polymyxa* bacteriophage, the amino acid sequence of PlyA revealed that AmiA-AmiC are zinc ion containing metalloenzymes [139]. The ability of these enzymes to bind zinc may explain their translocation via the Tat pathway.

The primary role of *N*-Acetylmuramyl-L-Ala amidases focuses on the biosynthesis, recycling and repair of the peptidoglycan sacculus. The PG sacculus largely resembles a net-like molecule comprising muramic acid residues linked via multiple peptide bonds [84]. Rearrangement of this sacculus during homeostasis and division is essential. This growth is simultaneously achieved through the insertion of newly synthesised PG subunits via PG synthases into gaps in the sacculus, created via the action of PG hydrolases which cleave the covalent bonds [140, 141]. This implies that the deletion of PG hydrolase genes would result in a bacillus which is unable to grow and divide. Despite multiple single- and multi-hydrolase knockouts, the phenotype of complete growth arrest has not yet been observed [129]. These data imply that there are multiple hydrolases, both known and unknown, which can compensate for the deletion of one or several knocked-out genes. Within *E. coli* alone, there exist 12 known hydrolases which reside in the periplasm [142]. These periplasmic hydrolases, in which amidases are included, are highly active during the growth and binary fission of the bacillus. In one round of replication, it is estimated that a single *E. coli* bacillus loses approximately 45% of its total peptidoglycan via the direct activity of cell wall hydrolases [143]. Considering the primarily single-layered structure of the PG, this percentage seems deleteriously high. The authors hypothesised that given the chemical compounds and turnover products involved, it is evident that the maintenance of the PG sacculus is achieved through the combined action of transglycosylases, endopeptidases and amidases. This is further elucidated in the separation of daughter cells via the cleavage of the cellular septum. Specifically, AmiA, an amidase homologue which is secreted into the periplasm of the *E. coli* cell, is an amidase_3 domain-containing protein whose deletion in *E.coli* results in atypical cell separation during division and the inclusion of multiple septa per cell [129, 137]. The bacterial

phenotype is that of a string of several connected daughter cells up to 15 µm long. Knockout of AmiC, another periplasmic amidase, resulted in a worsening of this phenotype which affected 20-30% of the *E.coli* population [137]. AmiB knockout did not display the elongated phenotype mentioned above, however, when knocked out in combination with AmiA, the additive effect worsened the atypical septation phenotype [137]. Further analysis of these filamentous mutants revealed that they displayed increased cell wall permeability and were more susceptible to antibiotic treatment [103, 144].

1.6.7 The Role of Peptidoglycan and Amidases in the Host Immune Response

Regarding the host immune response to bacterial PG, the recycling of cell wall material has both an energy benefit as well as plays a role in immune evasion. Previous studies have implied that PG recycling was largely observed in gram-negative bacteria; excessive PG fragments were detected in gram-positive culture milieu [123]. Several amidases have been shown to have roles in the recycling of extracellular murein, and thus it is probable that the knockout of these enzymes may also affect the host immune response. [122].

Bacterial peptidoglycan, or the peptidoglycan fragments N-acetylglucosamine (NAG) and N-acetylmuramic acid (MurNAc or NAM), are a potent antigen for the induction of an effective host immune response for many species. In the *Drosophila melanogaster* model, muramyl tripeptide, a muropeptide released after the digestion of the peptidoglycan during a bacterial challenge, is recognised via peptidoglycan recognition proteins, or PGRPs, and subsequent classical Toll-like receptor (TLR) recognition which is essential for the induction of an efficient immune response [145]. Interestingly, many peptidoglycan recognition proteins are amidases, and in *Drosophila melanogaster* two main eukaryotic amidases, PGRP-SB1 and PGRP-LB, are intrinsically involved in the hydrolysis of the stem peptide of the peptidoglycan layer [146, 147]. The reduced ability of peptidoglycan recognition proteins to identify muropeptides in *Drosophila melanogaster* leads to a lessening of the TLR response and subsequent immune signalling. The role of TLRs in PG recognition is controversial. TLRs are transmembrane-spanning proteins which are found on the surface of both cells and intracellular endosomes. Initially, TLR2 was hypothesized to be the main pattern recognition receptor (PRR) responsible for the detection of PG [148-150]. In contrast to that work, a subsequent study postulated that the TLR2 activation observed in those studies was as a result of lipoteichoic acids and lipoproteins found within the cell wall as opposed to the PG itself [151]. In those studies, the authors show that these molecules often coprecipitate with bacterial PG and that with, sufficient purification, the host immune response facilitated via TLR2 activation can be ablated. Further, they showed that the pure PG activates NOD2 in TLR2 knockout macrophages. However, an alternative study proposed

that PG was, in fact, a TLR2 ligand [152]. In this study, the authors showed that purified soluble PG extracted from penicillin-treated bacteria, which was not incorporated into the cell wall and was thus lacking lipoteichoic acids and lipoproteins, was able to activate TLR2 and induce TNF. These differing results have been attributed to varying purification techniques, PG structure, bacterial species and PG cross-linking [153]. Together, these studies have highlighted the uncertainty of TLR2 as the PRR of PG.

In mammals, four PG recognition proteins (PGLYRP1- PGLYRP4) have been identified [153]. They detect and elicit antibacterial activity through the detection of, and binding to, muramyl pentapeptide or tetrapeptide on the bacterial cell wall (Fig. 15) [154]. The cytosolic nucleotide-binding oligomerization domain-containing protein 1 (NOD1) and nucleotide-binding oligomerization domain-containing protein 2 (NOD2) proteins are the two most well-characterized detectors of PG.

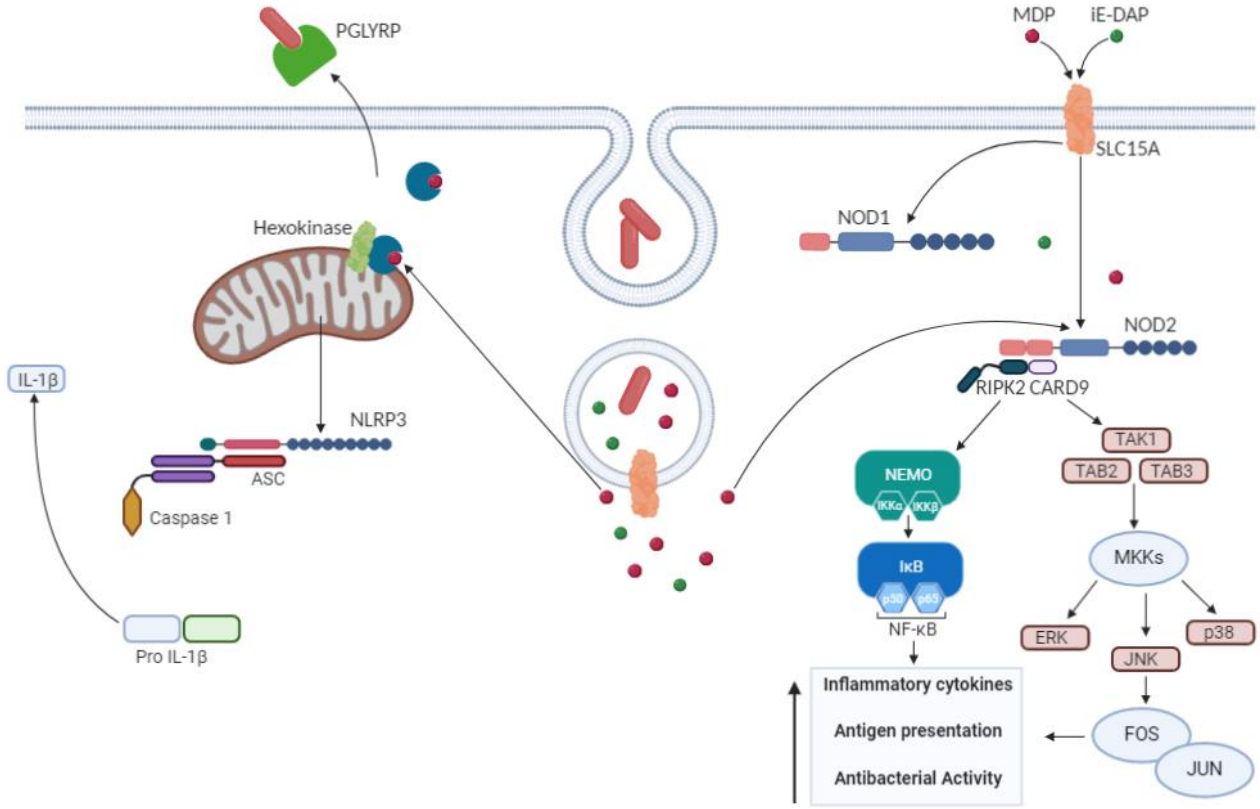

Figure 15: **Mammalian Innate Immune Signalling Pathways in Response to Bacterial Peptidoglycan.** Adapted from [153]

It has been reported that NOD1 identifies PG through the binding of the muropeptide γ-d-glutamyl-meso-diaminopimelic acid (iE-DAP) [155, 156]. Further, NOD2 identifies PG via muramyl dipeptide (MDP) which is formed via the acetylation of MurNAc otherwise known as NAM [157, 158]. For NOD1 or NOD2 to detect these fragments, antigen needs to be present either outside the cell or within

phagosomes. Currently, solute carrier family 15 member 4, or SLC15A4, is hypothesised to be the most likely transporter of PG antigen (iE-DAP and MDP) in both instances [159] (Fig. 15). The binding of these ligands to either NOD1 or NOD2 respectively results in the oligomerisation to RIPK2, which subsequently results in the activation of two pathways, namely the inhibitor of nuclear factor-κB (IKK) complex leading to activation of nuclear factor-κB (NF-κB), or activation of mitogen-activated protein kinase kinase kinase 7 (TAK1) and the mitogen-activated protein kinase (MAPK) signalling cascade [160]. Both of these pathways initiate the production of inflammatory cytokines and chemokines which are essential for the host immune response and antigen presentation [160].

Bacteria have evolved several strategies to mitigate immune detection, elicit chronic infection and increase virulence. The most effective methods of immune evasion occur through various modifications to the PG. Studies in *Streptococcus pneumoniae*, *Listeria monocytogenes* and *Staphylococcus aureus* have demonstrated that these pathogens can evade the host immune system and enhance their pathogenicity through the deacetylation or the acetylation of the PG sugar backbone via the genes, *pdgA* and O-acetyltransferase, respectively. [161-163]. More specifically, the deacetylation of NAG or MurNAc has been shown to abrogate NOD1/2 and inflammasome activation [164]. Additionally, Mtb has displayed the ability to evade the NOD1 host immune response via the amidation of the meso–diaminopimelic acid (mDAP), thus removing the substrate required for the formation of iE-DAP, the ligand of NOD1 [127, 165]. However, NAM residues within the PG polymer, which have been glycolylated, are well recognised via NOD2 and facilitates the induction of inflammatory cytokines in macrophages infected with Mtb [166, 167]. *Mycobacterium tuberculosis* muropeptides have been shown to potently induce the host innate immune response and can modulate immunity to infection [166]. Further, *Mycobacterium tuberculosis* muropeptides have been shown to play an important role in normal granuloma formation [168-170].

The dysregulation of the genes - and thus enzymes - which may play key roles in the remodelling of the mycobacterium cell wall, as well as the contribution of degraded peptidoglycan, may result in modulation of the host immune response to Mtb.

1.6.7.1 Mycobacterial-Specific Amidases

The mycobacterial cell wall is a unique structure which is distinct from that of well characterised bacterial models such as *E. coli*. As such, the inherent role of PG remodelling enzymes is expected to vary relative to the PG hydrolases observed in other model systems. The exact role of amidases in the context of mycobacterial homoeostasis and replication remains unclear. However, two recent studies have identified the crystal structure of Rv3717 (herein referred to as Ami1), a mycobacterial amidase which shares structural similarity to amidase_3 domain-containing amidases and has the functional

ability to cleave peptidoglycan [171, 172]. The hydrolytic activity of this enzyme was functional with the cell wall constituents of other bacteria, highlighting the degree of structural conservation observed [172]. In-depth biochemical analysis Rv3915 (herein referred to as Ami2), a peptidoglycan hydrolase isolated from Mtb, revealed distinct amidase activity [97]. In addition to Ami1 and Ami2, two more amidases have been identified in Mtb and *Mycobacterium smegmatis* alike. These enzymes have been designated the names Ami3 (Rv3811, MSMEG_6406) and Ami4 (Rv3594, MSMEG_5315) [98]. Both Ami3 and Ami4 are classified under the amidase_2 domain-containing family of cell wall hydrolyzing enzymes [98]. Ami1-Ami4 are potentially integral peptidoglycan remodelling enzymes in Mtb, however, this is yet to be fully elucidated.

As mentioned above, previous studies which have looked at the function of these enzymes in model organisms such as *E. coli* have found that the knockout of amidase homologues resulted in a bacterial phenotype which displayed atypical septation during binary fission and drastically increased the incidence of filamentous-like bacteria aggregates composed of multiple individual bacteria [103, 128, 173]. More recently, a similar phenotype was observed in non-pathogenic *Mycobacterium smegmatis* where Ami1 was knocked out via using two-step allelic exchange mutagenesis [174]. The amidase knockout again was shown to display a phenotype of dysfunctional septation and atypical filamentous growth, which was reversed via complementation (Fig. 16) [174]. Interestingly, the authors observed a two- to fourfold increased susceptibility to a range of cell wall targeting antimicrobial agents, as well as increased cell permeability in Ami1 defective bacteria [174].

These lines of evidence suggest that amidases play an important role in normal mycobacterial cell wall remodelling, most notably during binary fission, as well as potentially preserving tolerance to cell wall targeting antibacterial compounds. Inhibition of peptidoglycan remodelling enzymes may potentially I.) convey a pharmacokinetic advantage to existing TB treatments due to dysfunctional cell division or II.) improve host immune responses that ameliorate disease outcome. The immune response, phagocytic ability, and virulence of these Mtb mutants in both the human and murine model of Mtb infection remain a key gap in the knowledge of the field which needs to be verified.

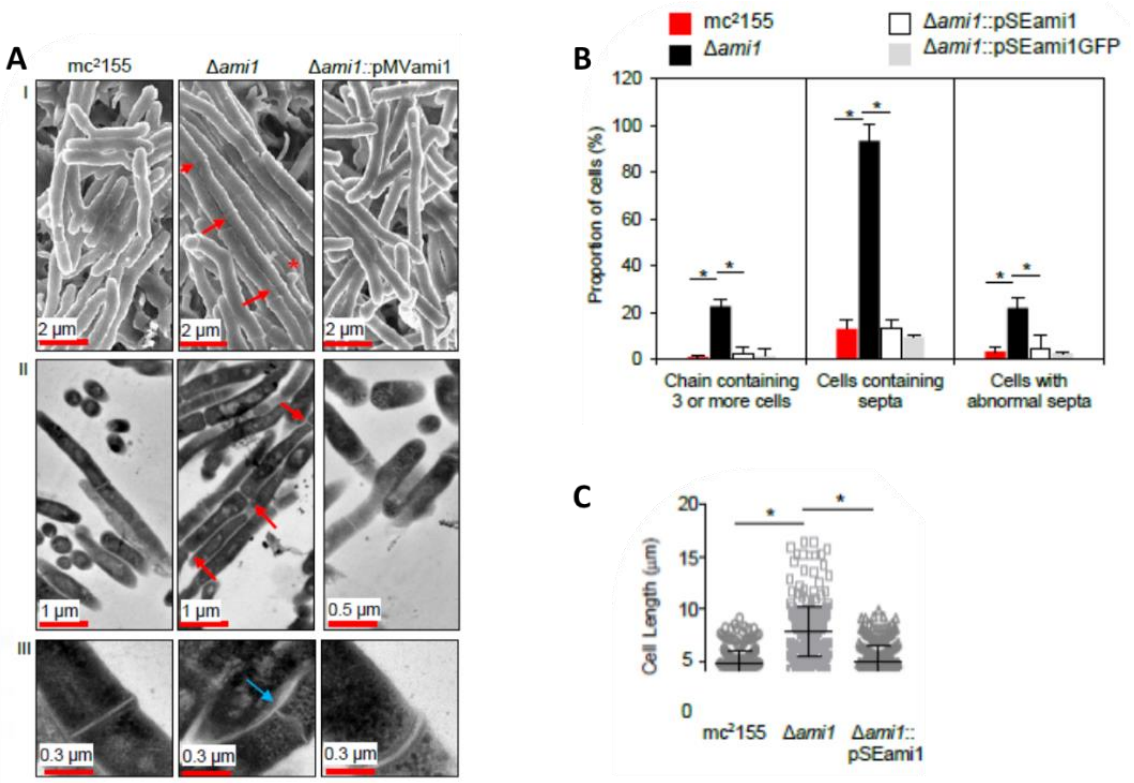

Figure 16: **Knockout of Ami1 in *Mycobacterium smegmatis* A)** Scanning electron microscopy displaying filamentous phenotype and atypical septation relative to WT (mc^{2}155) **B)** Ami1 knockout resulted in a mutant strain with an increased proportion of septa-contain cells which are composed of multiple cells resulting in **C)** a significant increase in length. Adapted from Senzani et al. 2017 [174].

1.7 The Role Epigenetics in Tuberculosis – Importance and Implications.

Mtb can tolerate, as well as proliferate, within the intracellular environment of innate immune cells. Infected individuals can be segregated into two categories: active disease patients, and individuals who are latently infected with Mtb (LTBI). The factors which contribute to the chronic persistence of Mtb to the host immune response and its later activation remain poorly understood. Some reports have shown that several bacterial factors are involved with the alteration of the Mtb virulence and induction of dormancy, without hampering their ability to enter cells. For example, resuscitation promoting factors (RPFs) have been shown to play integral roles in this phenomenon [175]. The epigenetic modulation of host nucleic acid can alter various cellular mechanisms ranging from gene expression, DNA repair and recombination, and may play a significant role in the resuscitation and subsequent immune response to Mtb. Whilst not always heritable, epigenetic alterations may be passed along during cell division, homeostatic growth and repair processes. These changes are not terminal and may be altered or deleted during the ontogeny of the cell. Methylation, acetylation, phosphorylation and ubiquitylation are all methods by which these alterations are achieved [176,

177]. Several microorganisms, including pathogenic species, have exhibited the ability to alter the host epigenome to disrupt key cellular processes involved with immunity, apoptosis and other defensive cellular mechanisms [178]. Mtb has been reported to exploit these methods, specifically histone modification, the expression of non-coding RNAs (ncRNAs), and DNA methylation to facilitate its persistence in the human lung and evade immune control.

1.7.1 *Mycobacterium tuberculosis* and Histone Modification

Histone modification refers to the alteration of the amino acid residues situated on histone tails, the primary protein components of the eukaryotic chromatin system within the nucleus. These alterations change the organisation and functional ability of the chromatin, thus affecting the ability of the chromosome to interact with nuclear RNA and proteins. This change in the ability of the chromatin to function has implications for gene expression, cellular growth and division, as well as the establishment of a successful host immune response. Chromatin alteration is facilitated through the actions of multiple enzymes, namely: histone deacetylases (HDACs), histone acetyltransferases (HATs), histone demethylases (HDMs), histone methyltransferases (HMTs), kinases, and phosphatases [179]. These chromatin modifications can also determine how densely the genetic material is organized into the complex structures by either active chromatin or inactive chromatin. Active chromatin is linked to post-translational modification of histone-3-lysine-4 residue trimethylation, whilst inactive chromatin is linked to histone-3-lysine-9 residue trimethylation [180].

During Mtb infection, the host immune system upregulates the production of IFN-γ which binds to, and activates, innate antigen-presenting cells (APCs) such as macrophages, thus increasing their antimicrobial activity. This is accomplished primarily through the upregulation of MHCII genes. Mtb can subvert this process. The binding of IFN-γ to surface receptors of APCs activates the Janus tyrosine kinase-signal transducer and activator of transcription1 (JAK-STAT1) pathway which, among other functions, can upregulate the class II transactivator (CIITA) which subsequently upregulates MHCII genes and is essential for the presentation of antigen [181]. In 2012, a study interrogated the different methylation patterns associated with BCG vaccination in immune-compromised (SCID) mice [182]. Those authors found that mice which received the BCG vaccination led to increased survival relative to unvaccinated control mice. Further, they showed that this survival benefit was facilitated by the epigenetic modifications of histone H3 trimethyl lysine4 (H3K4me3), which resulted in the reprogramming of the NOD2 gene within monocytes. A previous study reported that Mtb can prevent the gene expression of the CIITA transactivator via the secretion of a 19-kDa protein called Rv3763, which directly prevents the acetylation of histones 3 and 4 [181]. Further, it has been shown that Mtb can induce both methylation and acetylation marks in host DNA [183]. In this study, the authors

reported that Mtb infection significantly reduced H3K4 methylation as well as CIITA acetylation in primary macrophages following infection. In the absence of this protein, the host immune response was significantly more robust. Recently, Mtb was shown to modulation host autophagy through the increasing the acetylation at histone H3 [184]. Further, Rv3423.1, first isolated from Mtb infected primary macrophages, was shown to confer intracellular survival when incorporated into *M. smegmatis* via its histone acetyltransferase activity at H3K9 and H3K14 [185]. More recently, Koo et al. showed that a chronic immune response against Mtb (CDC1551), a susceptible lab strain, was sufficient to clear the pathogen. However, under the same conditions utilising the hypervirulent strain HN878, the immune response was unable to clear the infection [186]. Whilst the exact mechanism was not reported in that paper, their results reinforce the hypothesis that Mtb can alter the host immune response to encourage immune evasion and intracellular survival. Further illustrating the mechanisms of intracellular Mtb-macrophage epigenetic dynamics, a 2016 study highlighted the role of Alu element transposition during the early host innate immune response [187]. Specifically, they showed that, during infection, histone modifications to H3K4me1 resulted in the detection of a significant number of transcription factor binding sites, which are important in macrophage differentiation and immune responses during infection [187]. Further, they provided evidence to show that, through this epigenetic reprogramming, Mtb-infected macrophages can alter their cholesterol metabolism and apoptotic characteristics to kill Mtb.

1.7.2 *Mycobacterium tuberculosis* and DNA methylation

DNA methylation is utilised in a myriad of organisms in the regulation of gene expression, cellular development and differentiation, as well as genetic reprogramming [50]. The silencing of genes can be achieved by the methylation of CpG sites, thus preventing the interaction of transcription factors to their specific CpG island [188]. DNA methylations, such as these, are hypothesised to be less reversible and are more stable than histone modification [188].

In human cell line studies, significant epigenetic changes have been observed in Mtb infected THP-1, a human monocyte-like cell line, relative to uninfected controls, with the caveat that the degree of epigenetic change is variable depending on the strain and virulence of the Mtb isolates used during infection [189]. It has also been reported that Mtb-induced methylation may play a role in stress response [190]. Here, the authors provide evidence showing that a DNA methyltransferase in Mtb, called MamA, plays an important role, albeit Mtb strain-specific response, to hypoxic stress. More recently it was shown that Mtb can produce Rv2966c, a 5-methylcytosine-specific DNA methyltransferase, which is secreted by Mtb and is translocated to the host nucleus [191]. There, Rv2966c methylates host DNA in a non-canonical non-CpG specific manner to repress the host

immune response and promote bacterial survival. Further, it has been shown that Rv1988, a secreted Mtb methyltransferase, can translocate to the host nucleus and methylate histone H3 at H3R42 [192]. This methylation was then shown to be correlated with the inhibition of anti-TB genes and increased the ability of Mtb to survive in macrophages and mice.

In a recent clinical study, researchers interrogated DNA methylation patterns in patients suffering from TB [193]. In this study, they showed that TB patients possessed DNA hypermethylation patterns in the IL-2/STAT5, TNF/NF-κB, and IFN-γ intracellular signalling pathways. Further, they identified specific methylated genes within these pathways, which were correlated with decreased immune cell functionality and a worsened host immune response to Mtb [193]. This study illustrates the ability of Mtb to subvert the host immune response via the action of DNA methylation.

DNA methylation markers may probably be used as a reliable diagnosis of active and latent TB in the future. A recent study has already highlighted the feasibility of this [194]. In that paper, the researchers show that, via the assessment of the DNA methylome, it may be possible to identify not only TB positive individuals but also to distinguish between latent and active infection [194].

1.7.3 *Mycobacterium tuberculosis* and the regulation of non-coding RNAs

Current research has exhibited the critical roles of non-coding RNAs (ncRNAs) during various homeostatic mechanisms such as oncogenesis, apoptosis and cellular ontogeny [195]. Small ncRNAs, such as microRNAs (miRNAs), are important regulatory molecules which alter gene expression at a post-translational level [82, 196]. This occurs via the binding of the miRNA to the 3'UTR of mRNAs, thereby modifying their expression. Despite a growing interest in these molecules in TB, their roles in Mtb-host infection remains largely unknown [82].

Current research is increasingly informing on the intrinsic ability of Mtb-induced miRNAs to ameliorate the host immune response, thus contributing to pathogenesis. To illustrate this point, it has been shown that Mtb-infected dendritic cells and macrophages display a significant difference in the expression of numerous miRNAs relative to uninfected controls [197, 198]. Further, variations in strain and virulence have also been shown to induce differing miRNA expression profiles [199, 200]. Within the human-Mtb model of infection, it has been reported that BCG can suppress the activity of several IFN-γ producing immune cells such as natural killer (NK), and $CD8^+$ and $CD4^+$ T cells via the downregulation of miR-29 [201].

In mice, it has been shown that the targeted knockout of miRNA, miR-155, resulted in a heightened susceptibility to Mtb infection, highlighting the critical role this miRNA plays in the immune response to Mtb [202]. Further, in the human model of Mtb infection, Mtb-induced miR-155 was shown to

promote intracellular survival through the subversion of autophagy via its action on ATG3 [203, 204]. Additionally, Mtb has been shown to ameliorate the host immune response through the induction of miR-125b [205]. In that study, the authors show that miR-125b can inhibit the secretion of TNF during Mtb infection in mice. More recently, the roles of microRNA-143 and microRNA-365 in Mtb infection were elucidated [206]. In the study, the authors show that these miRNAs can promote bacterial growth in alternatively activated macrophages via their interaction with several transcription and host factors. Among others, several notable miRNAs have been identified which are induced by Mtb and result in a reduction of the host immune response: miR-99b [207], miR-125a [208], miR-33 [209], miR-132[210], miR-26a[210, 211], miR-20b [212] and miR-144 [213].

Like miRNAs, long non-coding RNAs (lncRNA) are believed to play important roles in TB pathogenesis. RNA sequencing data has shown an increased abundance of these molecules in the lungs of infected mice [214], however, few studies have managed to identify specific Mtb-induced lncRNAs which may modulate the host immune response [82]. Recently, the lncRNA, PCED1B-AS1, which is downregulated in Mtb infected patients, was shown to act as a molecular sponge to miR-155, thus enhancing autophagy and decreasing macrophage apoptosis *in vitro* [215]. Other lncRNAs which have been shown to be associated with TB are detailed in Table 3 below.

Table 3: **Additional Long non-coding RNAs which are upregulated/downregulated during Mtb infection.** Adapted from Fathizadeh et al., 2020 [216]

LncRNA Name	↑/↓	Experimentally Validated Role in TB	Reference
NR_038221, NR_003142 and ENST00000570366	↑	Associated with Impaired T cell activation and host immune response	[217]
ENST00000422183	↓	Associated with Impaired T cell activation and host immune response	[217]
Lnc-AC145676.2.1-6	↓	Impaired TLR signalling	[218]
Lnc-TGS1-1	↓	Associated with thrombocytopenia during TB treatment and impairment of TLR signalling	[218]
XLOC_014219	↑	Associated with impaired $CD8^+$ T cells activity	[219]
ENST00000427151	↑	Associated with B cell activation during TB	[220]
ENST00000354432	↑	Associated with renal dysfunction during TB	[220]
NEAT1	↑	Associated with prolonged Mtb infection via the reduction in IL-6	[221]
BC050410	↑	Associated with downregulation of IFN-γ and TNF-α	[222]
MIR3945HG V1 and MIR3945HG V2	↑	May be beneficial as a TB biomarker	[223]
LOC152742	↑	May be beneficial as a TB biomarker and in anti-TB treatment	[224]

Taken together these lines of evidence emphasise the significant impact that ncRNAs may have on the course of TB pathogenesis. Further, this evidence shows the intrinsic ability of Mtb to epigenetically reprogram the host immune response to elicit a survival benefit of the bacillus. Finally, these data illustrate that modern sequencing technologies have emerged as a robust, unbiased and powerful toolset by which we can interrogate host-pathogen interactions. Utilising these, and future, technologies will allow researchers to discover and characterise numerous ncRNAs which remain to be discovered and may be of far-reaching therapeutic and clinical significance.

1.8 What is RNA-seq?

Traditionally, gene expression changes were first measured via polymerase-chain-reaction, or PCR utilising primers, dNTPs and *Taq polymerase* in a method which was, famously, first pioneered by Kary Mullis in 1983 [225, 226]. Theoretically, this technology allowed for the single-copy detection and amplification of gene transcripts. Soon after the discovery, this technology was improved upon through first the addition of fluorescent dyes, such as SYBR green, and later by probes, such as commercially available *Taq*Man® which bind to the cDNA products. This innovation allowed for not only the detection of specific gene transcripts but quantification of them as well [225, 227].

RNA sequencing (RNA-seq) greatly improves further on the traditional PCR and qPCR methodology by the high throughput parallel sequencing of RNA. Its advent, more than 10 years ago, has been quoted to have facilitated the "second transcriptomic revolution" [228]. RNA-seq was developed from existing next-generation sequencing platforms which were actively used for high throughput analysis of DNA. In RNA-seq, RNA samples are reverse transcribed into a cDNA library which is then sequenced. The subsequent reads (sequence data) are then bioinformatically analysed *in silico*. "Depth" is the technical term used in sequencing studies, which alludes to the number of reads that was acquired. This data is generally used to assess differential gene expression (DGE) or identification of novel transcripts. The first genome-wide studies which utilized RNA sequencing were run in 2008. These studies were carried out in both mice and humans and yielded a range of 5- to 150-million reads with short read length in the range of 25 -32bp [229, 230]. Other species were subsequently sequenced. The first bacterial RNA-seq data provided approximately 5 million reads with an average length of ±37 bp [231-234]. Current short-read RNA sequencing technologies can sequence almost 100 - 1000 times more reads per run, whilst the long-read application can sequence fragments which are in the range 1 -50 kb [235].

RNA-seq technology, and its continued improvement, have shaped our understanding of biology and disease by revealing the presence and action of non-coding RNAs [236, 237], enhancer RNAs [238], as well as highlighting the extent of RNA splicing [239] in a myriad of biological models and species. In

the future, the utilisation of this technology will allow us to leverage the insights it brings to improve health, fight disease and better understand the natural world.

1.9 A Dual RNA-seq Approach to Studying Disease

RNA sequencing is a powerful tool which has allowed researchers to better elucidate unknown cellular mechanisms in a range of organisms in a high throughput, robust fashion. Among the most intricate interactions which RNA-seq can inform on is that of between a host and pathogen during infection. During infection, a vast number of cellular processes are activated both within the host immune system and within the invading pathogen. These complex interactions are made more multifarious by the action of unknown genes, RNAs and molecules which may be contributing to immune evasion or sensitivity. Recent studies have illustrated that the unbiased interrogation of changing global transcriptional profiles within the host and pathogen thus remains a key method to elucidating these immune events, and may provide key knowledge to develop and refine treatment strategies [240]. A dual RNA-seq approach is beneficial as it allows for the parallel understanding of both transcriptomic changes within the pathogen as well as within the host, with both accuracy and depth.

Initially, viral, parasitic and fungal infection models, whose transcripts were structurally similar to the host, were the first to be interrogated using dual RNA-seq [241-244]. However, the intrinsic biological difference between bacteria and eukaryotic cells (Table 4) are namely total RNA availability and composition eukaryotic cells typically have as much as two orders of magnitude more RNA than bacterial cells)., These obstacles required additional refinement of the experimental protocols and advancement of available technologies [240]. Vogel et al. [228] were one of the first research groups to postulate the feasibility of this technology to a bacterial infection model, and were the first to coin the term “dual RNA-seq”. In a later study, the same group demonstrated that with sufficient improvement of available technologies not only could dual RNA-seq work but that it could also provide valuable insights into novel regulatory ncRNAs elicited during host-pathogen interactions [245]. Despite early bacterial-host dual RNA-seq studies being exploratory, many have provided new understandings to the host immune response during infection.

Table 4: **Different Types of RNA in Bacteria and Eukaryotes**. Adapted from Westerman et al., 2012 [228]

Transcript class	Proportion (%)	Subcellular localization	Transcript features
Bacterial cell			
rRNA	± 80	n/a	• Cleaved from precursor transcripts • 120nt (5S), 1,500nt (16S), 2,900nt (23S)
tRNA	14-15	n/a	• Cleaved from precursor transcripts • 75–95nt
mRNA	4-5	n/a	• Polycistronic • Uncapped • Variable polyadenylation state (<50 As)
tmRNA	<1	n/a	• Processing similar to that of tRNA • 230–400nt
sRNA	Varies	n/a	• Processed or unprocessed • ~50–300nt
Eukaryotic Cell			
rRNA	± 80	Cytoplasm	• Processed or unprocessed • 120nt (5S), 160nt (5.8S), 1,874nt (18S), 4,718nt (28S)
tRNA	± 15	Cytoplasm	• Cleaved from precursor transcripts • 75–95nt
snRNA	± 5	Nucleus	• U-rich • ~150nt
snoRNA		Nucleolus	• U-rich • ~60–300nt • Two major classes (H/ACA and C/D box)
scaRNA		Cajal bodies	• Similar to snRNAs
mRNA		Cytoplasm/nucleus	• Processed from pre-mRNA via splicing • 5' capped • 3' polyadenylated (~250 As)
miRNA		Cytoplasm/nucleus	• Processed • 21–23nt
siRNA		Cytoplasm/nucleus	• Processed • 20–25nt
piRNA		Cytoplasm/nucleus	• Processed • 24–31nt
lncRNA/lincRNA		Cytoplasm/nucleus	• Heterogenic

Early *Chlamydia trachomatis* dual RNA-seq studies reported evidence showing that iron acquisition, coupled with host immune dampening, was one of the strategies which allowed these bacteria to infect human epithelial cells and induce fibrotic scarring [246]. Later, another study utilizing this technology found that whilst uropathogenic *Escherichia coli* (UPEC) – host responses were similar

when assessed for differing bacterial strains, transcriptomic differences were observed when compared to the pathogenicity of the strains used [247]. Further, the parallel analysis of host-pathogen transcriptomes in the *Haemophilus influenza* mucosal epithelial cell model highlighted the critical role of oxidative host responses, as well as the subsequent strategies by which this was evaded by the pathogen [248]. Very recently, dual RNA-seq was used to differentiate distinct macrophage-lineages within the murine Mtb infection model via their transcriptomic gene signature [249]. From their sequence data, they were able to show that permissive Mtb infected alveolar macrophages sustained bacterial replication through increased association with iron and fatty acid storage pathways. In contrast, they showed that interstitial, or recruited macrophages, were able to restrict Mtb growth and were associated with iron sequestration and higher expression of NO [249].

Together, these studies highlight the power of dual RNA-seq to elucidate the intrinsic cross-talk of pathogen and host which contribute to intra-macrophage survival or sensitivity and supports the hypothesis of unknown mechanisms in other disease models and during homeostasis. In the following study, we aim to explore and reconstruct the dynamics of epigenetic and transcriptional modifications and their effector proteins in human macrophages following Mtb infection, as well as identify associated noncoding RNAs which are correlated with these epigenetic changes.

1.10 Problem Statement

In recent years, TB has become the leading infectious killer worldwide with the highest-burden being experienced in developing countries within Sub-Saharan Africa and South-East Asia. The effectiveness of the host immune system, as well as the ability of first-line drugs to control Mtb, the causative agent of TB, is primarily hampered by, amongst other factors, the characteristically thick cell wall observed in Mtb. This wall is composed of mycolic acid, peptidoglycan and arabinogalactan which are all encompassed in a capsule. These multiple contributing layers are essential for normal physiological functioning, osmoregulation, structure, antibiotic resistance and homeostasis. The targeted dysregulation of the complex processes essential for the remodelling and repair of the cell wall during cell division may improve disease pathology or increase the efficacy of modern TB therapies. Further, a greater understanding of host-pathogen dynamics would allow for the discovery of novel gene targets which can be exploited for novel ant-TB treatment.

1.11 Aims

- We aim to explore mycobacterial survival and modulation of the host immune responses to infection of macrophages using amidase defective strains of Mtb. Further, we aim to assess the virulence of these amidase defective mutants and to test their sensitivity to existing drug therapies

both *in vitro* and *ex vivo* as to ascertain the potential of amidase homologues as future targets for novel drug development.

- Further, we aim to develop a reliable method for segregating both host and pathogen RNA in the Mtb – human macrophage model of infection. Utilising this methodology, we aim to longitudinally assess the transcriptional variation in both host and pathogen and correlate this to observable epigenetic changes in the host.

1.12 Hypothesis

Within the context of Mtb replication and the remodelling of the cell wall, we hypothesise that the disruption of cell wall remodelling processes, via the knockout of amidase homologues, has the potential to elucidate novel vulnerabilities in the restructuring of the peptidoglycan sacculus which is the prerequisite for successful cell division. These vulnerabilities have the potential to be exploited for novel drug design or the repurposing of existing therapies to improve TB outcome. Specifically, we hypothesise that amidase deficient mutants may display atypical septation, increased length and dysregulated binary fission which will modulate the host immune response. Lastly, we hypothesise that the segregation of the host and pathogen RNA is possible, even at relatively low MOI.

1.13 Objectives

To achieve the aims set out above, the general objectives of this study are as follows;

- To assess the immune response and mycobacterial survival in primary and cultured murine bone marrow-derived macrophages (BMDMs) which have been infected with amidase defective mutants (*Δami1*, Am1-Complement, Ami4, Ami4-Complement and H37RV) of Mtb.
- To assess the immune response and mycobacterial survival of the same Mtb mutants in human monocyte-derived macrophages (MDMs) and the human monocytic cell line, THP-1 cells.
- To assess the virulence of Mtb mutant's defective in amidase in the murine model of TB infection as well as to assess the host immune response to infection in vivo.
- The effect of first-line drugs as well as PG-specific antibiotics will be assessed *in vitro, ex vivo* and *in vivo*.
- The high-throughput generation of primary human monocyte-derived macrophages will be optimised for downstream Mtb infection experiments.
- Lastly, a protocol for the efficient segregation of human and mycobacterial RNA from Mtb-infected human macrophages will be optimised.

Chapter Two

General Materials and Methods

2.1.1 Ethics

All the experiments performed were done in accordance with the Animal Research Ethics Committee of South African National Standard (SANS 10386:2008) and University of Cape Town, South Africa for practice on animal procedures. The protocol (Permit number: 015/40 and 015/36) has been approved by the Animal Ethics Committee, Faculty of Health Sciences, University of Cape Town (Cape Town, South Africa). Further, this study has been ethically approved for the experimentation with human tissues (MDMs) within the context of the research question detailed above (Human ethics protocol: HREC 732/2015).

2.1.2 Cells and Reagents

To analyse the virulence and host protective responses of the Ami-deficient Mtb mutants within the murine model of infection, and the optimisation of the dual-RNA seq methodology, three model systems were investigated;

2.1.2.1 Human Monocyte-Derived Macrophages (MDMs)

For human monocyte-derived macrophages (MDMs), healthy-donor leukopaks were acquired from donors from the South African National Blood Service in Cape Town, South Africa. Leukopaks were standardised for age, sex and race. Standard pathological testing is conducted by the Western Cape Blood Transfusion Service (WCBTS) on all blood to ensure its free from HIV, Hepatitis B and C, and Syphilis. PBMCs were isolated via density centrifugation. Classical ($CD14^{++}CD16^{-}$), non-classical ($CD14^{+}CD16^{++}$) and intermediate ($CD14^{++}CD16^{+}$) monocytes were purified via negative selection utilising the MojoSort™ Human Pan Monocyte Isolation Kit (Biolegend) and were differentiated into monocyte-derived-macrophages (MDMs) in standard RPMI media supplemented with 10% fetal calf serum and 50 ng/uL recombinant human M-CSF over 7-days.

2.1.2.2 Murine Bone Marrow-Derived Macrophages (BMDMs)

To generate BMDMs, pluripotent stem cells were extracted from the femur and tibia bones of the C57BL/6 mouse strain. These cells were differentiated for 10-days at 37°C to bone marrow-derived macrophages in standard Plutznik media comprising of Inactivated Fetal Calf Serum (10% v/v), Inactivated Horse Serum (5% v/v), L929 conditioned medium (30%), 2mM L-glutamine, 1 mM sodium pyruvate, 50 U/ml penicillin, 50 ug/ml streptomycin, 50uM β-Mercaptoethanol and DMEM (50%) as described previously [250]. Post-differentiation, BMDMs were then harvested and plated into 96-well plates (Nunc, Denmark) and cultured overnight to ensure adequate adherence. To polarise these cells, they were cultured in DMEM media (Gibco) supplemented with 10% FCS and IFN-γ (100 U/ml, BD Biosciences, San Jose, CA). Activated BMDMs were then infected with Mtb at an MOI of 1.

2.1.2.3 THP-1 Cell Line

THP-1 were utilised for the optimisation of RNA extraction as well as other experimental troubleshooting. The THP-1 (ATCC® TIB-202™) cell line was purchased from the ATCC. The cells were cultured at 37°C and CO2 (5%). A cellular concentration of 0.5 x10^6 cells/ml was maintained at all times in RPMI-1640 media (Gibco) supplemented with β-mercaptoethanol (0.05 mM) and fetal bovine serum (10% v/v). The cells were passaged every 2-3 days. For cryopreservation, approximately 10-20 x10^6 were resuspended in culture media supplemented with DMSO (5% v/v) and stored at -80°C.

2.1.3 Bioinformatics and Experimental *Mycobacterium tuberculosis* Strains

M.tb mutants utilised in this study were generated by our collaborators at the University of Witwatersrand (Dr Sibusiso Senzani and Professor Bavesh Kana). For a full breakdown of methods and results, please reference the original PhD dissertation [251].

In short, Mtb strains deficient in four amidase-encoding genes; Rv3717 (Ami1), Rv3915 (Ami2), Rv3811 (Ami3) and Rv3594 (Ami4) were constructed using two-step allelic replacement with a suicide plasmid and a selectable lacZ and counter-selectable sacB markers [174]. This involved the cloning of homologous upstream and downstream regions to create in-frame, unmarked gene deletions that were transferred to the mycobacterial chromosome. Vectors for genetic complementation were generated by cloning wild-type genes, with upstream promoter elements or associated genes into a vector that will integrate into the mycobacterial chromosome. Mycobacterial colonies were streaked on 7H11 media and left at 37°C for 14 days. Single colonies were then picked and incubated in liquid 7H9 broth at 37°C until an optical

density (OD600) of at least 0.6 was reached. Stocks were stored down in 2 mL cryovials at -80°C and thawed as needed.

2.1.3.1 PCR Validation of Amidases Deficient Mycobacterium tuberculosis strains

To ensure that the strain-specific knockout was present, Mtb amidase deficient strains were assessed via PCR. In brief, *Mycobacterium* stocks were then streaked on 7H11 agar plates and incubated at 37˚C for 2-4 weeks. A single colony was then picked and inoculated in 50 µL sdH_2O and heat-inactivated at 95°C for 10 min. 25 µL chloroform was added, and the solution was centrifuged at maximum speed for 10 minutes. The top layer was removed to a new Eppendorf and 2 µL was used for standard PCR using the Super-Therm Taq polymerase and the primers detailed below (Table 5). The cycling conditions used were as follows 95°C for 4 min followed by 35 cycles of 95°C for 30 secs, 60°C for 30 secs and 72°C for 1 min and a final 72°C for 7 min step. The product was then run on a 2% agarose gel containing SYBR-safe and visualised using the G:Box gel documentation system.

Table 5: **Primers for the PCR Validation of Amidase Deficient Mutants/Complement Strains of *Mycobacterium tuberculosis***

Primer Name	Primer Sequence (5'-3')	Primer Length (bp)
TB Ami1 SC F Primer	TGGACCTACGAGTTGGCC	18
TB Ami1 SC R1 Primer	GCCGAGTAGTTGACGTGGA	19
TB Ami1 SC R2 Primer	CCCTAGTCCTCGACAACTGC	20
TB Ami4 SC F Primer	AGGCATCCGGAGGTATCC	18
TB Ami4 SC R1 Primer	CACTCGACGCCAATCATGT	19
TB Ami4 SC R2 Primer	CCGGTTGACATCGTTGCA	18

2.1.4 Cytokine Analysis via Enzyme-Linked Immunosorbent Assays (ELISA)

BMDM supernatants were removed from wells and placed in 96-well filter plate (Cornin FiltrEX™) and spun at 1500rpm for 5min at 4°C to remove residual *Mtb* bacilli. A 96-well microplate was coated with 50 µL of primary antibody (IL-12p40, IFN-y, IL-6, CCL2, G-CSF, IL-1α, TNFα, GM-CSF, IL-17, CCL3, TGFβ, IL-10, IFN-β, CXCL2, CCL5, CXCL1, CXCL5, CXCL10, IL-1β, IL-4, IL-12p70 and IL-23) and incubated overnight at 4° C. The wells were then washed four times with washing buffer (0.02% (w/v) KCL, 0.02% (w/v) KH_2HPO_4, 0.15% (w/v) $Na_2HPO_4.2H_20$, 0.8% (w/v) NaCl and 0.05% (v/v) Tween-20) followed by treatment using 200 µL of blocking buffer (2% BSA) and incubated at 37° C for 2 hours. A two-fold dilution series of recombinant mouse protein was prepared over 12 wells using an initial concentration of 100 ng/mL. Sera from

unknown samples were plated in duplicate and 3-fold dilution series of the samples were prepared over 3 wells. Approximately 50 µL of unknown sera and the diluted standard was then transferred to the corresponding wells of the washed ELISA plate and incubated at 4°C overnight. Each well of the washed ELISA plate was first treated with 50 µL of secondary biotinylated rat anti-mouse antibody and incubated at 37° C for 2-3 hours. Following this incubation, 50 µL of streptavidin-alkaline phosphate (1:100) was added and the plate was incubated at 37°C for 1 hour. Finally, 50 µL of 4-nitrophenyl disodium salt-hexahydrate (PNP) (0.1 g/mL) was added to each well and the OD_{405} was measured with Plate Reader (SpectraMax ID3) and analysed using the SoftMax programme (V6).

2.1.5 Histology and Alveolar Space Assessment

Lungs from mice infected with the amidase mutant, the complemented strain, and wild-type H37Rv were isolated and fixed using formalin solution and stained with haematoxylin and eosin as per previously published studies [252]. Analysis of lung sections and assessment of alveolar space was performed using NIS advanced software on a Nikon (Tokyo, Japan) 90i microscope. Additionally, lung weight index (LWI) was utilised as a proxy for inflammation intensity [253]. LWI was calculated using the following equation:

$$LWI = \sqrt{\left[\frac{Lung\ weight\ (mg)}{\frac{Mouseweight(g)}{10}}\right]}/10$$

2.1.6 Flow Cytometry

Briefly, single-cell suspensions from the lung tissues were prepared by chopping them into small pieces followed by incubation in Dulbecco's Modified Eagle Media (DMEM) containing 0.18 mg/ml Collagenase Type I (Sigma, St. Louis, MO), 0.02 mg/ml DNase I (Sigma, St. Louis, MO) for 1 hour at 37°C under constant rotation, followed by mechanically passing through a 100 µm and 70 µm cell strainer sequentially. Erythrocytes were lysed using red blood cell (RBC) lysis buffer (155 mM NH4Cl, 12 mM NaHCO3, 0·1 mM EDTA). A single-cell suspension ($1x10^6$ cells) from infected lung tissue was stained for the following surface markers suspended in FACs buffer comprising of PBS supplemented with 1% BSA and 0.1% NaN_3: CD64 (Clone X54-5/7 PeCy7, BioLegend), Ly6C (Clone AL-21 PerCPCy5.5, BD Biosciences), CD11b (Clone M1/70 V450, BD Biosciences), MHCII (Clone M5/114.15.2 AF700, BioLegend), CD103 (Clone M290 PE, BD Biosciences), CD11c (Clone HL3 APC, BD Biosciences), SiglecF (Clone E5-2440 APC-Cy7, BD Biosciences), Ly6G (Clone 1A8 FITC, BD Biosciences), F4/80 (Clone BM8 PeCy7, eBiosciences), CD4 (Clone RM4-5 BV510, BD Biosciences), CD44 (Clone IM7 PE, BD Biosciences), CD3 (Clone 500A2 AF700, BD Biosciences), CD62L

(Clone MEL-14 V450, BD Biosciences), CD19 (Clone 1D3 PerCPCy5.5, BD Biosciences) and CD8 (Clone 53-6.7 APC, BD Biosciences). The acquisition of samples was conducted using BD LSR Fortessa, and data analysis was performed with FlowJo v10 software (Treestar, Ashland, OR, US).

2.1.7 Statistical Analysis

All experimental data were analysed using Graph-Pad Prism 8.0.2, one-way ANOVA was used. A *p-value of less 0.05 was considered significant, with *$p < 0.05$, **$p < 0.01$, ***$p < 0.001$ and ****$p < 0.0001$ n=3-6. Sample size determined using G*Power (version 3.19.7). Optimally, a total sample size of 18 (n=6 per group) with an expected effect size (f=1.5) and an α=0.5 allowed for a statistical power of 99%. Alternatively, a minimum sample size of 9 (n=3 per group) allowed for 87% should mice be limiting (Supp. Fig 4).

Chapter Three

Loss of putative amidases in Mycobacterium tuberculosis does not affect the ability to colonize macrophages and mice

4.1 Introduction

Tuberculosis (TB) causes the largest number of human deaths attributable to a single human pathogen [21]. It is estimated that globally 1 in 4 people are infected with *Mycobacterium tuberculosis* (Mtb), the causative agent of TB [21]. The rapid emergence of drug-resistant TB and the continued failure to create a universally efficacious vaccine have highlighted the need for new effective therapies. The discovery and characterization of novel gene targets for therapeutic intervention thus remain a key area of TB research. The biosynthesis of the bacterial cell wall and remodelling of the complex macromolecules which comprise it are essential processes under strict regulatory control to facilitate normal cell division, growth, virulence, as well as resistance to antibiotics [100-102]. This dynamic balance of cell wall biogenesis vs. degradation is achieved via the coordinated action of multiple enzymes and dysregulation thereof has deleterious implications for the mycobacterial cell, an effect that can potentially inform novel drug design [141, 173, 254, 255]. In the past, such a strategy has served as the basis for the successful development of many commercial antibiotics and similar approaches may be beneficial for TB [256].

Peptidoglycan (PG) is unique to the bacterial cell wall and is essential for the maintenance of cytoplasmic turgor and cell morphology. PG is made up of crosslinked N-acetylglucosamine (NAG) and N-acetylmuramic acid (MurNAc or NAM), which are potent bacterial antigens that are detected by multiple host pattern recognition receptors (PRR) during infection [153]. Four PG recognition proteins (PGLYRP1-4), which directly bind to the PG of the cell wall have been identified in mammals. This detection is facilitated via recognition of the muramyl pentapeptide or tetrapeptide present on the bacterial cell wall and has been shown to elicit antibacterial activity [154]. Cytosolic nucleotide-binding oligomerization domain-containing protein 1 (NOD1) and nucleotide-binding oligomerization domain-containing protein 2 (NOD2) are the two most well-understood sensors of PG [153]. NOD1 identifies PG through the binding of the muropeptide γ-d-glutamyl-meso-diaminopimelic acid (iE-DAP) [155, 156]. NOD2 identifies PG via muramyl dipeptide (MDP), which is formed via the acetylation of MurNAc [157, 158]. The binding of these ligands to either NOD1 or NOD2 respectively ultimately results in the activation of two pathways, namely;

the inhibitor of nuclear factor-κB (IKK) complex leading to activation of nuclear factor-κB (NF-κB), or activation of transforming growth factor beta-activated kinase 1 (TAK1) and the mitogen-activated protein kinase (MAPK) signalling cascade [160]. Both of these pathways initiate the production of inflammatory cytokines and chemokines which are essential for the host immune response and antigen presentation [160]. Additionally, NOD-, leucine-rich repeat receptor (LRR-) and pyrin domain-containing 3 (NLRP3) have also been implicated in the sensing of PG [164], whereas the role of toll-like receptors (TLR) in PG recognition remains controversial.

Bacteria have evolved several strategies to subvert immune detection to elicit chronic infection and prolonged survival. Often, this is facilitated via the remodelling of the PG sacculus. Previous studies in model pathogenic bacterial species have demonstrated that these organisms can evade the host immune system and enhance their pathogenicity through the deacetylation or the acetylation of the PG sugar backbone via the genes, *pdgA* and O-acetyltransferase, respectively. [161-163]. More specifically, the deacetylation of NAG or MurNAc has been shown to abrogate NOD1/2 and inflammasome activation [164]. Additionally, Mtb can evade the NOD1 host immune response via the amidation of the meso–diaminopimelic acid (mDAP), thus removing the substrate required for the formation of iE-DAP, the ligand of NOD1 [127, 165].

During growth and division, PG is remodelled via the action of several remodelling enzymes such as transpeptidases, endopeptidases, carboxypeptidases, amidases, and transglycosylases [84, 141, 257]. These enzymes have important roles in the hydrolysis, synthesis, crosslinking and remodelling of the PG sacculus and also mediate repair of damaged cell wall material [84, 88]. In this study, we have investigated the role of two N-acetylmuramoyl-L-alanine amidases (Ami1 and Ami4) in Mtb. This class of enzymes is important for PG degradation during cell division, PG recycling and the homeostatic regulation of osmotic pressure via the hydrolysis of the bond between the glycan strand and stem peptide [88]. In *Escherichia coli*, the deletion of several amidases resulted in arrested cell separation after cytokinesis leading to the formation of bacterial chains and altered antibiotic susceptibility [137]. The role of amidases in Mtb requires further work. The crystal structure of Rv3717 (herein referred to as Ami1), a mycobacterial amidase has been solved and bears structural similarity to amidase_3 domain-containing amidases observed in *E. coli*, with demonstrated ability to cleave PG [171, 172]. Whilst lacking efficient hydrolase activity relative to Ami1, Ami2 is essential in regulating cell growth via phospho-relay mechanisms [258, 259]. In addition to Ami1 and Ami2, two more amidase-2-domain containing amidases have been identified in Mtb, designated Ami3 (Rv3811) and Ami4 (Rv3594) [98]. In *Mycobacterium smegmatis*, Ami3

is stabilized by mannosylation and subject to degradation by the HtrA protease as dysregulated levels of this protein resulted in cell death. Ami1 deletion in *M. smegmatis* was found to confer dysfunctional septation, resulting in the formation of cellular chains, with a two-to-four-fold increase in susceptibility to a range of cell wall targeting antimicrobial agents [174].

In Mtb, an Ami1 deficient mutant is defective for survival in chronic infection in mice where Ami1 appears to play a synergistic role with RipA, another cell wall endopeptidase in mediating survival and tolerance [99]. In this study, we further investigate host immune responses in murine macrophages and mice infection with Ami1 and Ami4 defective mutants and assess the changes in antibiotic susceptibility that may occur upon deletion of amidases in Mtb.

4.2 Methods and Materials

4.2.1 Mice

8-12 weeks age, male wild-type C57BL/6 mice (Jackson Labs) were utilized for all mouse infection studies as well as the generation of bone-marrow-derived macrophages for this study. Following infection, mice were housed in a biosafety level 3 containment facility, maximum six per individually ventilated cage with filter tops (type 2 long), as well as dried wood shavings and shredded filter paper as floor coverings. The temperature range was set at 22 to 24 °C and 12-to-12-hour light cycles.

4.2.2 Ethical Statement

All experiments were conducted this study were done in accordance with the Animal Research Ethics Committee of South African National Standard (SANS 10386:2008) and the University of Cape Town, South Africa for practice on animal procedures. The protocol (Permit number: AEC 015/40 and AEC 015/36) was approved by the Animal Ethics Committee, Faculty of Health Sciences, University of Cape Town (Cape Town, South Africa).

4.2.3 Generation of BMDMs

The generation of murine bone marrow-derived macrophages was achieved through the extraction and subsequent differentiation and polarisation of murine pluripotent stem cells as previously described [41]. Post differentiation, BMDM were cultured in standard DMEM medium supplemented with 10% fetal calf serum (FCS) at 37°C. Cells were adhered over 12 -24 hours in 96-well plates (Nunc, Denmark) at a concentration of 2 x 105 cells per well. Post adherence, the cell media was supplemented with 100 U/mL recombinant IFN -γ (BD Biosciences) for 24 hours. Cells were infected with Mtb strains at a multiplicity of infection (MOI) of 1 for indicated time points.

4.2.4 Mycobacterium tuberculosis Strains and CFU Analysis

The Mtb deletion mutants (*Δami1*, *Δami4*) and complemented strains (*Δami1*::*ami1*, *Δami4*:: *ami4*) were constructed by Dr Sibusiso Senzani and Dr Melissa Dalcina Chengalroyen (DST/NRF Centre of Excellence for Biomedical TB Research, Faculty of Health Sciences, University of the Witwatersrand, National Health Laboratory Service, Johannesburg, 2001, South Africa) from wild-type H37Rv (ATCC 25618) as described previously (Table S1 and S2). Cells were cultured at 37°C in 7H9 medium supplemented with 10% Middlebrook OADC Growth Supplement OADC and glycerol (1%) to at OD of ~0.6. To ensure single-cell stocks, the Mtb culture was vortexed vigorously using sterile glass beads. The culture was then centrifuged at 700 rpm for 5 min. The upper clump-free volume was removed to a new tube and stored at -80°C in 15% glycerol. To

determine CFU, infected cells were lysed in 10% Triton X-100 (Sigma) and the cell lysate was plated on 7H11 agar supplemented with 10% Middlebrook OADC Growth Supplement and 0.5% glycerol. Plates were cultured for 2 -3 weeks at 37°C.

4.2.5 Genotyping and Confirmation of Amidase deletion

Mycobacterium tuberculosis amidase deficient mutant strains were assessed via polymerase chain reaction (PCR). *Mycobacterium* stocks were streaked on 7H11 agar plates and incubated at 37˚C for 4 weeks. A single colony was then picked and inoculated in 50 µL sdH_2O and heat-inactivated at 95°C for 10 min. 25 µL chloroform was added, and the solution was centrifuged at maximum speed for 10 minutes. The top layer was used for standard PCR. The primers used for verification of the genotypes were as follows Ami1 SC F 5'-TGGACCTACGAGTTGGCC-3', Ami1 SC R1 5'- GCCGAGTAGTTGACGTGGA-3', Ami1 SC R2 5'-CCCTAGTCCTCGACAACTGC-3', Ami4 SC F 5'- AGGCATCCGGAGGTATCC-3', Ami4 SC R1 5'-CACTCGACGCCAATCATGT-3' and Ami4 SC R2 5'- CCGGTTGACATCGTTGCA-3'. The cycling conditions are as follows 95°C for 4 min followed by 35 cycles of 95°C for 30 secs, 60°C for 30 secs and 72°C for 1 min and a final 72°C for 7 min step. The PCR product was then run on a 2% agarose gel containing SYBR-safe and visualised using the G.Box (Syngene) and Genesnap (Syngene).

4.2.6 *In vivo* Mtb infection and CFU analysis

Anaesthetized C57BL/6 mice were infected intranasally with approximately 100-CFU in sterile saline. Infected mouse lungs were homogenised to produce a single-cell suspension. To determine lung CFU at 3- weeks and 6-weeks post-infection and to determine bacilli uptake at 1-day post-infection, whole lung homogenates were plated on 7H11 agar plates containing 10% OADC and 0.5% glycerol for 2–3 weeks.

4.2.7 *In vitro* / *in vivo* Antibiotic Sensitivity Assessment

AlamarBlue: Antibiotic sensitivity testing was performed in clear 96-well plates (Nunc). The outermost wells were filled with sterile, distilled water to prevent dehydration from the sample wells. Initial drug concentrations were made up in sterile, distilled water; Meropenem (8 ug/mL), pyrazinamide (400 ug/mL), isoniazid (0.2 ug/mL) and rifampicin (0.2 ug/mL) (Sigma). The drug was then diluted two-fold in 7H9 in the 96-well plate. Approximately, $1x10^5$ CFU was added per well. The drug only, media only, and Mtb only controls were included on each plate. The plates were incubated at 37°C for 14-days. On day 14, 20 uL AlamarBlue™ was added to all wells and the plates were incubated overnight. The microwell plates were read at an

absorbance of 570 nm or fluorescence of 585/610 nm using a Spectromax i3X (Molecular Devices) plate reader. Mean fluorescence was calculated from triplicate wells.

BMDM Antibiotic Assay: BMDMs were generated as above. 2×10^5 cells were plated in a clear 96 well plate and rested for 12 hours. Cells were then infected with *Δami1*, *Δami4*, *Δami1*::*ami1*, *Δami4*:: *ami4*, and H37Rv at an MOI of 1. All mutant strains were transformed to express constitutive mCherry. At 4-hours post-infection, drug dilution was carried out as above. Plates were read at 8 days post-infection. Fluorescence was read the excitation wavelength of 585 and emission wavelength 610.

In vivo antibiotic sensitivity assessment: C57/BL6 were infected intranasally with 100-CFU. Infection was allowed to progress for 2 weeks, before the initiation of drug treatment comprising of isoniazid (100mg/L) in the drinking water for a further 2 weeks as previously published [260]. CFU were analysed at 0-, 2-, 4- and 6-WPI as described above.

4.2.8 Flow Cytometry

Briefly, single-cell suspensions from the lung tissues were prepared by chopping them into small pieces followed by incubation in Dulbecco's Modified Eagle Media (DMEM) containing 0.18 mg/ml Collagenase Type I (Sigma, St. Louis, MO), 0.02 mg/ml DNase I (Sigma, St. Louis, MO) for 1 hour at 37°C under constant rotation, followed by mechanically passing through a 100 µm and 70 µm cell strainer sequentially. Erythrocytes were lysed using red blood cell (RBC) lysis buffer (155 mM NH4Cl, 12 mM NaHCO3, 0·1 mM EDTA).A single-cell suspension (1×10^6 cells) from infected lung tissue was stained for the following surface markers suspended in FACs buffer comprising of PBS supplemented with 1% BSA and 0.1% NaN_3: CD64 (Clone X54-5/7 PeCy7, BioLegend), Ly6C (Clone AL-21 PerCPCy5.5, BD Biosciences), CD11b (Clone M1/70 V450, BD Biosciences), MHCII (Clone M5/114.15.2 AF700, BioLegend), CD103 (Clone M290 PE, BD Biosciences), CD11c (Clone HL3 APC, BD Biosciences), SiglecF (Clone E5-2440 APC-Cy7, BD Biosciences), Ly6G (Clone 1A8 FITC, BD Biosciences), F4/80 (Clone BM8 PeCy7, eBiosciences), CD4 (Clone RM4-5 BV510, BD Biosciences), CD44 (Clone IM7 PE, BD Biosciences), CD3 (Clone 500A2 AF700, BD Biosciences), CD62L (Clone MEL-14 V450, BD Biosciences), CD19 (Clone 1D3 PerCPCy5.5, BD Biosciences) and CD8 (Clone 53-6.7 APC, BD Biosciences). The acquisition of samples was conducted using BD LSR Fortessa, and data analysis was performed with FlowJo v10 software (Treestar, Ashland, OR, US) using the gating strategies detailed in the supplementary figures (Supp. Fig. 1 and 2).

4.2.9 Histology and Alveolar Space Assessment

Lungs from mice infected with the amidase mutant, the complemented strain, and wild-type H37Rv were isolated and fixed using formalin solution and stained with haematoxylin and eosin as per previously published

studies [252]. Analysis of lung sections and assessment of alveolar space was performed using NIS advanced software on a Nikon (Tokyo, Japan) 90i microscope. Additionally, lung weight index (LWI) was utilised as a proxy for inflammation intensity [253]. LWI was calculated using the following equation:

$$LWI = \sqrt{\left[\frac{Lung\ weight\ (mg)}{\frac{Mouseweight(g)}{10}}\right]}/10$$

4.2.10 The enzyme-linked immunosorbent assay

The supernatant extracted from the whole lung homogenate was isolated from infected murine lungs via centrifugation. Filtered supernatant was used to detect IL-12p40, IL-12p70, IFN-γ, IL-6, CCL2, GM-CSF, TGFβ, IL-4 (BD Biosciences), G-CSF, CXCL2, CCL3, CCL5, CXCL1, CXCL5, CXCL10, IL-1β (R&D Scientific) IL-1α, TNF, IL-17, IL-10, IFNβ, and IL-23 (BioLegend) via the enzyme-linked immunosorbent assay (ELISA) according to manufacturer suggested dilutions. Chemokine and cytokine protein expression was measured using SoftMax Pro 6.

4.2.11 Statistical Analysis

All experimental data were analysed using Graph-Pad Prism 8.0.2, one-way ANOVA was used. A *p-value of less 0.05 was considered significant, with *$p < 0.05$, **$p < 0.01$, ***$p < 0.001$ and ****$p < 0.0001$ n=3-6. Sample size determined using G*Power (version 3.19.7). Optimally, a total sample size of 18 (n=6 per group) with an expected effect size (f=1.5) and an α=0.5 allowed for a statistical power of 99%. Alternatively, a minimum sample size of 9 (n=3 per group) allowed for 87% should mice be limiting (Supp. Fig 4).

4.3 Results

Genomic maps of Mtb amidase knockout Mtb strains

The genomic map of the relevant locus is shown for the H37Δ*ami1* strain, H37Δ*ami4* and the wild-type H37Rv strains below (Fig. 17a-b). Also shown on the left is the PCR confirmation of the genotype and Southern blotting is shown on the right. For PCR confirmation of Ami1 and Ami4, chromosomal DNA was used to amplify the Ami1 alleles from the wild type and mutant strains using the primers described in Table S1 and indicated as red arrows above. The expected sizes of the amplicons are as follows: Ami1:1526 bp and *Δami1*: 580 bp; *ami4*, 1711 bp and Δ*ami4*, 460 bp. For the Southern blot analysis, chromosomal DNA from the parental and mutant strain was digested with ApaI.

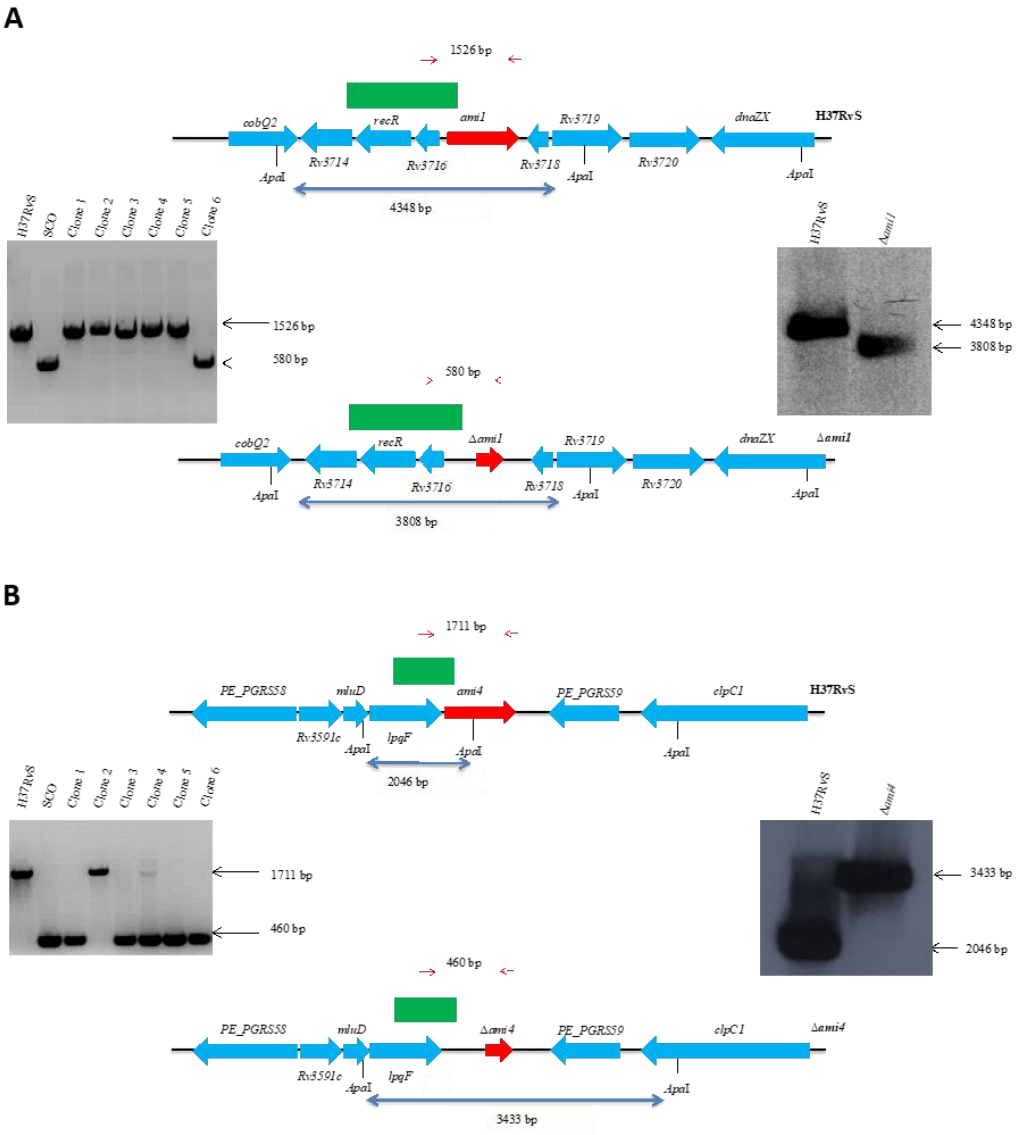

Figure 17: **Genotypic analysis of the amidase Mb strains by PCR and Southern blot analysis. A)** The genomic map of the relevant locus is shown for the **A**) H37Δ*ami1* strain B) H37Δ*ami4* strain and the wild-type H37Rv strain. The probe used for hybridisation is shown as a solid green box and the expected sizes are indicated by the blue arrows. The figures are not drawn to scale. All mutant strains generated for this study and the figure above were created by Dr Sibusiso Senzani and Dr Melissa Dalcina Chengalroyen, DST/NRF Centre of Excellence for Biomedical TB Research, Faculty of Health Sciences, University of the Witwatersrand, National Health Laboratory Service, Johannesburg, 2001, South Africa.

Genotypic Validation of Amidase Mutant Strains Post Culture

Bulk experimental stocks of the amidase mutants (*Δami1* and *Δami4*), their complements (*Δami1::ami1 and Δami4::ami4*) and wild-type, H37Rv were generated from single culture aliquots in liquid broth. Previous, work showed that there was no difference in the growth rate observed between strains (Supp. Fig. 3). Post liquid culture, the fidelity of the mycobacterial strains was assessed to ensure the knockouts where still

phenotypically distinct from the complement and WT strains. To assess this, the Mtb strains were cultured on agarose gel plates for approximately two weeks. Subsequently, colonies were picked and lysed to extract the bacterial DNA. Via PCR, the genotypes of the mycobacterial strains to be used in this study were then verified (Fig. 18). For the Ami1 mutant (Fig. 18a), the knock-out possessed a single band which was approximately 750 bp large. The complemented strain possessed the expected two bands which corresponded to approximately 650 bp and 400 bp in size, respectively. Lastly, the wildtype strain possesses a single 400 bp band. Similarly, the Ami4 (Fig. 18b) mutant strain possessed a single band which was approximately 300 bp in size. The complemented strain had two bands which were approximately 300 bp and 400 bp in size. The wildtype amplicon was approximately 400 bp in size.

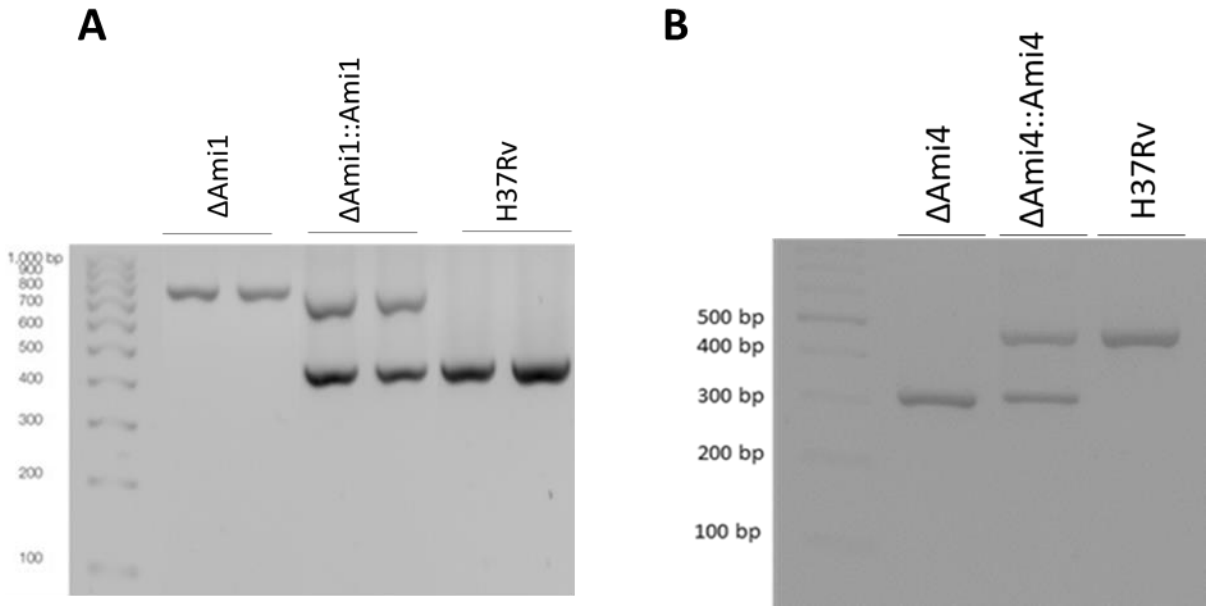

Figure 18: **Genotypic validation of experimental strains utilised in this study post high-throughput culture**. **A**) Ami1 and **B**) Ami4 mutant strains, their respective complemented strains (*Δami1*::*ami1* and *Δami4*::*ami4*) and the wild-type control, H37Rv, post stock culture.

Mtb Amidase 1 and 4 deletion mutants induce an elevated proinflammatory response in macrophages

Mutants defective for the Ami1 and Ami4 genes were generated using two-step allelic exchange mutagenesis and genotyped by PCR and Southern blot (Fig. 17a-b and Fig. 18a-b). To evaluate if Mtb amidases regulate host immune responses, the Δ*ami1* and Δ*ami4* mutants were assessed for cytokine and chemokine production in macrophages following infection. Using Cell Titer Blue assay, we observed that the cell viability of murine bone marrow-derived macrophages (BMDM) was not affected following infection with either Δ*ami1* and Δ*ami4* mutants when compared to the wild-type Mtb H37Rv and genetically complemented strains (Fig. 19a-b). Furthermore, both mutants were equally sensitive to the IFNγ-induced antimicrobial activity of BMDMs

relative to the wild-type and *Δami1* complemented strain as measured by classical colony-forming unit (CFU) enumerations (Fig. 19c-d). The Δ*ami1* mutant infection in BMDMs induced a prominently proinflammatory cytokine response through increased secretion of IL-1α, IL-6, and IL-12p40 (Fig. 20a). In addition, the CCL2 chemokine, responsible for monocyte recruitment [261], was significantly increased in the Mtb Δ*ami1* mutant infection when compared to the wild type or genetically complemented strains (Fig. 20a). Similarly, infection of BMDMs with the Mtb Δ*ami4* mutant resulted in significantly increased production of IL-1α, IL-1β, IL-6, and IL-12p40 (Fig. 20b). Together, these results demonstrate that Ami1 and Ami4 are dispensable for growth in macrophages. However, the deletion of either Mtb amidases can induce increased proinflammatory cytokine and chemokine responses during macrophage infection.

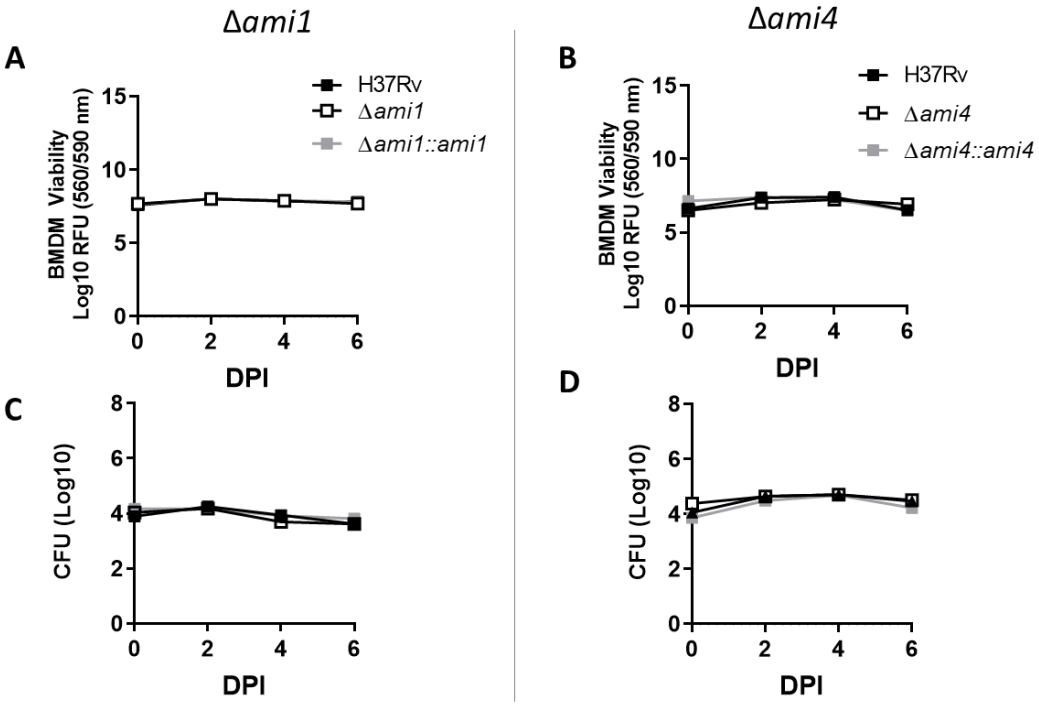

Figure 19: **Mtb infection of macrophages with the *Δami1* and *Δami4* mutant has no effect on macrophage cell viability and intracellular Mtb growth. A, B**) Cell viability of BMDM infected with the Ami mutants (*Δami1* and *Δami4*), complemented strains (*Δami1*::*ami1* and *Δami4*::*ami4*) and wild-type H37Rv was measured via Cell Titer Blue at 0 (4 hours), 2, 4 and 6-days post-infection. **C, D**) CFU counts of BMDMs infected with the *Ami* mutants (*Δami1* and *Δami4*), complemented strains (*Δami1*::*ami1* and *Δami4*::*ami4*) and wild-type H37Rv at 0 (4 hours), 2, 4 and 6-days post-infection (*P ≤ 0.05, **P ≤ 0.01, ***P ≤ 0.001, ****P ≤ 0.0001, one-way ANOVA, n=3). DPI=days post-infection.

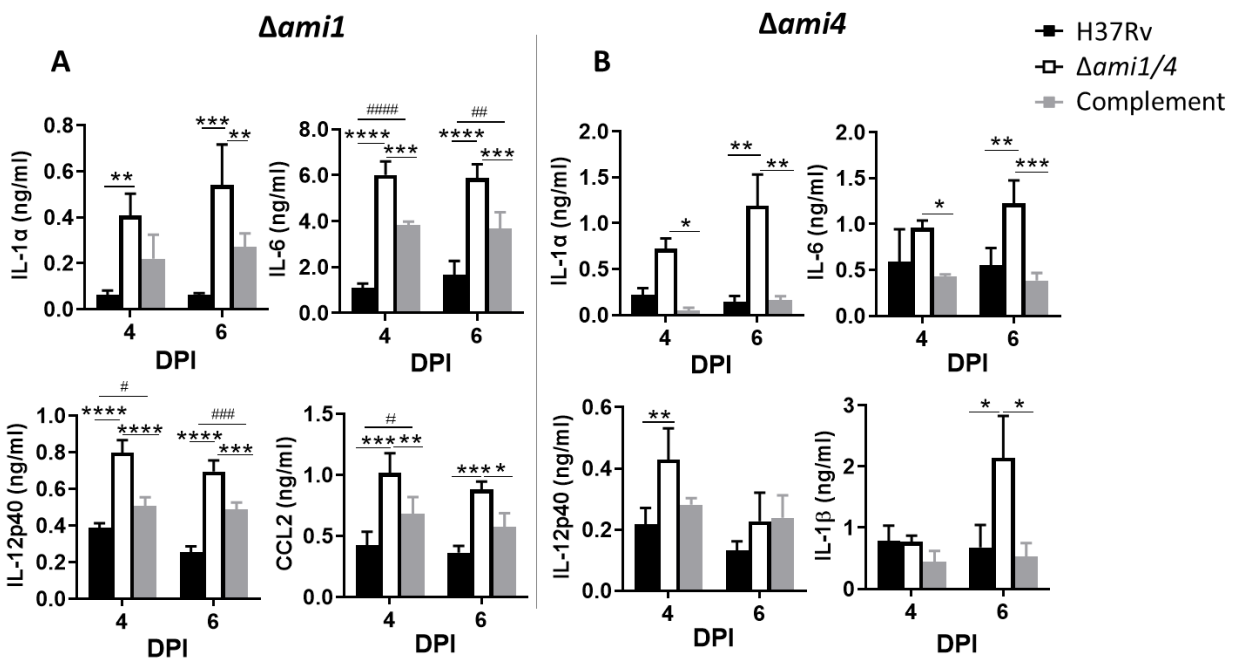

Figure 20: **Mtb infection of macrophages with the *Δami1* and *Δami4* mutant induces a heightened proinflammatory response.** At 4- and 6-days post-infection, the proinflammatory cytokine and chemokine production of infected macrophages was measured via ELISA using **A**) Δ*ami1, Δami1*::*ami1* and *Δami1*::*ami1* and H37RV and **B**) *Δami4, Δami4*::*ami4* and H37RV. * = *Δami1/4* vs. WT, # = complemented strains vs. WT (*/#P ≤ 0.05, **/##P ≤ 0.01, ***/###P ≤ 0.001, ****/####P ≤ 0.0001, one-way ANOVA, n=3). DPI=days post-infection.

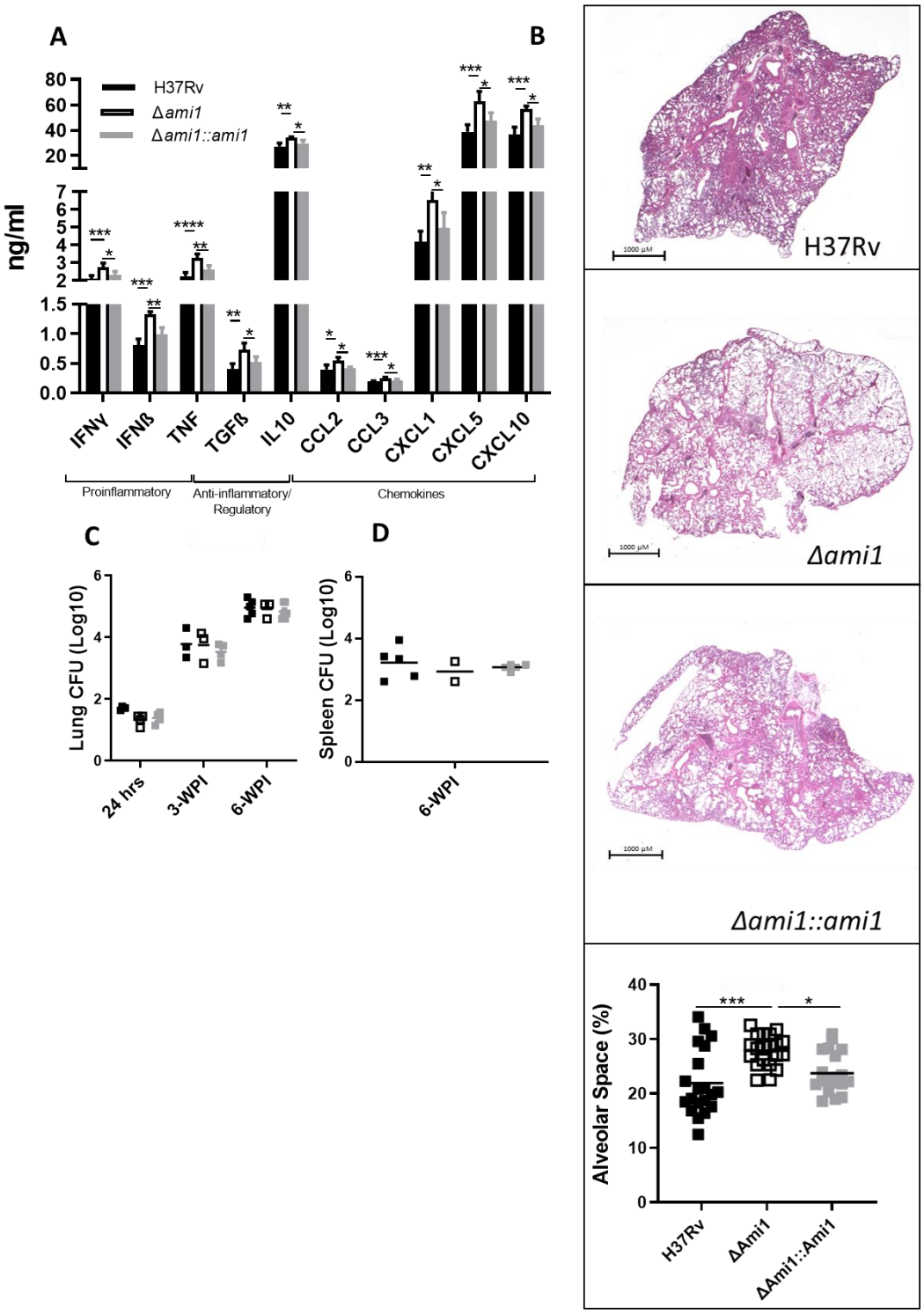

Figure 21: **Infection of mice with the *Δami1* mutant displays immune response at 3-WPI which is absent at 6-WPI.** C57BL/6 male mice were infected intranasally with 100-CFU of the Mtb Δ*ami1* mutant, complemented *Δami1*::*ami1* and WT, H37Rv. At 3-WPI infected mice were sacrificed and the lungs were collected to quantify **A)** Cytokine and chemokine levels from whole lung homogenate of Mtb-infected mice were measured by ELISA **B)** H&E histology staining of Mtb-infected lungs at 3-WPI. Inflammation was quantified as a measure of alveolar space. Scale bars = 1000 µm **C**, **D**) At 3- and 6-WPI infected mice were sacrificed to measure mycobacterial burden by CFU enumeration in the lungs and spleen (*P ≤ 0.05, **P ≤ 0.01, ***P ≤ 0.001, ****P ≤ 0.0001, one-way ANOVA, n=5-6). WPI=weeks post-infection.

Mtb Ami1 knockout results in a heightened acute immune response which is subsequently lost during chronic phase infection in mice

To investigate if the elevated pro-inflammatory responses elicited by the amidase 1 and 4 deletion Mtb mutants during macrophage infection translate to elevated immune responses *in vivo*, we infected C57BL/6 mice intranasally with the Mtb *Δami1* or *Δami4* mutant strains. In the acute phase, at 3-weeks post-infection (WPI), the *Δami1* mutants significantly increased the production of several proinflammatory cytokines (IFNγ and TNF), type 1 interferon (IFNβ), regulatory cytokines (TGFβ and IL-10), and chemokines (CCL2, CCL3, CXCL1, CXCL5, and CXCL10) in whole lung homogenates when compared to the *Δami1* complemented and WT H37Rv Mtb strains (Fig. 21a). Interestingly, Mtb *Δami1* mutants displayed reduced pulmonary histopathology, as measured by percentage alveolar spaces relative to the *Δami1* complemented and WT H37Rv Mtb strain (Fig. 21b). Despite the increased inflammatory cytokine and chemokine responses at 3-WPI, the mycobacterial growth rates of *Δami1* in the lungs and the spleen were similar to the *Δami1* complemented and WT H37Rv Mtb strains as measured by classical CFU enumerations at 3- and 6-weeks post-infection (Fig. 21c and d). Using flow cytometry, we measured numerous immune cell populations in the lungs at 3-weeks post-infection and determined that Mtb *Δami1* infection significantly exhibited decreased percentage of alveolar macrophages, CD11b DCs, neutrophils and monocytes (Fig. 22a) with a concomitant decrease in total CD4 cells, CD8 cells, effector $CD4^+$ as well as naïve, effector and memory $CD8^+$ T cells (Fig. 22c) when compared to WT Mtb. Within the mediastinal lymph node (LN), at 3-WPI, Mtb *Δami1* mutant infection resulted in an increased frequency of B cells (Fig. 23a). However, when calculated for total cell numbers within the lung and mediastinal lymph node, no measurable difference in cellular recruitment was observed between the groups (Fig. 22b, d and 23b). At 6-weeks post-infection, the percentages and numbers of cell populations (Fig. 25a-d, 26a,b), cytokine and chemokine expression, histopathology and percentage of alveolar spaces (Fig. 24a-c) were similar between the *Δami1* mutants, *Δami1* complement and wild-type H37Rv Mtb strains.

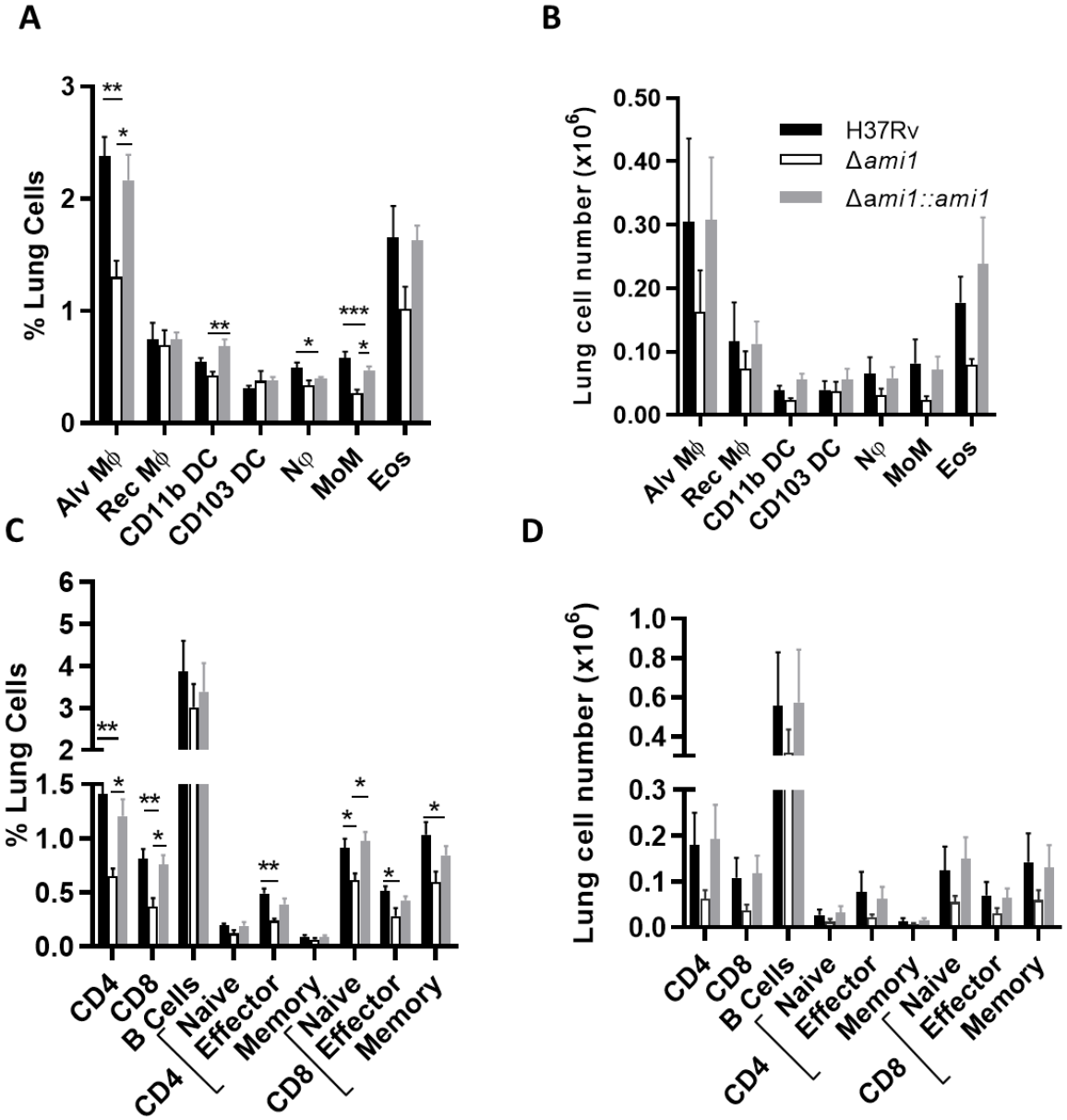

Figure 22: **At 3-WPI, *Δami1* mutant infection in mice reduces specific myeloid and lymphoid cell populations in the lung.** C57BL/6 male mice were infected intranasally with 100 CFU of *Δami1* mutants, *Δami1::ami1* and wild-type H37Rv. Infected mice were sacrificed at 3-WPI and lungs were collected to measure the frequency and cell numbers of **A, B)** myeloid and **C, D)** lymphoid cell populations. Cell surface markers used: Alveolar Mph (Alv MΦ) = $SiglecF^+CD11c^+$, recruited Mph (Rec MΦ) = $CD11c^+$ $SiglecF^-$, CD103 DCs = $MHCII^+CD11c^+CD103^+CD11b^-$, CD11b DCs = $MHCII^+CD11c^+CD103^+CD11b^+$, neutrophils (Nϕ) = $LY6G^+CD11b^+$, MoMs = $CD11b^+CD11c^+$, EOS = $SiglecF^+CD11b^+$, B cells = $CD19^+CD3^-$, $CD8^+$ T cells = $CD3^+CD4^-CD8^+$, $CD4^+$ T cells = $CD3+CD4^+CD8^-$, Naïve T cells = $CD62L^+CD44^+$, Memory = $CD62L^+CD44^-$ Effector = $CD62L^-CD44^+$(**P ≤ 0.01, ***P ≤ 0.001, one-way ANOVA, n=5-6).

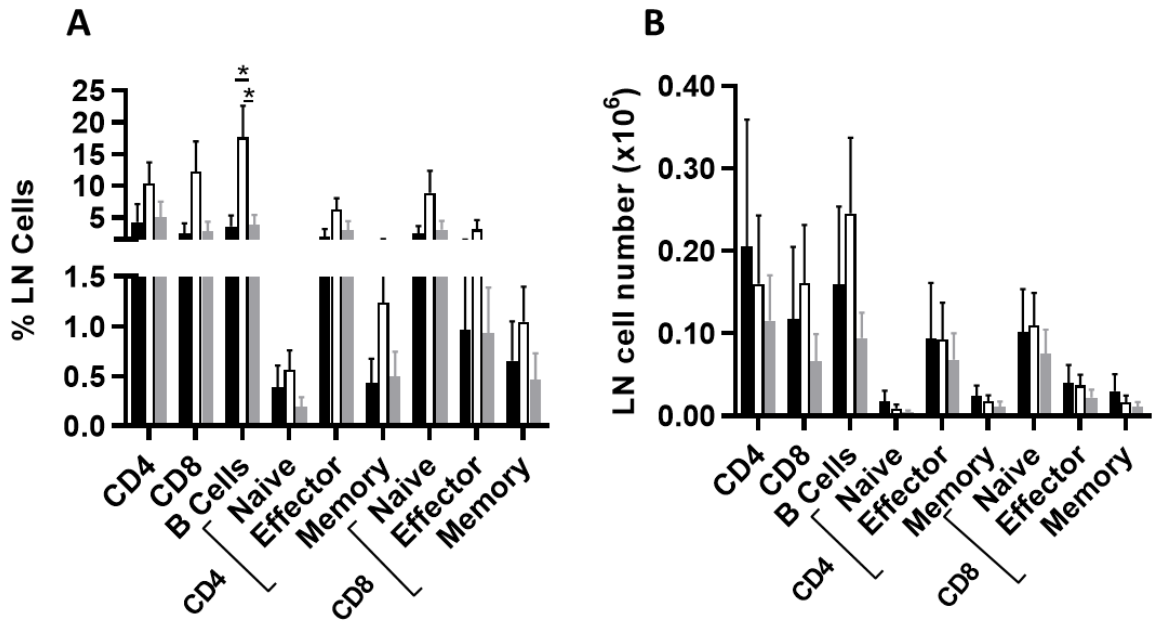

Figure 23: **At 3-WPI, *Δami1* mutant infection in mice recruits B cells in the mediastinal lymph node.** C57BL/6 male mice were infected intranasally with 100 CFU of *Δami1* mutants, *Δami1::ami1* and wild-type H37Rv. Infected mice were sacrificed at 3-WPI. **A, B)** The mediastinal lymph nodes were collected to determine the frequency and cell numbers of lymphoid populations. Cell surface markers used: B cells = $CD19^{+}CD3^{-}$, $CD8^{+}$ T cells = $CD3^{+}CD4^{-}CD8^{+}$, $CD4^{+}$ T cells = $CD3+CD4^{+}CD8^{-}$, Naïve T cells = $CD62L^{+}CD44^{+}$, Memory = $CD62L^{+}CD44^{-}$ Effector = $CD62L^{-}CD44^{+}$ (**P ≤ 0.01, ***P ≤ 0.001, one-way ANOVA, n=5-6).

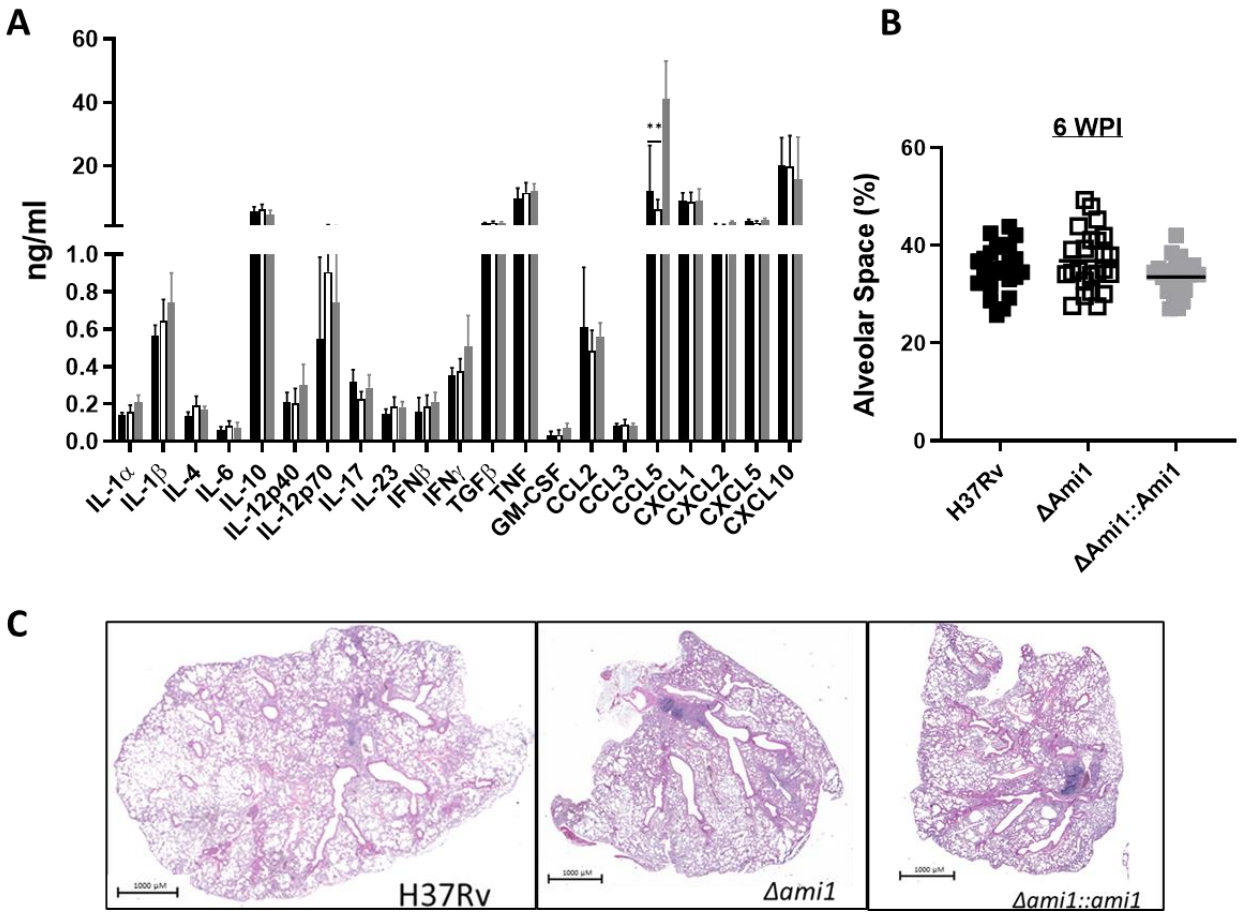

Figure 24: **At 6-WPI, *Δami1* mutant infection in mice induces similar inflammation in mice relative to wild-type.** Infected male mice were sacrificed at 6-WPI and the lungs were collected to quantify the A**)** Cytokine and chemokine levels from whole lung homogenate of Mtb-infected mice were measured by ELISA. **B**) Lung inflammation at 6-WPI was quantified as a measure of alveolar space from **C**) H&E-stained infected lungs. Scale bars = 1000 µm (**P ≤ 0.01, one-way ANOVA, n=5-6)

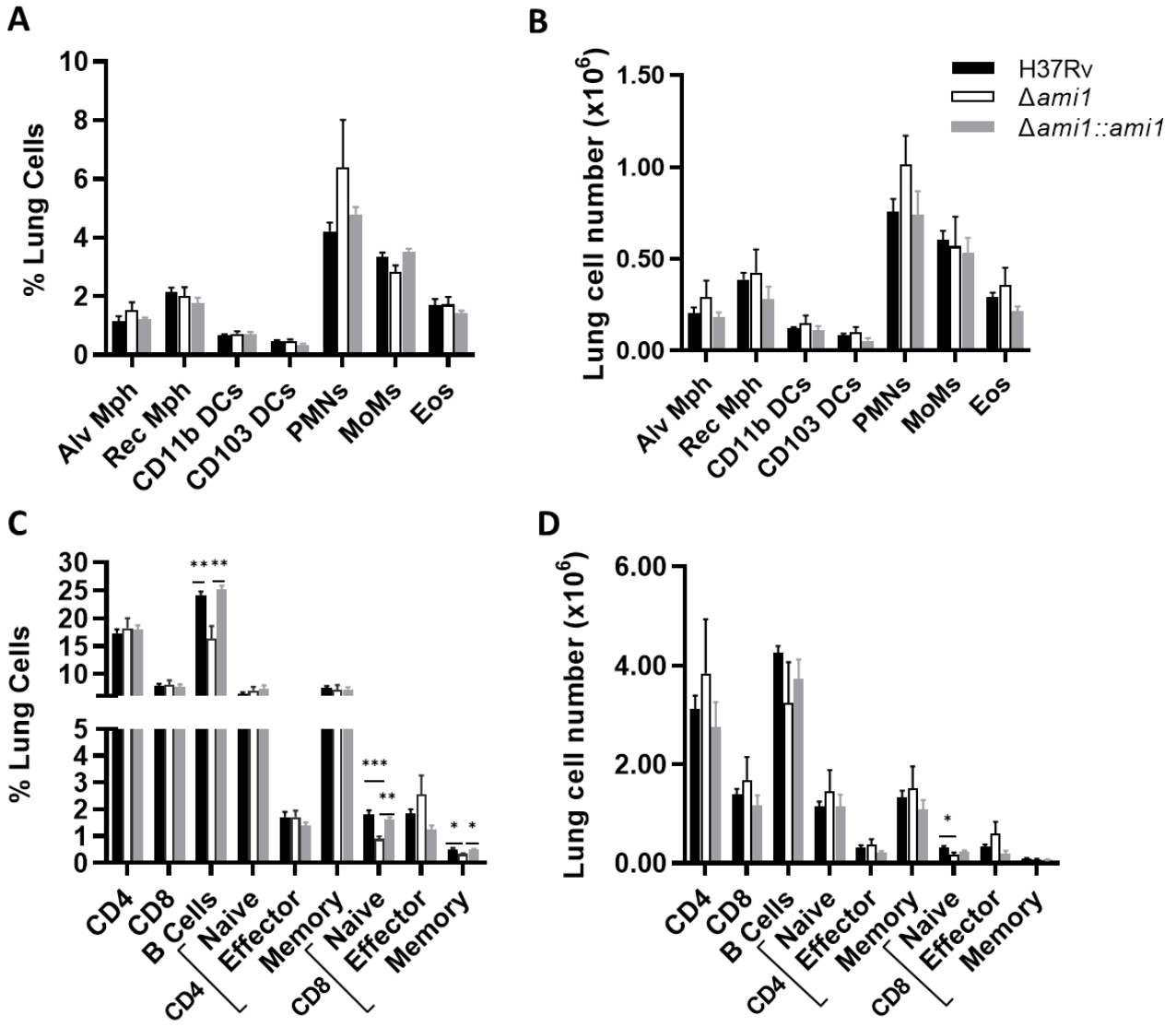

Figure 25: **At 6-WPI, Ami1 deletion induces similar myeloid cell populations in the lung.** C57BL/6 male mice were infected intranasally with 100 CFU of *Δami1* mutants, *Δami1*::*ami1* and wild-type H37Rv. Infected mice were sacrificed at 6-WPI and lungs were collected to measure the frequency and cell numbers of **A, B)** myeloid and **C, D)** lymphoid cell populations. Alveolar Mph (Alv MΦ) = SiglecF$^+$CD11c$^+$, recruited Mph (Rec MΦ) = CD11c$^+$ SiglecF$^-$, CD103 DCs = MHCII$^+$CD11c$^+$CD103$^+$CD11b$^-$, CD11b DCs = MHCII$^+$CD11c$^+$CD103$^+$CD11b$^+$, neutrophils (Nϕ) = LY6G$^+$CD11b$^+$, MoMs = CD11b$^+$CD11c$^+$, EOS = SiglecF$^+$CD11b$^+$, B cells = CD19$^+$CD3$^-$, CD8$^+$ T cells = CD3$^+$CD4$^-$CD8$^+$, CD4$^+$ T cells = CD3+CD4$^+$CD8$^-$, Naïve T cells = CD62L$^+$CD44$^+$, Memory = CD62L$^+$CD44$^-$ Effector = CD62L$^-$CD44$^+$(**P ≤ 0.01, ***P ≤ 0.001, one-way ANOVA, n=5-6).

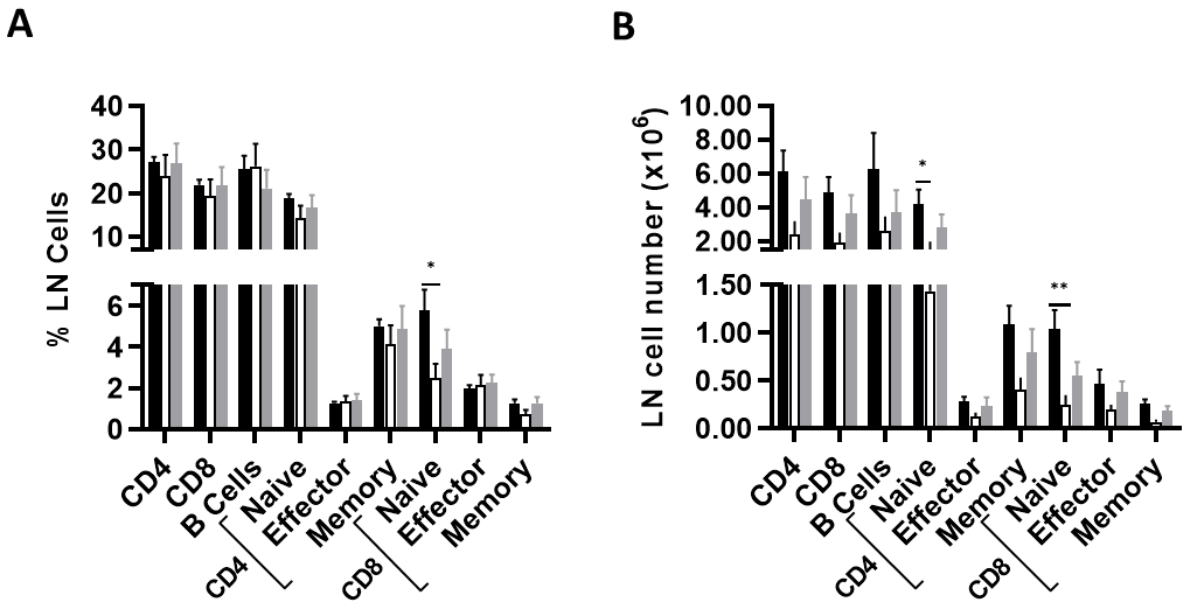

Figure 26: **At 6-WPI, Ami1 deletion results in marginally decreased lymphoid cells within the mediastinal lymph node.** C57BL/6 male mice were infected intranasally with 100 CFU of *Δami1* mutants, *Δami1*::*ami1* and wild-type H37Rv. Infected mice were sacrificed at 6-WPI. **A, B)** Mediastinal lymph nodes were collected to determine the frequency and cell numbers of lymphoid populations. B cells = $CD19^{+}CD3^{-}$, CD8 T cells = $CD3^{+}CD4^{-}CD8^{+}$, CD4 T cells = $CD3+CD4^{+}CD8^{-}$, Naïve T cells = $CD62L^{+}CD44^{+}$, Memory = $CD62L^{+}CD44^{-}$ Effector = $CD62L^{-}CD44^{+}$ (*P ≤ 0.05, **P ≤ 0.01, ***P ≤ 0.001, one-way ANOVA, n=5-6).

Ami4 deletion does not affect the host immune response during acute and chronic Mtb infection

We further investigated the acute and chronic host immune response to Mtb Ami4 deficiency using the *Δami4* mutants. The bacterial burden (Fig. 27a), inflammation assessed by histopathology (Fig. 27b) and cytokine/chemokine expression (Fig. 27c-d) were similar between all groups. In the lung, at 3-WPI, Ami4 deletion elicited decreased percentages of alveolar macrophages, CD11b DCs, CD103 DCs, monocytes and eosinophils (Fig. 28a). Additionally, within the lung, a reduction in $CD8^{+}$, B cells, naïve & memory $CD4^{+}$, as well as reduction in naïve CD8+T cells, was overserved when compared to WT Mtb (Fig. 28a and c). Further, within the lymph node at 3-WPI, Ami4 deletion elicited decreased naïve and memory $CD4^{+}$- and $CD8^{+}$T cells by percentages when compared to WT Mtb (Fig. 29a). However, when calculated for total cell numbers within the lung and mediastinal lymph node, no measurable difference in cellular recruitment was observed between the groups. At 6-WPI, within the lung, Ami4 deletion elicited decreased alveolar macrophages, memory $CD4^{+}$ and $CD8^{+}$ T cells with a concomitant increase in total $CD4^{+}$-, $CD8^{+}$ T cells and naïve $CD4^{+}$T cells and effector CD8+ T cells by percentage when compared to WT Mtb (Fig. 30a and c). Within the lymph node, Ami4 deletion elicited increased effector $CD4^{+}$T cells by percentages when compared to WT Mtb (Fig 31e). However, when calculated for total cell numbers within the lung and mediastinal lymph node, no measurable difference in

cellular recruitment was observed between the groups, except for reduced memory $CD4^+$- and $CD8^+$T cells. Together, these data imply that whilst Mtb Ami1 is more immunomodulatory relative to Ami4, the deletion of either gene can slightly alter cellular recruitment in lung and lymph node but is, ultimately, insufficient to ameliorate the disease progression at 3- and 6-weeks post-infection.

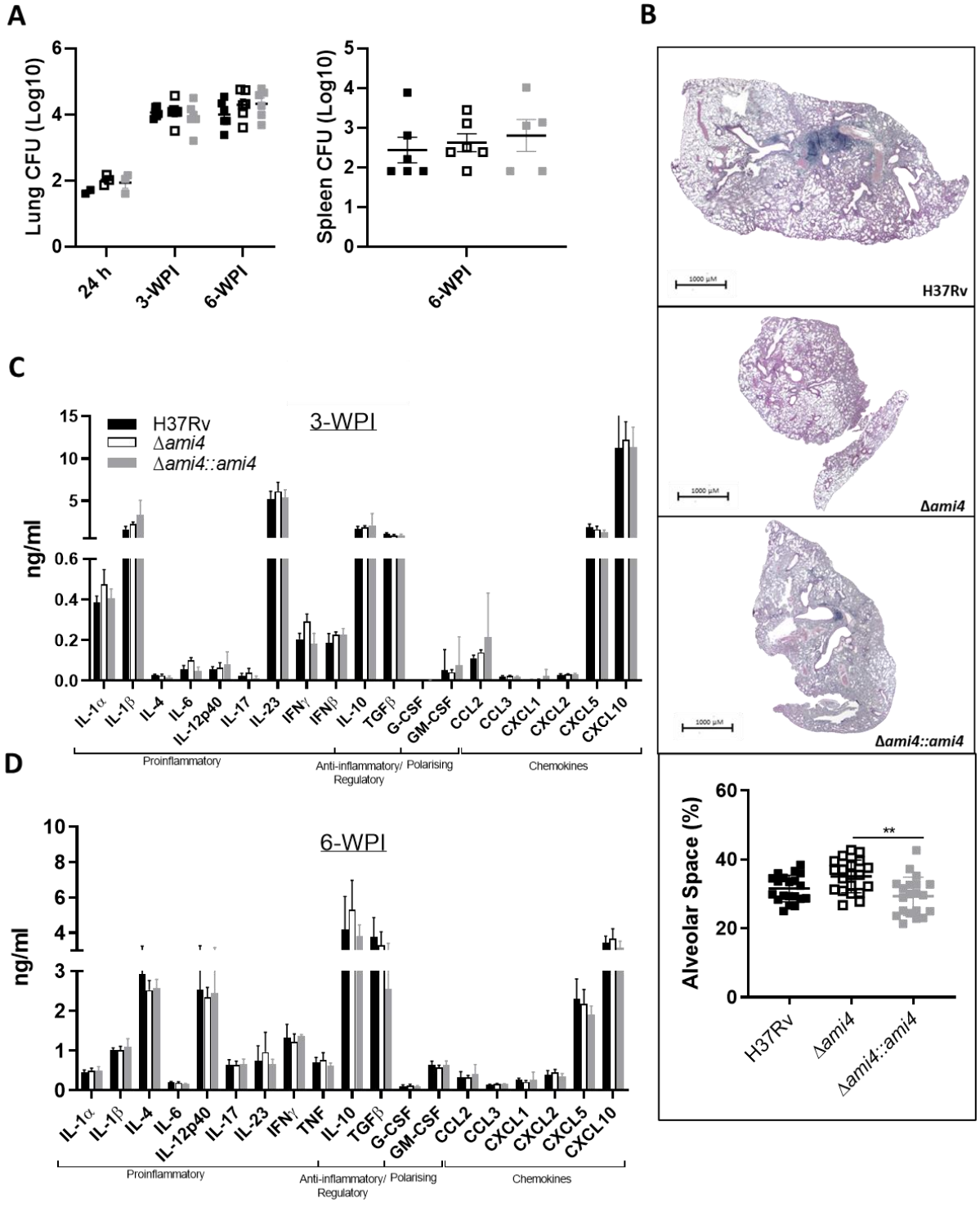

Figure 27: **Mtb Ami4 is dispensable for the modulation of the host immune response during acute and chronic phase infection in mice.** C57BL/6 male mice were infected intranasally with 100 CFU of the *Δami4* mutant, *Δami4*::*ami4* and H37Rv. **A)** Infected mice were sacrificed at 3- and 6-WPI to measure mycobacterial burden by CFU enumeration in the lungs and spleen. **B**) General inflammation in the lung was assessed via the lung-weight index. Cytokine and chemokine levels from whole lung homogenate of Mtb-infected mice were measured by ELISA at **C)** 3-WPI and **D)** 6-WPI (n=5-6).

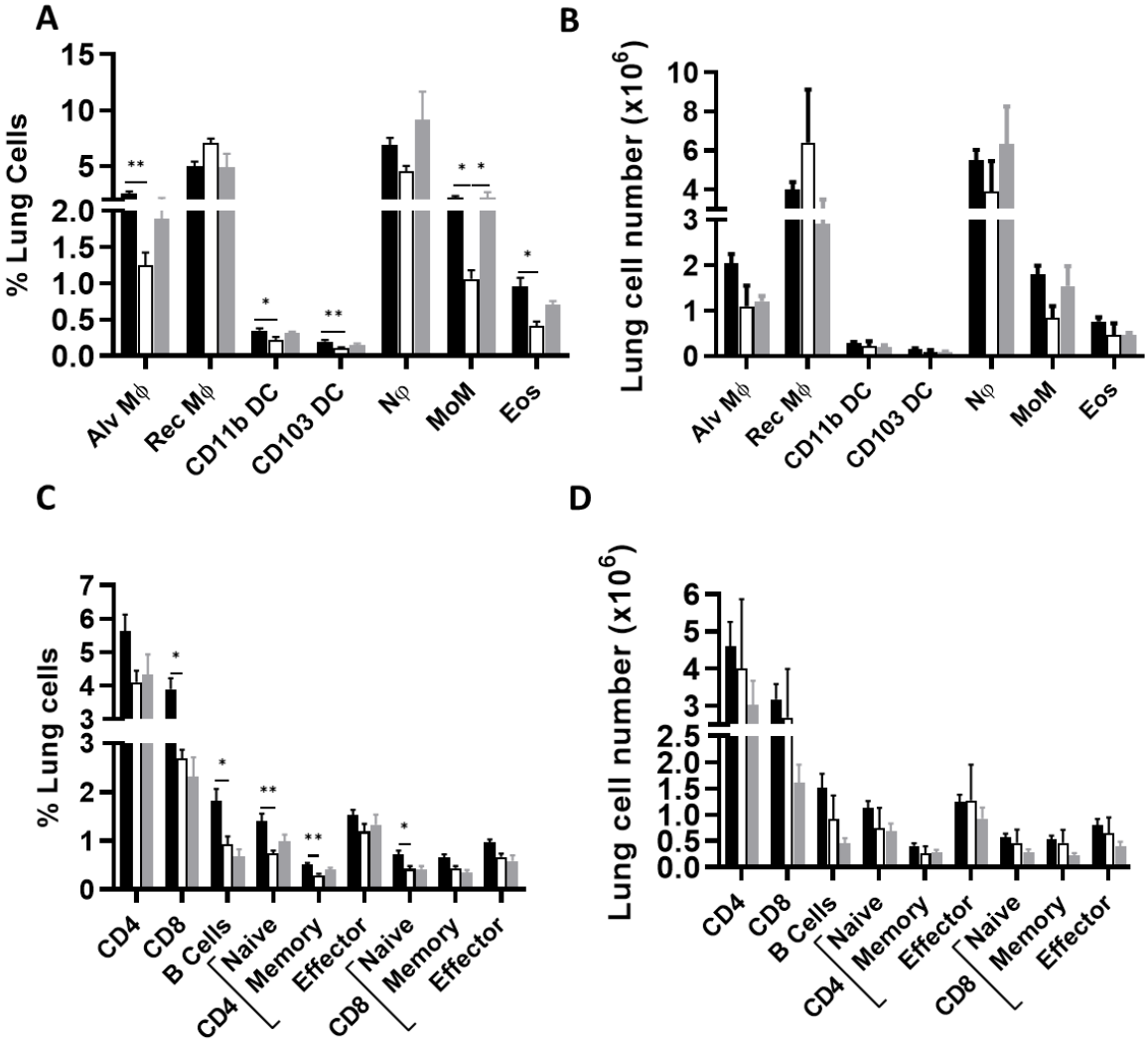

Figure 28*:* **At 3-WPI, *Δami4* mutant infection in mice reduces specific cell populations within the lung.** C57BL/6 male mice were infected intranasally with 100 CFU of the *Δami4* mutant, *Δami4*:: *ami4* and wild-type H37Rv. Infected mice were sacrificed at 6-WPI and lungs were collected to measure the frequency and cell numbers of **A, B)** myeloid and **C, D)** lymphoid cell populations. Alveolar Mph (Alv MΦ) = SiglecF$^+$CD11c$^+$, recruited Mph (Rec MΦ) = CD11c$^+$ SiglecF$^-$, CD103 DCs = MHCII$^+$CD11c$^+$CD103$^+$CD11b$^-$, CD11b DCs = MHCII$^+$CD11c$^+$CD103$^+$CD11b$^+$, neutrophils (Nϕ) = LY6G$^+$CD11b$^+$, MoMs = CD11b$^+$CD11c$^+$, EOS = SiglecF$^+$CD11b$^+$, B cells = CD19$^+$CD3$^-$, CD8$^+$ T cells = CD3$^+$CD4$^-$CD8$^+$, CD4$^+$ T cells = CD3+CD4$^+$CD8$^-$, Naïve T cells = CD62L$^+$CD44$^+$, Memory = CD62L$^+$CD44$^-$ Effector = CD62L$^-$CD44$^+$(**P ≤ 0.01, ***P ≤ 0.001, one-way ANOVA, n=5-6).

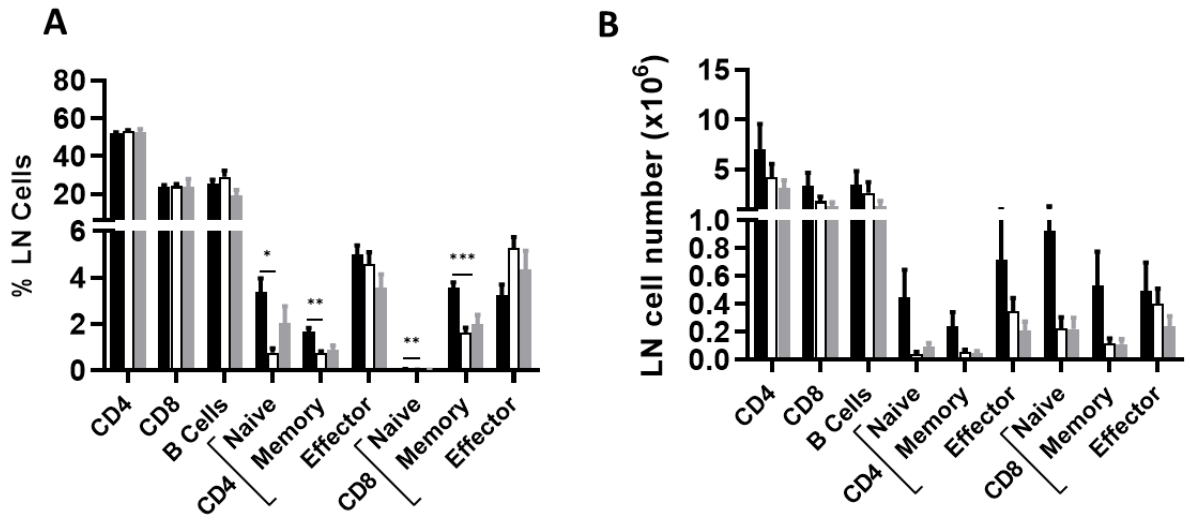

Figure 29: **At 3-WPI, *Δami4* mutant infection in mice reduces specific cell populations within the mediastinal lymph node.** Infected male mice were sacrificed at 3-WPI and the mediastinal lymph nodes were collected to determine the **A,** frequency and **B)** cell numbers of lymphoid populations. B cells = $CD19^{+}CD3^{-}$, CD8 T cells = $CD3^{+}CD4^{-}CD8^{+}$, $CD4^{+}$ T cells = $CD3^{+}CD4^{+}CD8^{-}$, Naïve T cells = $CD62L^{+}CD44^{+}$, Memory = $CD62L^{+}CD44^{-}$ Effector = $CD62L^{-}CD44^{+}$ ($*P \leq 0.05$, $**P \leq 0.01$, $***P \leq 0.001$, one-way ANOVA, n=5-6).

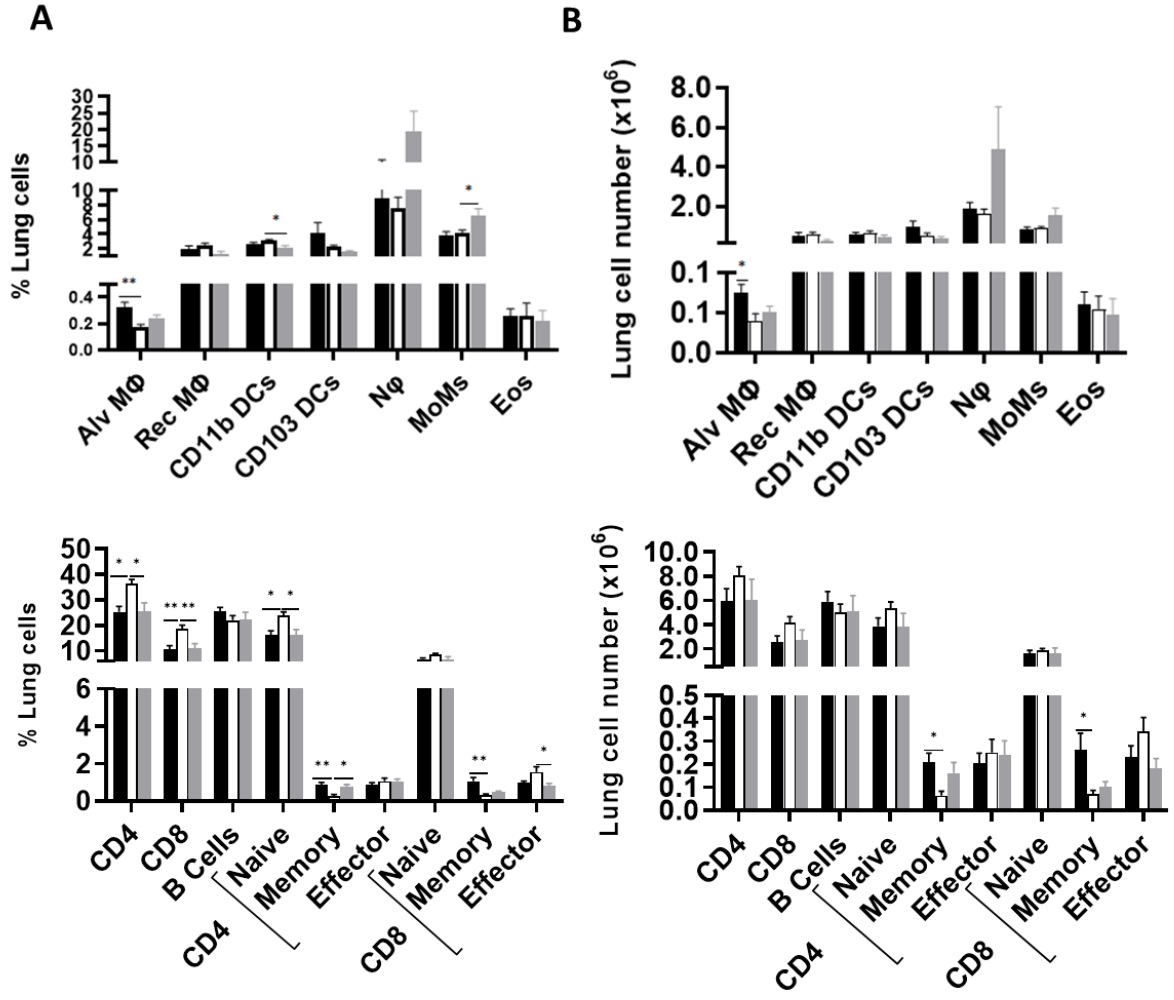

Figure 30: **At 6-WPI, *Δami4* mutant infection in mice induces lymphoid cells within the lung.** C57BL/6 male mice were infected intranasally with 100 CFU of the *Δami4* mutant, *Δami4*::*ami4* and wild-type H37Rv. Infected mice were sacrificed at 6-WPI and the lungs were collected to measure the frequency and cell numbers of **A, B)** myeloid and **C, D)** lymphoid cell populations. **E, F)** Mediastinal lymph nodes were collected to determine the frequency and cell numbers of lymphoid populations. Alveolar Mph (Alv MΦ) = SiglecF$^+$CD11c$^+$, recruited Mph (Rec MΦ) = CD11c$^+$ SiglecF$^-$, CD103 DCs = MHCII$^+$CD11c$^+$CD103$^+$CD11b$^-$, CD11b DCs = MHCII$^+$CD11c$^+$CD103$^+$CD11b$^+$, neutrophils (Nϕ) = LY6G$^+$CD11b$^+$, MoMs = CD11b$^+$CD11c$^+$, EOS = SiglecF$^+$CD11b$^+$, B cells = CD19$^+$CD3$^-$, CD8$^+$ T cells = CD3$^+$CD4$^-$CD8$^+$, CD4$^+$ T cells = CD3+CD4$^+$CD8$^-$, Naïve T cells = CD62L$^+$CD44$^+$, Memory = CD62L$^+$CD44$^-$ Effector = CD62L$^-$CD44$^+$(**P ≤ 0.01, ***P ≤ 0.001, one-way ANOVA, n=5-6).

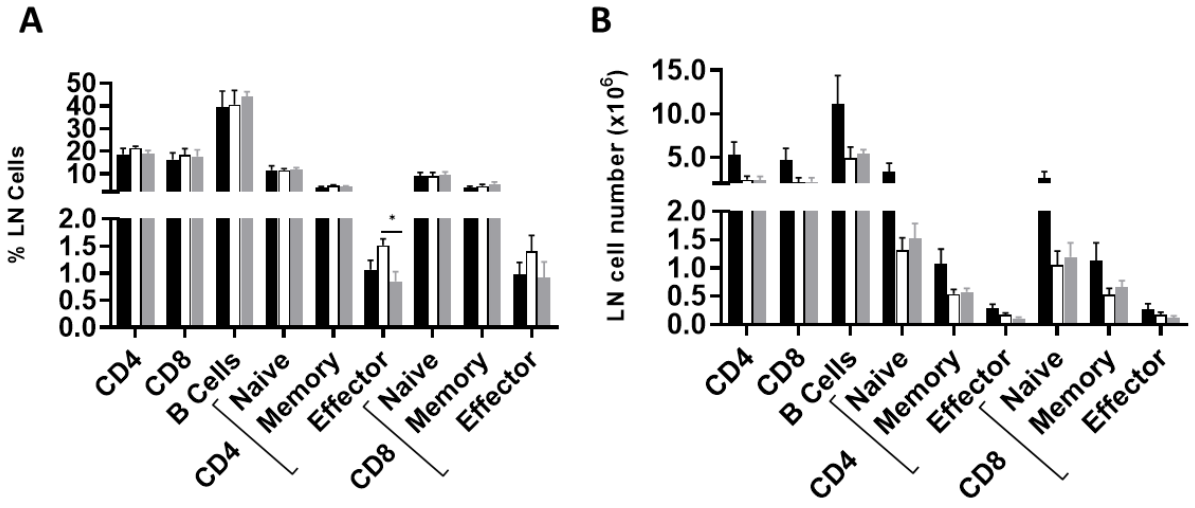

Figure 31: **At 6-WPI, *Δami4* mutant infection in mice induces effector CD4⁺ T cells within the mediastinal lymph node.** C57BL/6 male mice were infected intranasally with 100 CFU of the *Δami4* mutant, *Δami4*:: *ami4* and wild-type H37Rv. Infected mice were sacrificed at 6-WPI and the mediastinal lymph nodes were collected to quantify the **A)** frequency and **B)** cell numbers of lymphoid cells within the mediastinal lymph node. B cells = $CD19^+CD3^-$, $CD8^+$ T cells = $CD3^+CD4^-CD8^+$, CD4 T cells = $CD3+CD4^+CD8^-$, Naïve T cells = $CD62L^+CD44^+$, Memory = $CD62L^+CD44^-$ Effector = $CD62L^-CD44^+$ (*P ≤ 0.05, **P ≤ 0.01 one-way ANOVA, n=5-6).

Mtb Ami1 deficiency, but not Ami4, results in an increased sensitivity to anti-TB drugs in liquid culture which is abrogated during macrophage infection

Mycobacterial Ami1 deletion has been shown to confer antibiotic sensitivity to antimycobacterial drugs in *M. smegmatis* and Mtb models [99, 174]. To investigate if Mtb strains deficient in Ami1 and Ami4 alter their susceptibility to antibiotics, constitutively mCherry expressing Mtb *Δami1* mutants, Mtb *Δami1* complemented and wild-type Mtb H37Rv were cultured in the presence of the anti-TB drugs isoniazid, rifampicin, meropenem and pyrazinamide. Mycobacterial viability was assessed fluorometrically via AlamarBlue within 8-days of liquid culture. In line with the previously published results on the antibiotic sensitivity of Ami1 deficient mutant in *M. smegmatis* [174], Mtb *Δami1* mutants were found to be sensitive to antibiotic exposure in liquid broth culture. Here, the Mtb *Δami1* mutants displayed heightened sensitivity to isoniazid and meropenem (Fig. 32a). However, within macrophages, *Δami1* mutants were found to be equally susceptible to rifampicin and isoniazid as when compared to *Δami1* complemented and WT H37Rv Mtb strains (Fig. 32b). Further, the *Δami4* Mtb mutants were found to be equally susceptible to all drugs when assessed in liquid culture (Fig. 33). Together, these data imply that the presence of Ami1 in Mtb may contribute to a tolerance phenotype to isoniazid and meropenem when exposed to antibiotic stress in liquid growth culture, but not during macrophage infection.

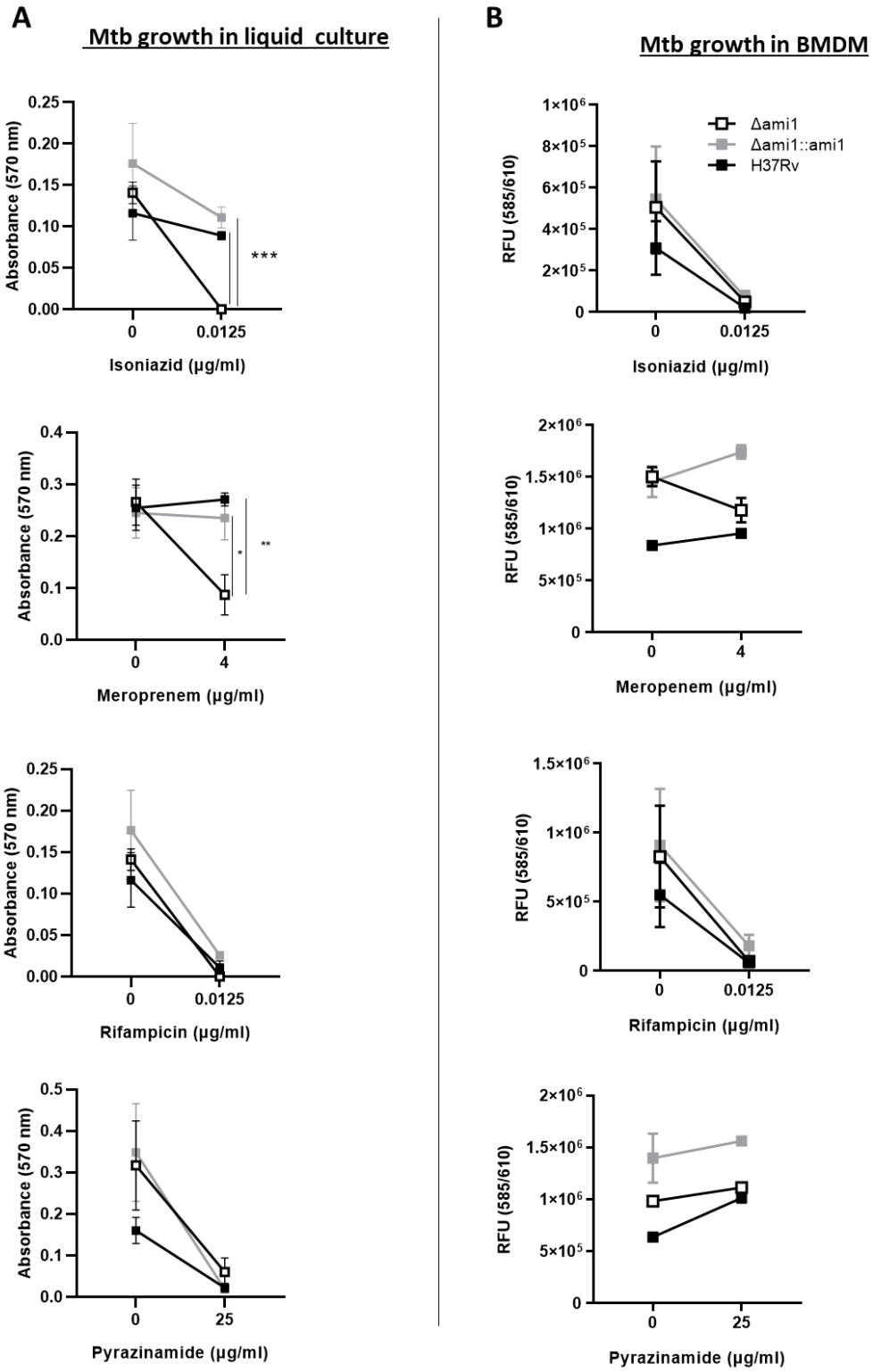

Figure 32: **Increased sensitivity of Mtb *Δami1* mutant to isoniazid and meropenem antibiotics in liquid culture. A)** The *Δami1* mutant, *Δami1*::*ami1* and wild-type H37Rv Mtb strains were cultured in 7H9 liquid broth culture for 14-days in the presence of isoniazid, rifampicin, meropenem or pyrazinamide. **B)** BMDMs were infected with a mCherry expressing *Δami1* mutant, *Δami1*: *ami1* and wild-type H37Rv Mtb strains. Isoniazid, rifampicin, meropenem or pyrazinamide were added 4-hours post-infection and macrophages were culture for 8-days to measure the fluorescence of Mtb strains (*P ≤ 0.05, **P ≤ 0.01, ***P ≤ 0.001, one-way ANOVA, n=3-4)

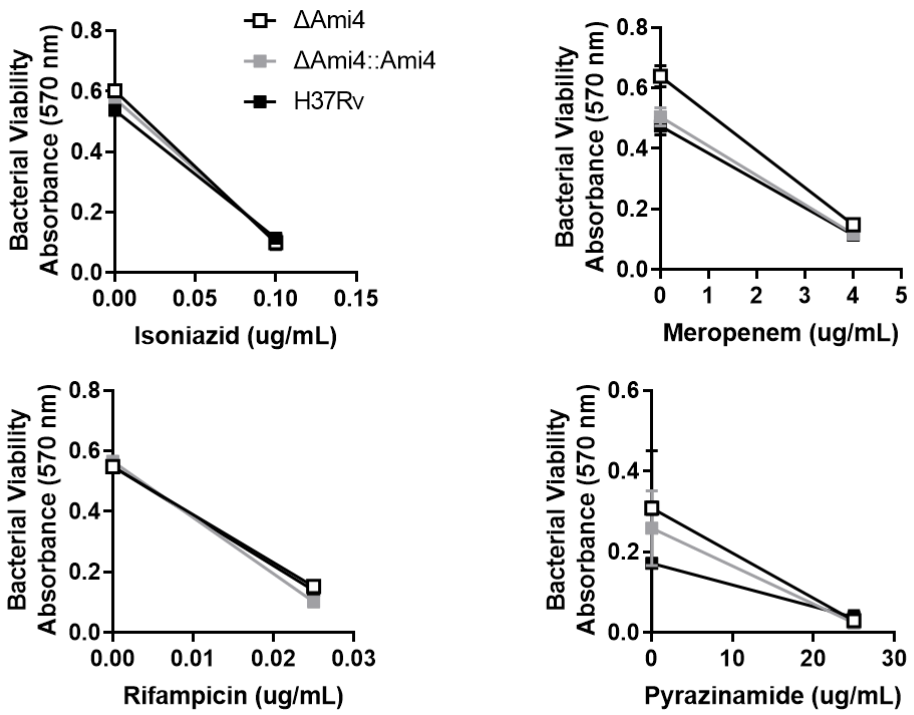

Figure 33: **The Mtb Ami4 deletion mutant is equally susceptible to antibiotics in liquid culture. The** *Δami4* mutant, *Δami4*::*ami4* and wild-type H37Rv Mtb strains were cultured in 7H9 liquid broth culture for 14-days in the presence of isoniazid, rifampicin, meropenem or pyrazinamide (*P ≤ 0.05, **P ≤ 0.01, ***P ≤ 0.001, one-way ANOVA, n=3-4)

Ami1 deficiency increases the resistance of Mtb to isoniazid single treatment in mice

Previously, increased sensitivity to anti-TB drugs in liquid culture was reported in *M. smegmatis* Ami1 deleted mutants [99, 174] We have also shown that *Δami1* Mtb mutants are more susceptible to antibiotic stress in liquid media (Fig. 32). However, the antibiotic susceptibility of amidase mutants *in vivo* remains to be elucidated. To test this, C57BL/6 mice were infected intranasally with Mtb *Δami1* mutants, Mtb *Δami1* complemented and wild-type Mtb H37Rv (Fig. 29). At two weeks post-infection, the drinking water was supplemented with 0.1g/L isoniazid. The mycobacterial burden in the lungs was assessed before treatment, 2- and 4-weeks post-treatment. Strikingly, after 2- and 4-weeks of isoniazid treatment, a significantly higher number of Mtb *Δami1* mutant colonies were observed when compared to *Δami1* complemented and wild-type Mtb H37Rv (Fig. 34). While no wild-type H37Rv colonies were detected following the 4-week course of antibiotics treatment (Fig. 34). Together with the axenic culture antibiotic data above (Fig. 32), the effect of Ami1 deletion within the *in vivo* model of infection resulted in a phenotypic reversal where the Ami1 mutants were observed to be tolerant to antibiotic stress.

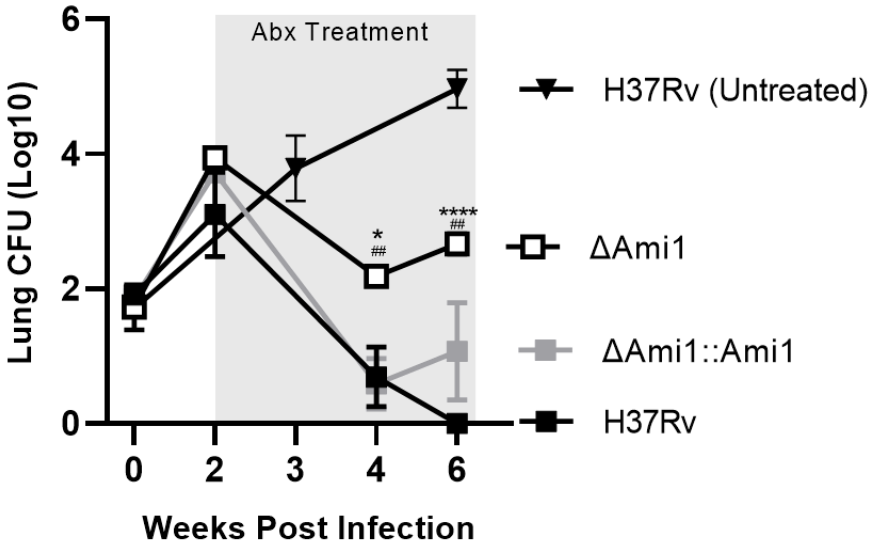

Figure 34: ***Δami1* mutants display increased tolerance to isoniazid treatment in mice.** C57BL/6 male mice were infected with *Δami1* deletion mutants, *Δami1::ami1* and H37Rv WT. At 14-days post-infection, Mtb-infected mice were treated with isoniazid (0.1g/L) in the drinking water for 14-days. **A)** Mice were sacrificed at 2- and 4-weeks post-treatment to measure bacillary counts by CFU enumerations. * = *Δami1* vs H37Rv, # = *Δami1* vs *Δami1::ami1* (*$P \leq 0.05$, $^{\#\#}P \leq 0.01$****$P \leq 0.0001$, one-way ANOVA, n=6).

4.4 Discussion

Cell wall amidases cleave the covalent bonds responsible for the stabilisation of the cell wall sacculus, thus represent potential autolytic enzymes that can be targeted for drug therapy. Further, the growth of *M. smegmatis* Ami1 deleted mutant strains in culture media resulted in the release of the mycobacterial cell wall material into the extracellular milieu [174]. In line with previous work, this material is probably highly antigenic. In the present study, we sought to elucidate the effect of Mtb amidase knockout (Ami1 and Ami4) on the host immune response. Despite the similarity of the crystal structures [171, 172] and genetic conservation between multiple species [129], few studies have fully assessed the loss-of-function effects of Mtb amidase 1 and 4 in and the host immune response. That these enzymes are so well conserved across different kingdoms and domains *implie*s that they may be intrinsic to a common pathway across these varying organisms. However, it is also possible that these enzymes may play variable and essential roles in mycobacterial ontogeny – especially during stress, such as has been observed in Ami2 [258]. Senzani et al. [174] provided evidence in *M. smegmatis* which revealed that the targeted knockout of Ami1 resulted in defective bacterial fission evident through the formation of ectopic lateral buds, the mislocalization of the cell elongasome, the bundling of the FtsZ ring and defective septal PG turnover [174]. Further, the authors also provided evidence that the Ami1 knockout *M. smegmatis* mutants experienced approximately 2x higher cell

wall permeability and were more sensitive to several antibiotics relative to the wild-type controls. In addition, Li [262], provided evidence that Ami1 knockout in *M. smegmatis* resulted in a defective ability of these filamentous mycobacteria to invade human alveolar epithelial cells [262]. In a recent *in vivo* infection study, C57BL/6 mice were infected with Ami1 deficient *M. smegmatis* mutants. Those authors displayed a diminished uptake of the mutants within the lungs, thus confirming the worsened invasion ability of these mutants observed *in vitro* [263]. Besides, the authors observed that the Ami1 deleted mutants induced less inflammation despite residing within the lungs twice as long relative to the wild-type and complemented strains before being cleared. Interestingly, this finding was verified in the Mtb model where Ami1 was found to be important to prolonging chronic Mtb infection [99].

These observations are both similar and conflicting to the results acquired in this study. Like the *M. smegmatis in vivo* model, we observed that acute phase Mtb mutant infection resulted in less inflammation by immunohistochemistry despite the increased detection of proinflammatory cytokines and chemokines relative to the complemented and wild-type strains. However, the uptake of the mutant bacilli and the final burden was unchanged relative to the complement and wild-type strains at both acute and chronic stages of infection. This implies that the invasion handicap observed in *M. smegmatis* does not occur in the Mtb model of infection. More recently Mtb Ami1 deletion mutants were tested for atypical cell division phenomena. Those authors found that under regular culture conditions, Ami1 deletion did not affect the length of daughter cells nor the number of division-septa they contained [99].

M. smegmatis is a fast-growing mycobacterial species that is both sensitive to the host immune response as well as being unable to proliferate intracellularly [263]. Conversely, Mtb is a slow-growing mycobacterial species, taking 6x longer to divide relative to *M. smegmatis.* Further, Mtb has been well studied in its ability to reside and proliferate intracellularly whilst simultaneously abrogating the antimicrobial host immune response through multiple mechanisms [82]. These key differences infer the likelihood of key differences observed in Ami1 deletion between Mtb and *M. smegmatis* models of infection. It is probable that, unlike the *M. smegmatis* model, the induction of filamentation in Mtb is highly stress-dependent and that Ami1 knockout may increase the speed to this defective phenotype only after uptake. This may explain why there is no uptake impairment within the Mtb model as the bacterial population of Ami mutants vs. the wild-type strain are phenotypically homogenous under favourable conditions. The lack of uptake impairment in Ami1-deficient Mtb mice within our study has recently been independently verified and further substantiates the hypothesis that the host immune effect of amidase deletion may only be detected/exacerbated *after* successful uptake and infection [99].

Wild-type Mtb bacilli which proliferate intracellularly within the phagosome of macrophages have been observed to exhibit filamentous bacterial chains and a dysregulated FtsZ ring phenotype [264]. Interestingly,

similar phenotypes have been observed in *Salmonella enterica* where the authors assessed the role of the AmiA and AmiC knockout - conserved orthologues of mycobacterial Ami1 and Ami4 [19]. They provided evidence showing that bacilli which were grown under low pH, high osmolarity and sublethal antimicrobial stress formed chains of cells that were more sensitive to the host immune response. Within our study, the lack of difference in bacterial burden observed between wild-type and amidase-deficient Mtb mutants may be attributed to a similar mechanism whereby the host immune milieu within the phagosome induces a filamentous phenotype in the wildtype and complemented controls to the same extent of the mutant strains at a chronic time point; thus, abrogating the potential deleterious/beneficial effect conferred by Ami1 and Ami4 knockout. This line of evidence may explain why we observe an enhanced immune response during the acute phase of *in vivo* infection with *Δami1* mutants relative to the control strains which subsequently disappears at chronic phase infection. Senzani *et al.* [174] showed that filamentous *Δami1 M. smegmatis* mutants extruded cell wall material into the cytoplasm during binary fission; this phenomenon may account for the enhanced acute immune response observed *in vitro* and *in vivo* whilst maintaining the bacterial burden in an unknown mycobacterial-specific manner. Previous studies have highlighted the importance of NOD2 in the detection and immune response to mycobacterial antigen [265, 266]. Certainly, the increased presence of PG muropeptide subunits, in the milieu has the potential to bind to NOD-like receptors and subsequently induce an enhanced proinflammatory cytokine response via canonical pathways. This may explain the increased pro-inflammatory immune response observed at 3-weeks post-infection, despite the lack of tissue inflammation.

In the present study, we assessed the sensitivity of amidase 1 and 4 knockout Mtb mutants to first-line anti-TB treatment. Mtb Ami1 knockout mutant bacilli were found to display increased sensitivity to isoniazid and meropenem relative to the complemented and wildtype controls (Fig 32a). However, within the cultured macrophages, this effect was abrogated (Fig. 32b). The apparent sensitivity of these Mtb Ami1 deletion mutants in broth has recently been independently verified [99]. In our study, the high efficacy of INH and RIF in cultured macrophages (Fig. 32b) shows that that the drugs can act on internalised Mtb, however, the lack of sensitivity observed in the Mtb *Δami1* mutant cell-free-bacilli MICs implies an innate host-pathogen interaction which neutralises the sensitivity observed in broth. Further, within the C57BL/6 mouse model, Mtb Ami1 deletion mutants were observed to be tolerant to INH treatment relative to infective controls at 4-WPI (Fig. 34). Further, this observation was significantly exacerbated at 6-WPI. This counter-intuitive phenotype-reversal which correlates with an increasingly complex host immune response under constant anti-TB drug treatments is interesting. From approximately 2-WPI, the adaptive arm of the host immune response is activated. Recruited lymphoid cells may contribute to the resistant phenotype observed in the mice infected with the mutant strain. At 6-WPI, lung inflammation between the *Δami1* mutants, complemented strains and the wild-type H37Rv infected mice is the same (Fig. 24a,b) despite a higher frequency of neutrophils and

effector CD8 cells within the lung (Fig. 25) of the mice infected with the mutant strain. This observation implies that whilst cellular recruitment is largely unchanged by Ami1 deletion, the cells have more of an effector phenotype. A similar observation of drug tolerance in the face of increased immune pressure was recently reported in 2016 [267]. In that study, the authors found that the tolerance of Mtb to anti-TB treatment was altered by the activation status of the myeloid cells isolated from the lungs of Mtb-infected mice. Within our study, we observe a heightened immune response at both *in vitro* (Fig. 20a,b) and at 3-WPI in mice infected with the Ami1 deletion mutant (Fig. 21a). Taken together, it may be possible that the increased proinflammatory response of the Ami1 deletion mutant and increased tolerance of this mutant to anti-TB therapy may be causally linked. The mixed phenotype observed in the complemented strain (Fig. 34) may be as of a consequence of the selection of plasmid-free bacilli, thus reverting the complemented stain to the knockout phenotype in the absence of hygromycin selection and resulting in increased resistance to INH treatment over the long duration of infection.

Within the phagosome, Mtb bacilli experience multiple stressors which are intended to restrict the growth of the pathogen and promote sterilisation; *viz*, hypoxia, nutrient starvation and ROS stress [268]. In 2016, Boutte *et al*. showed that CwlM, a protein homologous to mycobacterial PG amidases (Ami2) and the major substrate of PknB [259], facilitates PG synthesis activity in direct correlation to the nutrient status of the bacilli. During nutrient surplus, CwlM is activated via phosphorylation and associates with MurA, an enzyme responsible for the formation of the PG network. This association induces MurA's activity 30-fold and upregulating cell wall metabolism. However, under starvation conditions, the phosphorylation of CwlM and the subsequent association of CwlM to MurA does not occur resulting in decreased cell wall metabolism and a marked tolerance to antibiotics [258]. Ami1 may play a similar role to CwlM in Mtb, however, it is highly unlikely that Ami1 alone is responsible for the growth and maintenance of the bacterial PG sacculus. Further, other amidase isoforms may act as a complex to maintain the PG such as Heidrich *et al.*, [137] postulated from his observations in *E. coli*. In nutrient-rich, 7H9 broth and stressor-free conditions, Δ*ami1* mutant bacilli are more sensitive to INH and MER indicating possible compensatory mechanisms which may facilitate regular bacterial growth and maintenance. However, as nutrients become more limited, the knockout-effect of Ami1 may become more pronounced whilst the compensatory mechanism becomes increasingly more inefficient resulting in the induction of a tolerant phenotype despite the action of the other mycobacterial amidases.

One potential limitation of this study is that the immunological effect of Ami deletion was only analysed in male C57BL/6 mice. Recent reports have shown that male C57BL/6 mice are slightly more susceptible to Mtb infection relative to female mice [269, 270]. This observation has been correlated to secreted cytokine differences and B-cell follicle formation in the lung [269, 270]. Whilst sex-differences were not analysed in this study, they may further contribute to the immunological effects of Ami deletion reported here. The effect of sex should, therefore, be explored further in subsequent future experiments. Additionally, in Fig. 20a, some

of the *Δami1:ami1* samples induced a higher secretion of pro-inflammatory cytokines than the WT control. It is possible that any increase in elicitation of proinflammatory cytokines (IL6, IL12p40 and CCL2) may be as a possible artefact of a slightly incorrect MOI. Further, it is possible that without the selective pressure of hygromycin, the selection antibiotic under which the complemented strain was maintained in the media, the plasmid which allowed for the expression of Ami1, may have been ejected or inhibited. However, as the complement and wild-type data are largely in agreement for all subsequent experiments, I believe the artefactual dosing hypothesis to be the most likely.

In conclusion, we provide evidence describing the host immune response, both *in vitro* and *in vivo*, to two Mtb amidase knockouts; Ami1 and Ami4. *Δami1* mutant infection induced a largely pro-inflammatory immune response both *in vitro* and at 3-WPI *in vivo* relative to WT controls. However, the exacerbated host immune response was lost at 6-WPI. Neither Ami1 nor Ami4 deletion resulted in a reduction of bacterial burdens within the lung and spleen during acute and chronic phase infection. *In vitro* antibiotic studies have revealed that *Δami1* mutants were more sensitive to meropenem and isoniazid, whilst *Δami4* mutants were equally suspectable to all antibiotics tested. Interestingly, the antibiotic benefit observed under cell-free conditions is lost in macrophages and completely reversed *in vivo*. Future work elucidating this phenomenon as well as interrogating the effect of multi-amidase-knockout mutants may confer more understanding.

Chapter 4

The Optimisation and Establishment of a Dual-RNA-Seq Methodology to Detect Novel Host and *Mycobacterium tuberculosis* Transcripts from Infected Primary Macrophages.

5.1 Introduction

Tuberculosis (TB) has emerged as the world's most deleterious infectious disease effecting 1-in-4 people [21]. The etiological agent of TB, *Mycobacterium tuberculosis* (Mtb), has evolved the ability to evade the host immune response using several strategies [82]. These include the suppression of autophagy [271], phagolysosomal maturation [272-274], innate signally pathways [275], antigen processing [276] and the countering of host antimicrobial activity [277] among others. Combining these immune evasion strategies with the emergence of drug-resistant phenotypes has highlighted the need to better understand Mtb physiology and TB pathogenesis. Further, this emphasizes the need to develop novel therapeutic drug strategies that either act directly on the pathogen or fortify the host immune response to improve disease outcome. RNA sequencing (RNA-seq) is a powerful tool which has allowed researchers to better elucidate unknown cellular mechanisms in a range of organisms in a high throughput, robust fashion [278]. Among the most intricate interactions which RNA-seq can inform on, is that of between a host and pathogen during infection. During infection, a vast number of cellular processes are activated both within the host immune system and within the invading pathogen. These complex interactions are made more multifarious by the action of unknown genes, RNAs and molecules which may be contributing to immune evasion or sensitivity. Recent studies have illustrated that the unbiased interrogation of changing global transcriptional profiles within the host and pathogen remains a key method to elucidating these immune events, and may provide key knowledge to develop and refine treatment strategies [240]. *In vivo* dual RNA-seq studies are fraught with technical challenges [228]. However, a recent study utilising a dual-RNA seq methodology has been used to successfully examine the role of *in vivo* murine Mtb infection within alveolar and recruited macrophages, linked to nutritional immunity [249]. A dual RNA-seq approach is beneficial as it allows for the parallel understanding of both transcriptomic changes within the pathogen as well as the host, with both accuracy and depth.

Further, these processes are almost certainly programmed by underlying genetic changes in both the host and pathogen during pathogen challenge and subsequent host immune response. Recently, it has been shown that *Mtb* secretes two proteins (Rv1988 and Rv2966c) which directly acts on the host chromosome and promotes bacterial survival [191, 192]. However, many of the specific epigenetic changes that occur during infection and

contribute to immune evasion remain unknown. A dual-RNA seq approach has the potential to elucidate the mechanisms which occur during host-pathogen interactions. The correlation of transcriptional (RNA-seq data) with both epigenetic/histone modification (ChIP-seq) as well as DNA methylation patterns (BS-seq) data allows for the formation of strong hypotheses which can then be used to better understand the biology underpinning the host-pathogen interaction. Further, this information may elucidate novel gene targets and long non-coding RNAs for therapeutic treatment strategies.

In this study, we provide an optimised proof-of-concept methodology which allows for the extraction of host (primary human monocyte-derived-macrophages) RNA, DNA and nuclei whilst simultaneously allowing for the enrichment of pathogen (HN878) RNA from the same sample over a longitudinal time course. We show that despite low numbers of Mtb, meaningful RNA-seq data can be acquired. Combining sequence data from multiple sources we aim to explore and reconstruct the dynamics of epigenetic and transcriptional modifications, their effector proteins in human macrophages following *Mtb* infection, as well as identify associated noncoding RNAs correlated with these epigenetic changes.

5.2 Methods and Materials

5.2.1 Ethics

This study has been ethically approved for the experimentation with human tissues (MDMs) within the context of the research question detailed above (Human ethics protocol: HREC 732/2015).

5.2.2 Cells and Reagents

Leuokopaks from healthy donors, standardised for age, sex and race, were acquired from the Western Cape Blood Transfusion Service (WCBTS). Standard pathological testing is conducted by the WCBTS on all blood to ensure its free from HIV, Hepatitis B and C, and Syphilis. PBMCs are isolated via density centrifugation. $CD14^{+}CD16^{+}$ monocytes were purified via negative selection utilising the MojoSort™ Human Pan Monocyte Isolation Kit (Biolegend) and were differentiated into monocyte-derived-macrophages (MDMs) in standard RPMI media supplemented with 10% fetal calf serum and 50 ng/uL recombinant human M-CSF over 7-days.

5.2.3 *Mycobacterium tuberculosis* Strains

MDMs were infected with Mtb (HN878) at an MOI of 1. Host/ *Mtb* RNA and DNA was extracted at 0h, 4h, 12h and 24h utilising an optimised differential lysis and centrifugation protocol described below. Host cell nuclei were extracted and fixed at 0h and 4h post-infection for downstream ChIP-seq.

5.2.4 Nucleic Acid Extraction, Nuclei Preparation and Sequencing

Infected MDMs were differentially lysed in GTC buffer (5M guanidinium thiocyanate, 0.5% (w/v) sodium-N-lauryl sarcosine, 25mM tri-sodium citrate, 0.1M β-mercaptoethanol and 0.5% Tween80) for 5 min. The cell lysate was removed to a new Eppendorf tube. The lysate was then centrifuged at max speed for 3 min at RT to pellet out the infectious bacilli. The supernatant, containing host nucleic acid was removed to a new Eppendorf tube and stabilised using TRIzol (ThermoScientific). The mycobacterial pellet was sheared in TRIzol using the FastPrep-24 (MP Biomedicals) bead beater and BeadBug Eppendorf Tubes (Sigma). *Mtb* RNA, host RNA and DNA were then purified using the standard TRIzol protocol. Quantification of the RNA extracte d was approximated using the Nanodrop (Thermoscientific). The RNA quality was assessed using the Bioanalyzer (Agilent). Samples were sequenced by our collaborators at the Institute of Bioengineering, Moscow, Russian Federation using an Illumina NextSeq 500.

5.2.5 Bioinformatic Analysis

Bioinformatic analysis (Fig. 35) of sequence data was achieved using FastQC (version 0.11.8), HISAT2, HTSeq-count tool (version 0.11.2) with reference to the annotated human genome annotations downloaded from

GENCODE (Comprehensive gene annotation, Release 30 (GRCh38.p12)). Normalized counts were obtained by the DESeq2 R package and the statistics and plots were generated using custom R scripts.

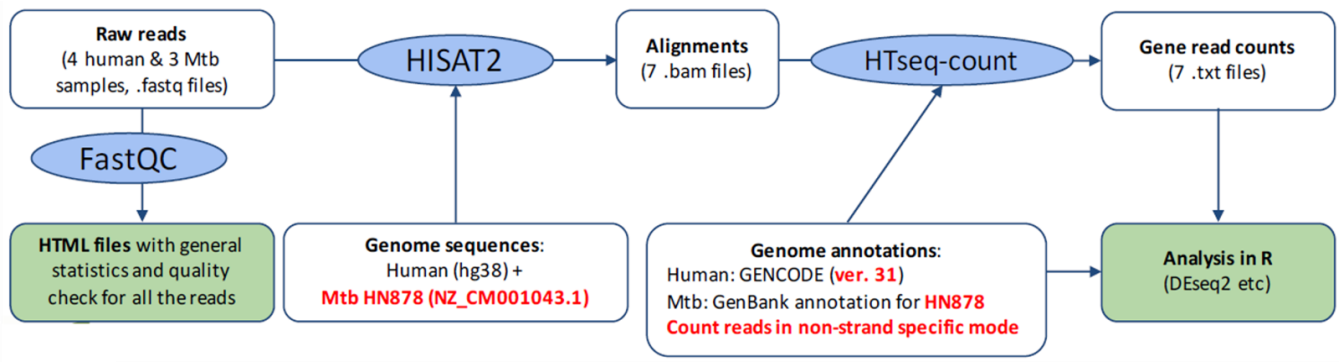

Figure 35: **Schematic representation of the RNA-seq bioinformatic-pipeline used for the assessment of sequence data from the host and pathogen**

5.3 Results

Optimal high throughput generation of MDMs can be achieved via negative immunomagnetic separation of monocytes and subsequent culture in media supplemented with serum

The generation of MDMs can be affected by the isolation method as well as by variation in the culture medium used. In this study, we initially assessed the effect of immunomagnetic separation (negative and positive selection) vs. plastic adhesion for the purification of $CD14^+/CD16^+$ monocytes before differentiation to MDMs. Further, we assessed the role of media supplemented with serum (FCS or Hab) or without serum (*Ex vivo* medium, Lonza) in the generation of the MDMs. Our data showed that adherence and the negative selection of monocytes elicited both similar yields and an estimated percentage adhesion of the cells after 7-days (Fig. 37a-b). The efficiency of differentiation was also calculated; the differentiation of monocytes isolated using negative selection was significantly more efficient than those isolated using adherence and positive selection (Fig. 37c).

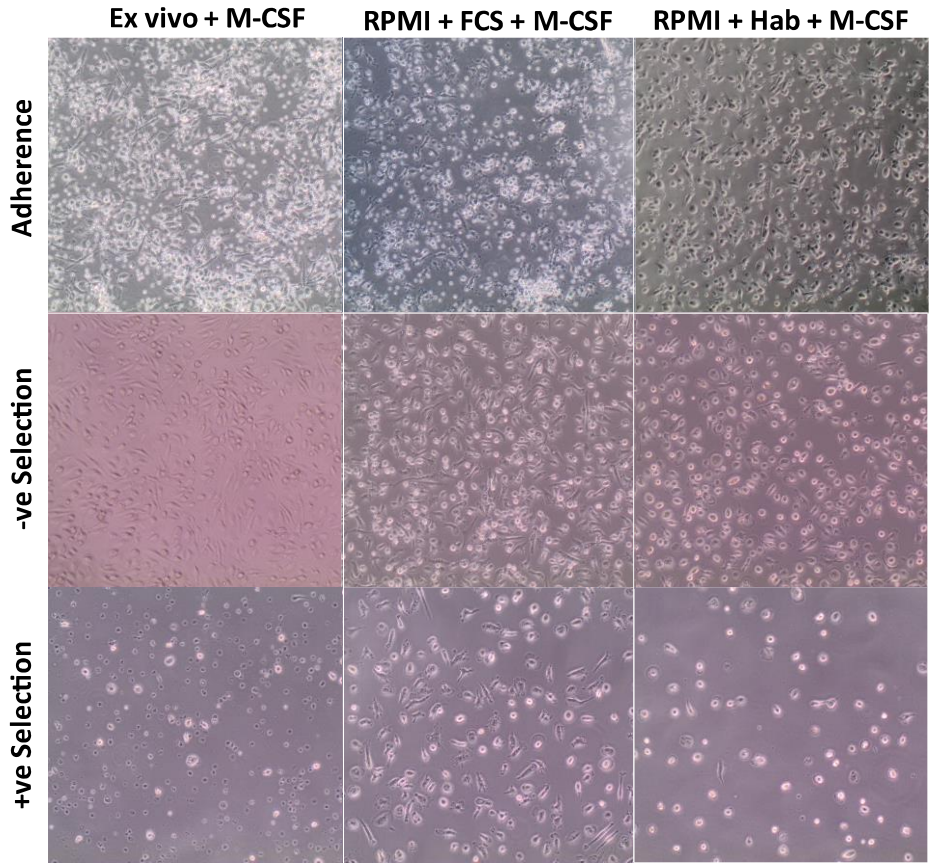

Figure 36: **Monocytes isolated via negative selection and cultured under serum-free conditions produced phenotypically homogenous monocyte-derived macrophages.** Monocytes isolated via plastic adherence or immunomagnetic separation in a range of culture media was observed to determine the degree of adherence and correct morphology of the MDMs after 7-days in culture.

The dual-RNA-seq methodology detailed in this study requires large amounts of primary human monocyte-derived macrophages. Further, from the same donor, additional cells are required for downstream ChIP-seq experiments, thus increasing the number of MDM required after differentiation. Therefore, to differentiate enough of these cells, approximately $1x10^9$ PBMCs are required per donor. As such, the high throughput method for the generation of MDMs required optimisation. Varying methods of MDM differentiation were investigated to assess macrophage adherence, yield and morphology. Monocytes were isolated by adherence or immune-magnetic separation via positive or negative selection. Additionally, the utilisation of human autologous serum, fetal calf serum and serum-free media supplemented with 50 ng/mL M-CSF was investigated. $CD14^+CD16^+$ monocytes, isolated via negative selection and differentiated in serum-free media, elicited macrophages which were morphologically homogenous and had the highest degree of confluence after 7-days, relative to the other culture methods assessed (Fig. 36).

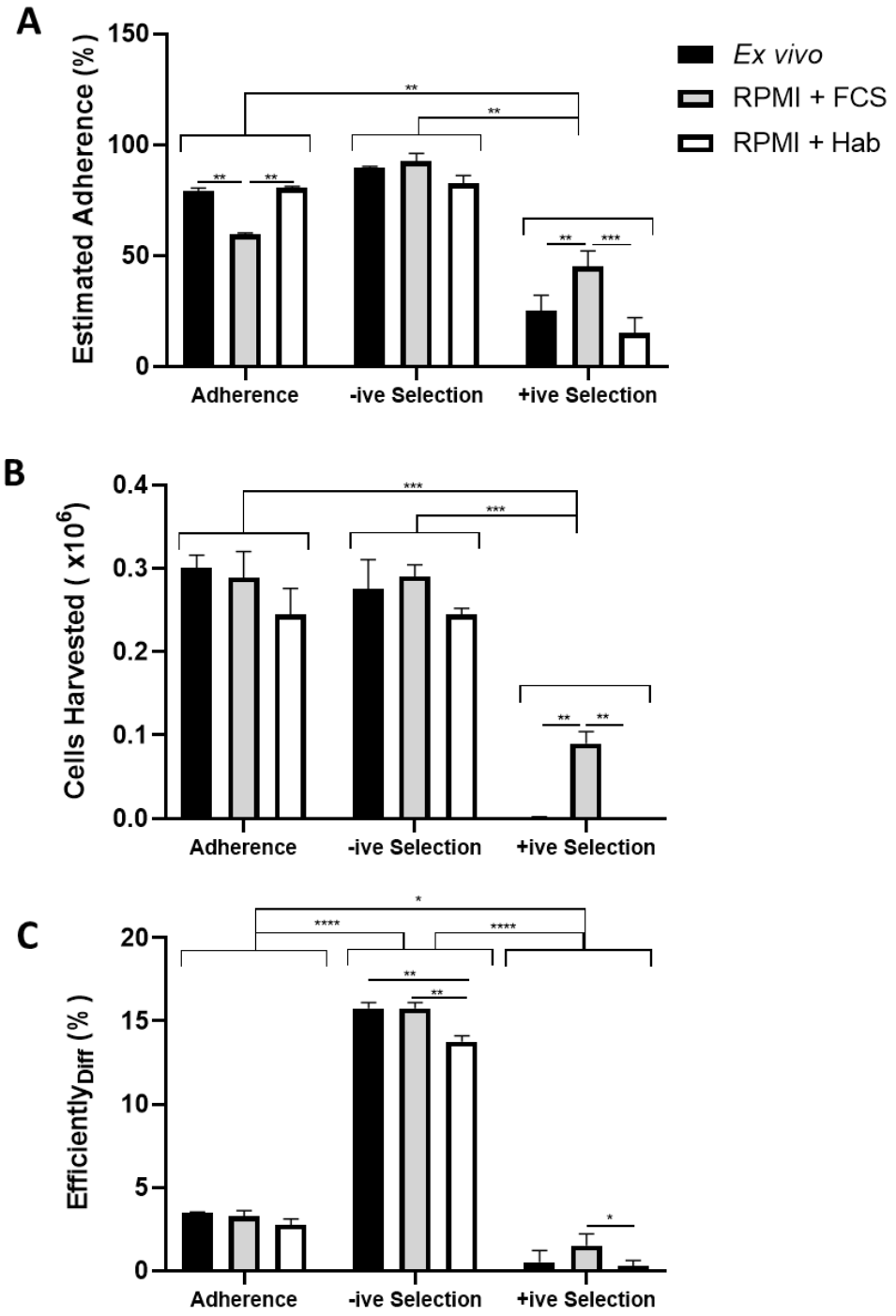

Figure 37: **Monocyte-derived macrophages isolated via negative selection, and grown in the presence of FCS, had superior differentiation efficiency and had similar yields and degree of adherence to MDMs isolated via plastic adherence.** Monocytes were isolated from PBMCs using adherence, negative selection or positive selection. Culture media with (RPMI + FCS or Hab) or without serum (Ex vivo media) was also assessed 7-day post culture. To determine the optimum method **A**) percentage adhesion. **B**) The yield of MDMs recovered after 7-days and **C**) Differentiation efficiency was determined via the percentage number of MDMs harvested from the initial number of cells seeded. (*P ≤ 0.05, **P ≤ 0.01, ***P ≤ 0.001, ****P ≤ 0.0001, one-way ANOVA, n=2).

Additionally, by flow cytometry and available human antibodies, we analysed the efficiency by which the negative immunomagnetic separation protocol was able to isolate monocytes from PBMCs. PBMCs were isolated via traditional density centrifugation. Analysis of the cells showed that via negative selection, magnetic beads efficiently purified $CD14^+$ monocytes from ~50% pre-isolation (Fig. 38a) to ~90% post-isolation (Fig. 38b). After 7-days of cell culture in differentiation media (RPMI + 10% FCS + 50 ng/mL), the adherent monocyte-derived macrophages were harvested and analysed via flow cytometry (Fig. 38c). The cells were found to be $CD3^-$, $CD11b^+$, $CD14^-$ and $HLA\text{-}DR^+$ in line with what is reported in the literature [279]. Further, the appearance of two distinct populations within the macrophage compartment ($CD14^+$ and $CD14^-$) implies a range of macrophage phenotypes generated after 7-days in the presence of M-CSF (Fig. 38c). In a recent study, it was reported that 50 ng/mL M-CSF can elicit two subsets of MDMs which differentiate into CD14 high and low populations and represent non-adherent and adherent MDM populations, respectively [279].

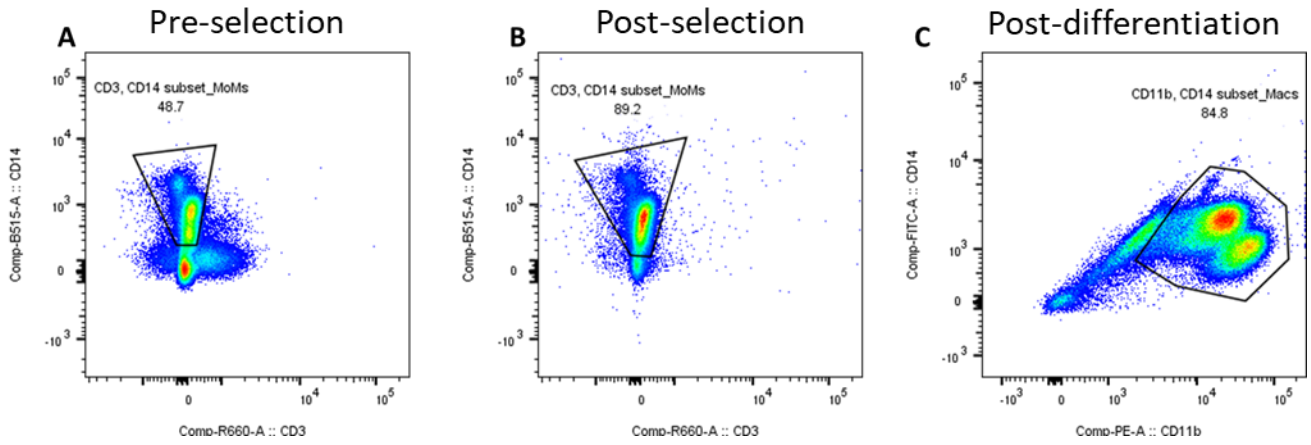

Figure 38: **Negative-selection efficiently purifies monocytes from PBMCs and allows for the generation of phenotypically distinct macrophages.** Monocytes and macrophages were analysed via Flow cytometry **A**) within PBMCs pre-negative selection, **B**) post-negative selection and **C**) after 7-day of culture in differentiation media. Monocytes (MoMs) = $CD14^+CD3^-$, monocyte-derived macrophages (MDMs) = $CD14^-CD3^-CD11b^+HLA\text{-}DR^+$. (p=n/a, n=1)

A brief explanation of the dual-GTC method used to isolate host and pathogen RNA

This study employs differential lysis and centrifugation steps to differentiate between host and pathogen nucleic acid (Fig. 39). Adherent, differentiated MDMs (~2×10^6) are infected with the hypervirulent Beijing Mtb strain (HN878) at an MOI of 1. Host cells are then incubated to allow for uptake of bacilli. At each time point, the culture media is removed, and the cells are lysed using the GTC buffer. This lysis buffer selectively lyses host cells whilst leaving Mtb bacilli intact. The lysate is then centrifuged to pellet out the engulfed Mtb and the lysate, containing host RNA and DNA, is removed to a separate tube for downstream purification. The Mtb pellet is then sheared using silica beads to ensure adequate extraction of pathogen nucleic acids. After

both lysates have been extracted, they are purified using established protocols to provide host RNA and DNA as well as pathogen RNA. Further, additional MDMs were plated for ChIP-sequencing.

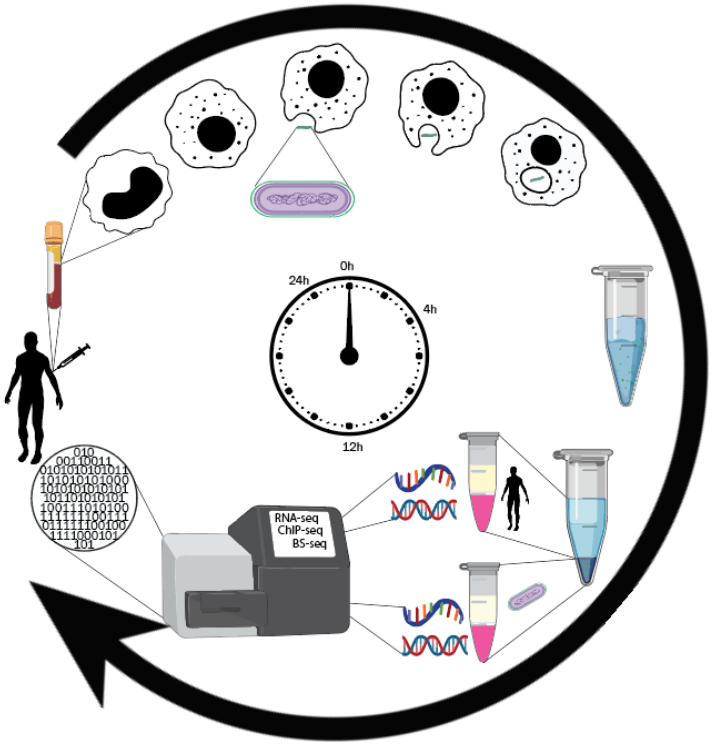

Figure 39: **General flow diagram of the dual-GTC methodology used in the optimisation of the dual RNA seq protocol.**

The dual-GTC method can successfully isolate host RNA as well as Mtb RNA

The host and Mtb RNA acquired from using the dual-GTC method detailed above were assessed for quantity and quality (Fig. 40) for downstream sequencing. The host samples were found to be of good quantity (~5.4 ug) and good quality (RIN = 8.6). Conversely, the Mtb RNA samples were of low quantity (~0.2 ug) and low quality as measured by a RIN value of 2.5. This finding was expected due to the low numbers of possible Mtb which could theoretically be phagocytosed by the MDMs.

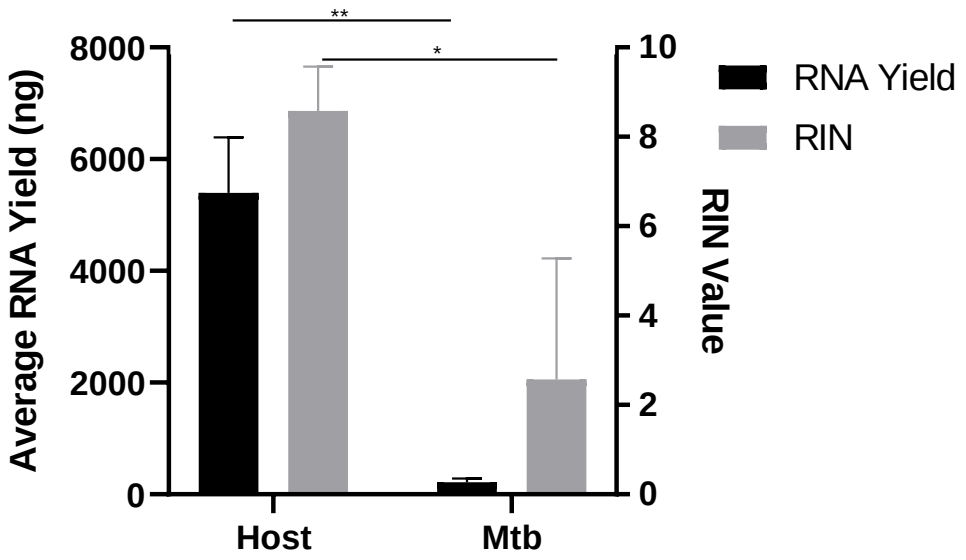

Figure 40: **The dual RNA-seq methodology isolated host RNA of high quality/quantity, whilst Mtb RNA was found to be of low quality/quantity.** RNA extracted from approximately 2 x 10^6 MDMs infected with Mtb an MOI of 1. RIN = RNA integrity number (*P ≤ 0.05, **P ≤ 0.01, students t-test, n=3/4).

RIN values are not a good predictor of RNA quality for samples with very low RNA concentrations

RIN values for the Mtb samples were deemed to be less than optimal for sequencing (RIN <7) (Fig. 40). To investigate this further, five independent experiments were pooled to assess the relationship between RNA quantity and RNA quality (RIN). From this analysis (Fig. 41), we observed a significant positive correlation between quantity and quality. As this study is limited by the number of host cells required for downstream analysis, increasing the number of Mtb by upscaling the MOI would negatively affect the viability of the MDMs. This is, therefore, an unfeasible alternative strategy for increasing the yield of Mtb RNA. From our data, it may be probable that the extracted Mtb RNA was near to, or below, the limit of detection for the Agilent Bioanalyzer 2100. However, we hypothesised that it may still be of sufficient quality for downstream sequencing applications. To test this hypothesis, we decided to sequence both sets of RNA (host and pathogen) to assess the fidelity of the dual-GTC RNA separation protocol.

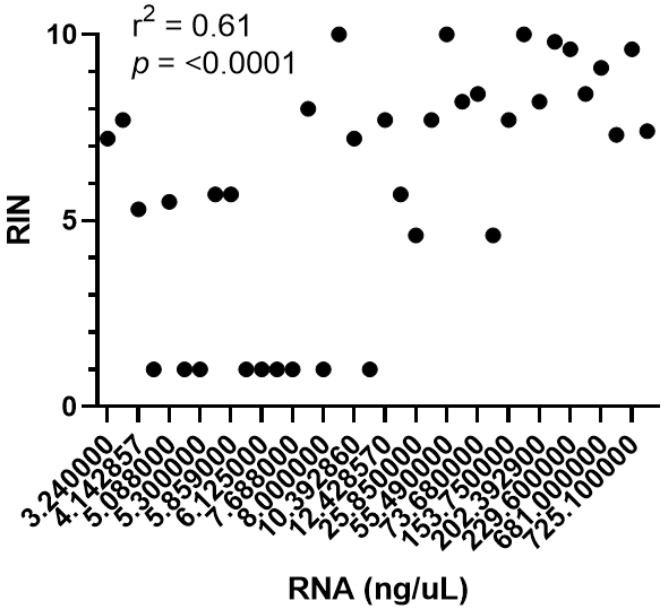

Figure 41: **High RIN values are positivity correlated with increasing RNA concentration.** RNA concentration and matched RIN data from five pooled independent experiments. (****P ≤ 0.0001, Pearson correlation, n=5).

Commercially available leukopaks provide enough cells for downstream RNA-seq and ChIP-seq

All donor blood samples purchased and utilised in the optimisation of this protocol were male and between the ages of 18-50-years old. The average age of 36 years was observed across the donor samples. Leukopaks are a blood product which is enriched for immune cells from peripheral blood. From our data, a single patient 75 mL PBMC sample can contain approximately 1.5 x 10^9 PBMCs (Table. 6). Using negative selection, approximately 13.7 x 10^9 (~10% of PBMCs) $CD14^+/CD16^+$ monocyte (MoMs) cells could be isolated via negative immunomagnetic separation. After 7-days in the differentiation culture medium, approximately 9 x 10^6 MDMs were harvested which equated to ~8% the monocytes seeded and ~0.8% of the initial PBMCs isolated.

Table 6: **Patient data and further information on subsequence cellular subsets isolated during the MDM differentiation protocol.**

Study Parameter	Average	Standard Deviation	P-Value
Donor Age	36.17	9.13	0.9993
PBMCs (x 10^9)	1.525	0.52	>0.9999
MoMs (x 10^7)	13.68	4.77	0.7989
MoMs (%)	10.10	4.98	0.9969
MDMs (x 10^6)	9.79	2.71	0.9989
MDMs (%)	7.73	2.60	0.9976

RNA-seq data confirm the ability of the dual-GTC methodology to enrich Mtb transcripts and extract meaningful data from the host and pathogen

The host and pathogen RNA were aligned to the *homo sapien* and Mtb genomes as detailed above. Within the human samples, approximately 18.0 – 26.0 M reads aligned uniquely to the reference genome, whilst a greater range was observed within the mycobacterial samples: *viz*, approximately 12.5 – 36.0 M reads (Fig. 42 and 43). Within the Mtb samples, a significant portion of the reads aligned uniquely to the *Homo sapien* genome. This observation is likely indicative of artefactual human RNA contamination within these samples during the differential lysis and centrifugation steps required by the dual-GTC methodology.

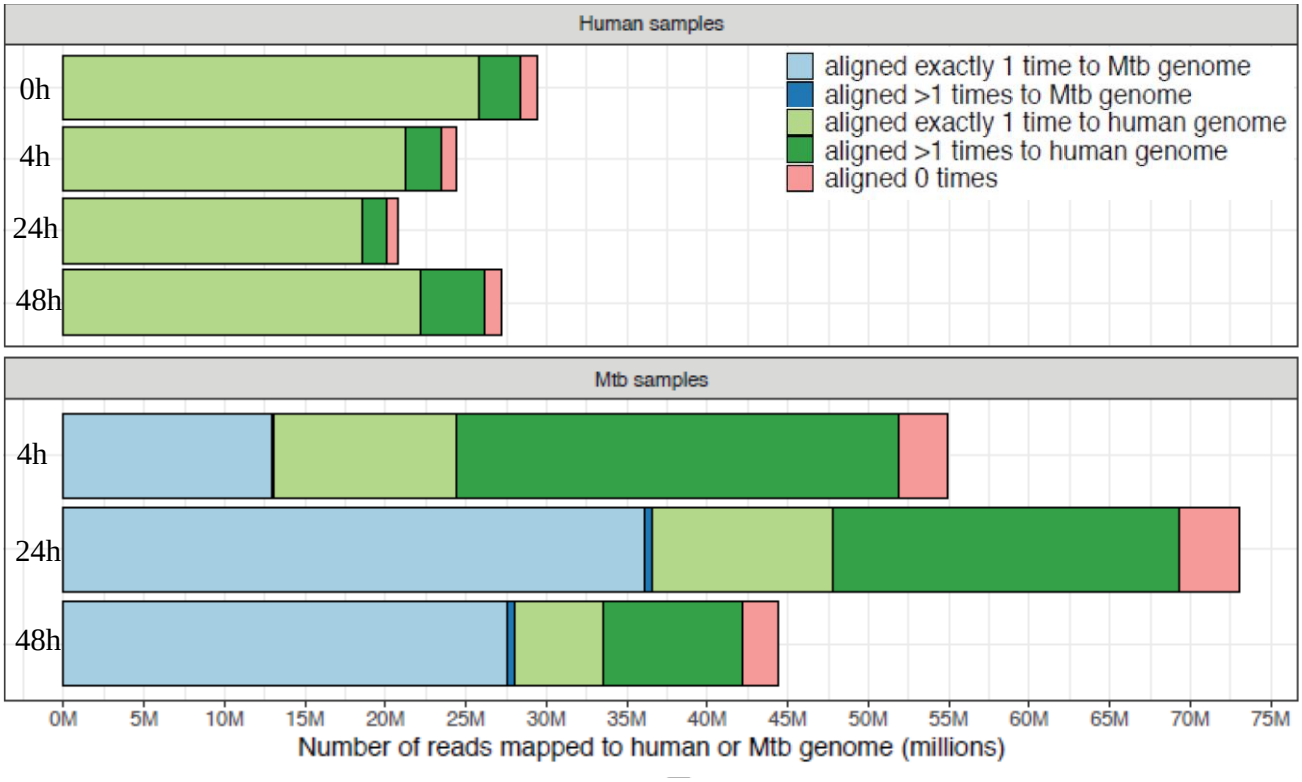

Figure 42**: RNA-seq data illustrated a sufficient number of unique reads for host and pathogen transcripts separately enriched using the dual-GTC methodology.** RNA samples were aligned to the **A**) human and **B**) *Mycobacterium tuberculosis* genomes at 4h, 24h and 48h post-infection. Analysis performed and graphs created by Dr Ivan Antonov at the Institute of Bioengineering, Moscow, Russian Federation (p = *n/a*, n=1)

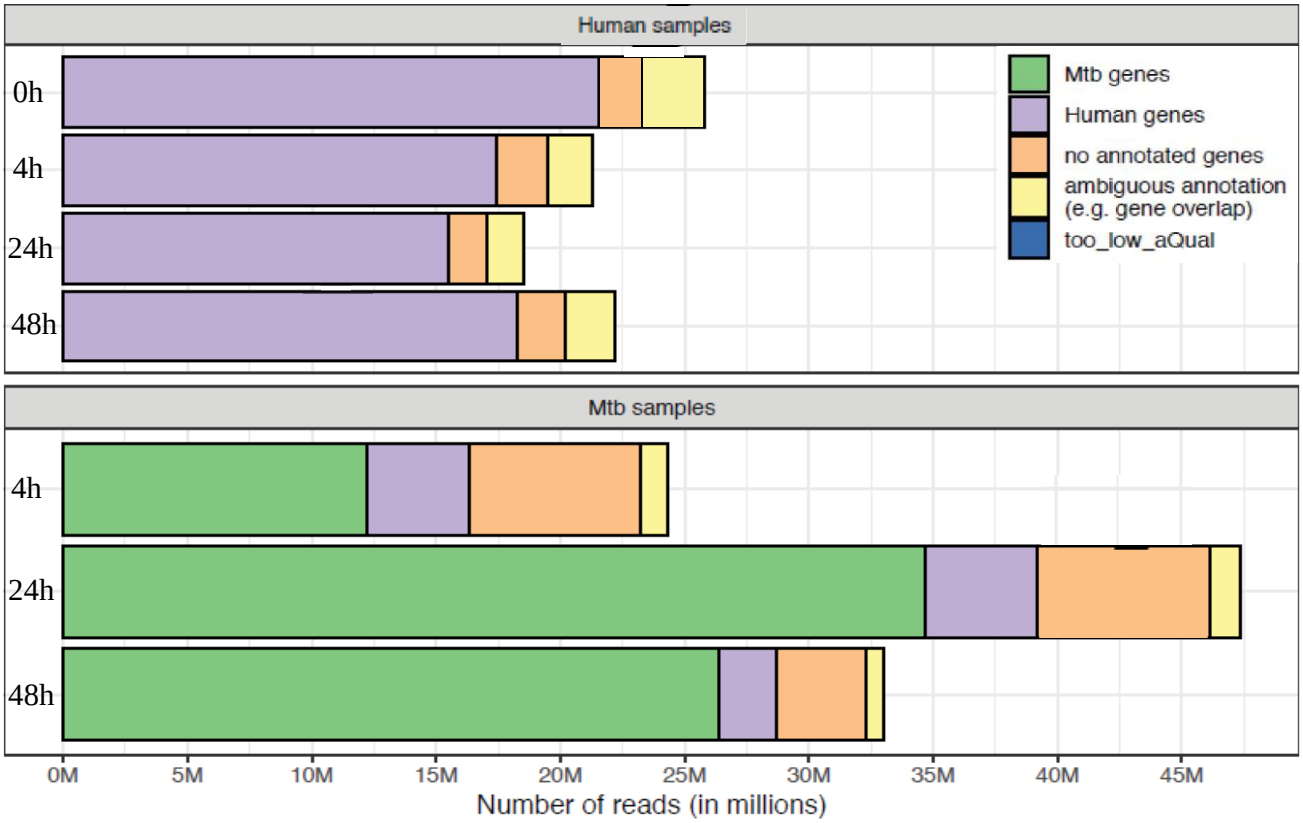

Figure 43**: The dual-GTC methodology allows for the segregation of host- and pathogen-specific transcripts.** RNA samples were purified from **A**) human primary MDMs and **B**) *Mycobacterium tuberculosis* genes at 4h, 24h and 48h post-infection**.** Analysis performed and graphs created by Dr Yulia Medvedeva and Dr Ivan Antonov at the Institute of Bioengineering, Moscow, Russian Federation (p = *n/a*, n=1)

Human and bacterial reads were aligned to known annotated gene entries *in silico*. On average, approximately 81% of the human reads were aligned to annotated genes, whereas 67% of reads within the Mtb samples were aligned to known Mtb genes. Within the Mtb samples, ~5 million reads were aligned to the human genome (Fig. 43). This phenomenon is likely as a result of residual host RNA left behind during segregation of host/pathogen RNA via centrifugation.

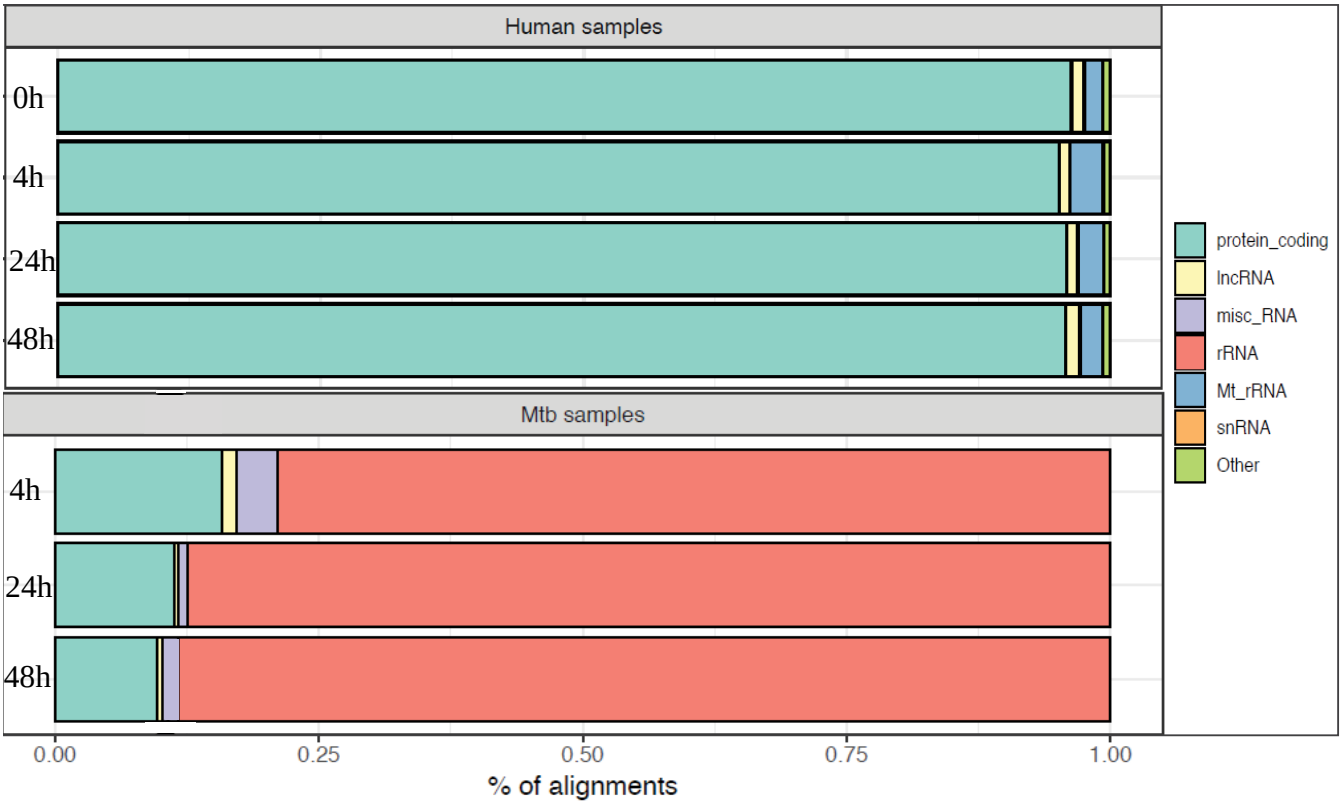

Figure 44: **mRNA and rRNA are the main transcripts identified for host and pathogen RNA, respectively.** RNA was isolated from **A)** human primary MDMs and **B)** internalised *Mycobacterium tuberculosis* at 4h, 24h and 48h post-infection. Analysis was performed and graphs created by Dr Yulia Medvedeva and Dr Ivan Antonov at the Institute of Bioengineering, Moscow, Russian Federation (p = *n/a*, n=1)

The gross majority of reads within the human samples aligned to protein-coding genes, followed by a small proportion of mitochondrial ribosomal RNA (Mt_rRNA) and long-non-coding RNA (lncRNA) (Fig. 44). Due to the low number of Mtb hypothesised to be phagocytosed by the MDMs, a bead abased rRNA clean-up of the rRNA was anticipated to have a catastrophic effect on the already-limited yield of coding and non-coding RNA. Thus, within the Mtb enriched samples, the greatest percentage of reads were identified as ribosomal RNA (rRNA) followed by protein-coding genes and then lncRNA.

Table 7: **Summary of Average RNA Sequence Data.**

			Aligned to Human Genome				Aligned to Mtb Genome			
			Unique		Not Unique		Unique		Not Unique	
	Total Reads	Not Aligned	*Reads (#)*	*rRNA (%)*	Reads (#)	rRNA (%)	Reads (#)	rRNA (%)	Reads (#)	rRNA (%)
Human	25.465M	0.95M	21.96M	2.5	2.54	0.1	40	86.7	0	0
Mtb	57.41M	2.95M	9.39M	19.33	19.22	0.1	25.49M	84.86	0.38M	52.2

In summary, the RNA sequence data for the human samples were more than sufficient for statistical analysis and identification of important transcriptomic changes (Table. 7). Despite the technical and MOI-limiting phenomenon for the Mtb RNA samples, sufficient reads were also acquired for robust downstream statistical analysis.

The dual-GTC method proved sequence data representative of Mtb and human genomes

Figure 45 informs on the range of uniquely annotated reads acquired for the host and pathogen using this dual-RNA methodology. For the host samples, an average of 16135.75 genes aligned uniquely to the host reference genome, with an average number of ~3000 reads per gene (Fig 45a). This estimate is similar to the anticipated number of protein-coding genes in the human genome [280, 281]. Within the Mtb samples, an average of 4078 uniquely aligned genes was detected with an average number of approximately 2500 reads per gene (fig. 45b). Together, these indicate that that the dual-GTC mythology provides robust RNA which is representative of both the host as well as the pathogen.

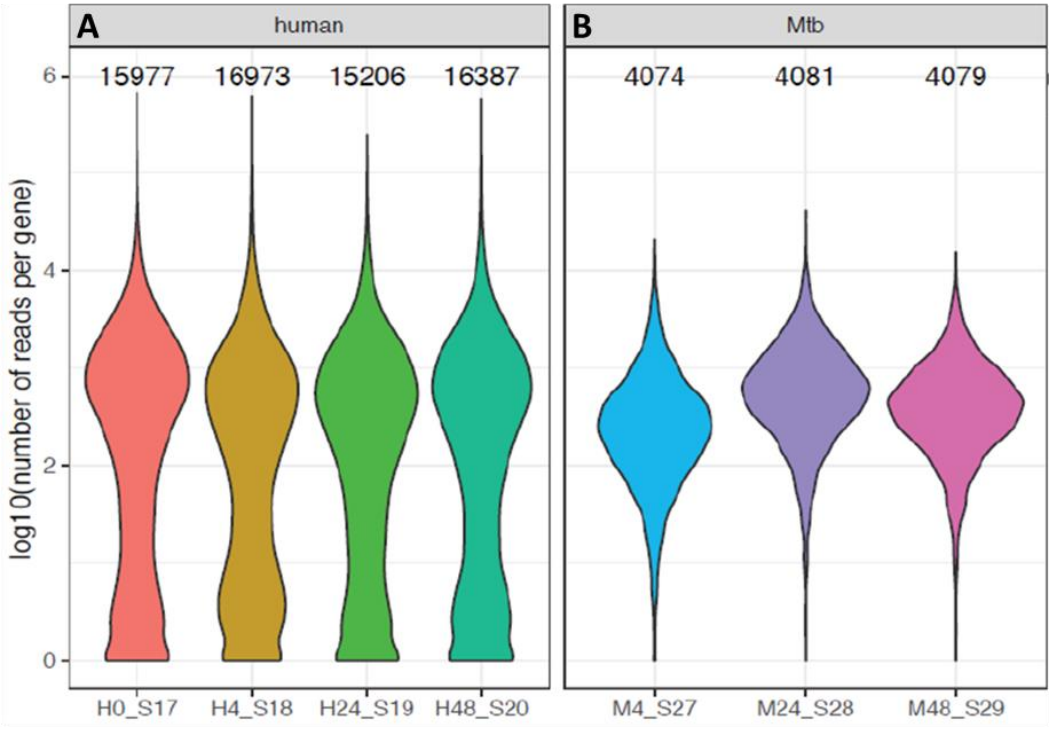

Figure 45: **The total number of reads and the number of unique genes identified per timepoint in all samples.** Read data and the number of genes which aligned uniquely for **A**) human MDM samples and **B**) Mtb samples at 4-, 24- and 48-hours post-infection. Analysis performed and graphs created by Dr Yulia Medvedeva and Dr Ivan Antonov at the Institute of Bioengineering, Moscow, Russian Federation (p = *n/a*, n=1)

Gene expression profiles are characteristic of Mtb infection

To assess the final fidelity of the dual-GTC methodology, several marker genes were assessed from both the host and the pathogen sequence data. In human MDM Mtb infection, IL1α, IL1β, IL10, CCL1, CXCL8, TLR2, IRF7, CCL7, CXCL1, CXCL3, PTGS2 and IL12β were all found to be upregulated by Mtb infection (Fig. 46). Further, several common Mtb genes were also identified from the RNA-seq data.

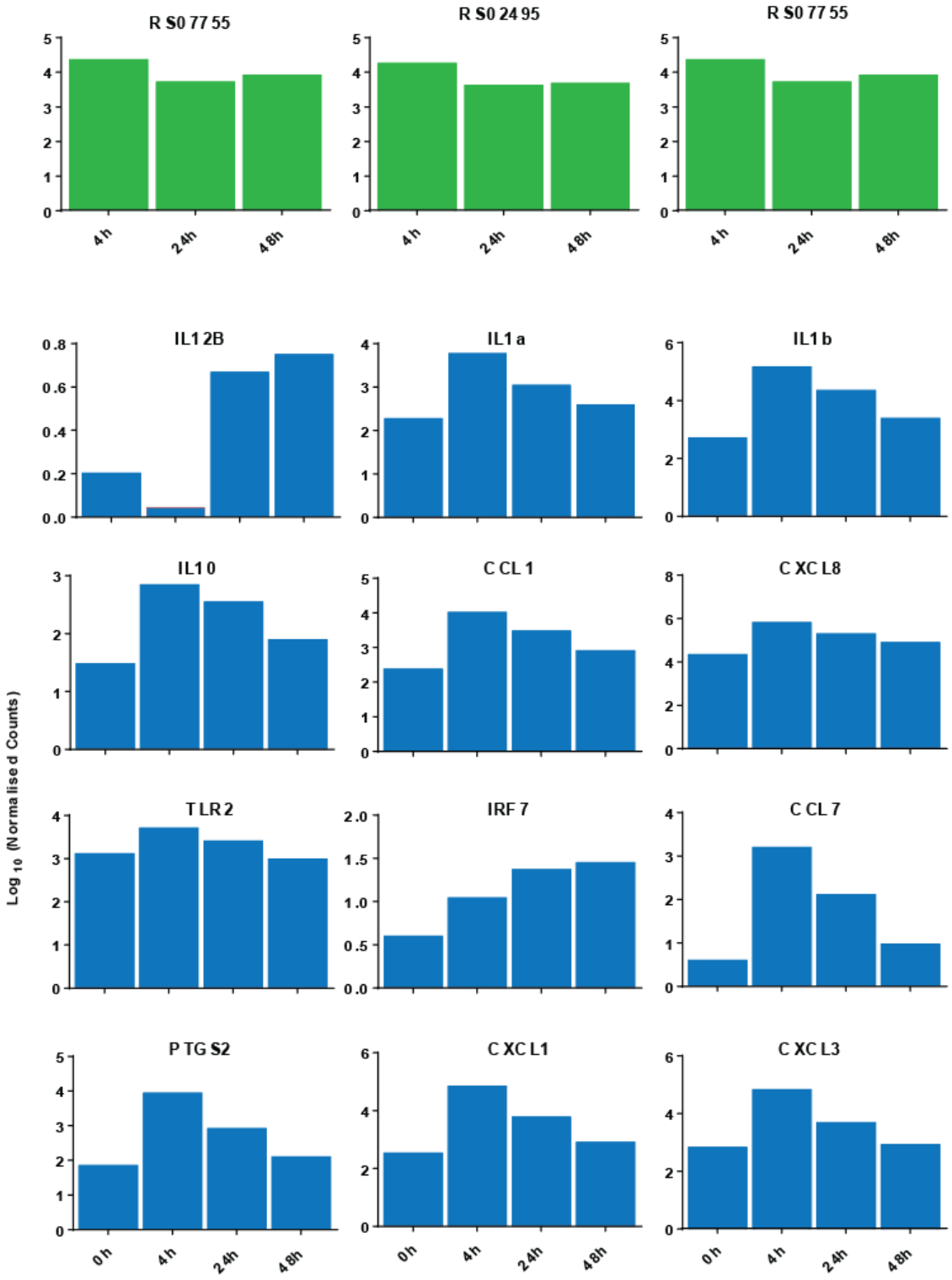

Figure 46: **Normalised gene counts from primary MDMs (Blue) and internalised mycobacteria (green) post-infection illustrate the success of segregation and analysis of host/pathogen transcriptomic profiles.** Data extrapolated from RNA-seq data for a single pilot donor. Samples sequenced by the Institute of Bioengineering, Moscow, Russian Federation (p = *n/a*, n=1)

5.4 Discussion

The ability to elucidate and correlate transcriptional and epigenetic changes, that occur within both the pathogen and the host at the same time point, has two primary benefits. Firstly, this approach can add to the knowledge of TB pathogenesis, and secondly, this method may highlight novel targets for therapeutic intervention. The dual RNA-seq method described in this study has several advantages; namely, (i) it allows for the bulk generation of MDMs in quantities sufficient for a longitudinal assessment of dual RNA-seq, ChIP-seq and BS-Seq Data on a per human donor basis; (ii) it allows for the cost-effective enrichment of phagocytosed *Mtb* bacilli without the need for FACs sorting such as previously shown in other studies [249, 282]; (iii) it only requires basic laboratory equipment; and (iv) serves as a good starting point before validatory PCR and more in-depth single-cell RNA-seq studies.

To date, few *in vivo* or *ex vivo* mycobacterial dual RNA-seq studies have been published. This phenomenon is largely due to the technical difficulties inherent with this approach. For example, increased depth, RNA yield differences between eukaryotic cells and rRNA depletion are some of the obstacles that need to be optimised [228]. To by-pass these issues, several studies have explored the transcriptional changes in macrophage-like cells lines [283, 284]. These studies have informed on the role of nutrient dynamics and altered metabolism of mycobacteria *in vitro*. In the *ex vivo* leprosy model, dual RNA-seq has been used to identify specific gene signatures which result in different clinical manifestations, highlighting the importance of understanding site-specific inflammation caused by pathogenic mycobacteria and disease progression [285]. Very recently, dual RNA-seq has been used in *in vivo* murine-Mtb infection models to assess the host response to Mtb and nutrient immunity [249]. *In vivo* human-Mtb dual RNA-seq infection studies, in combination with epigenetic sequencing experiments, are still technically unfeasible due to the number of human immune cells and engulfed Mtb required. Our study attempts to circumvent this obstacle though the examination of *ex vivo* primary MDMs. However, this protocol is limited by the large amount of terminally differentiated MDMs required to acquire adequate DNA, RNA and host nuclei for downstream sequencing applications. From our data, we observed that approximately 10% of donor PBMCs were monocytes and that post-differentiation, ~8% of monocytes could be differentiated to macrophages (Table. 6). These percentages are similar to previously published studies [286]. Further, whilst it is assumed that the large majority of Mtb are phagocytosed by the MDMs, some bacilli may not be internalised or washed away during the processing steps before the lysis of the MDMs. This phenomenon may introduce sequence noise in the analysis, as these bacilli would have likely experienced other non-immune linked stressors. Additional optimisation has shown that, at an MOI of 5, approximately 20% of cultured macrophages are infected with Mtb after four hours of uptake (data not shown). Higher MOI's may infect more macrophages, however, this is at the cost of macrophage viability and a compromised host

transcriptome. For this reason, we chose to use a lower MOI of 1 within this study. Whilst conserving macrophage viability, a low MOI creates other experimental issues which need to be overcome.

In previous bulk RNA sequencing studies which have investigated Mtb transcriptomic profiles, Mtb cultures grow to the mid-log phase prior to lysis and nucleic acid extraction [284, 287]. This constitutes a culture containing hundreds of millions of colony-forming units (CFUs) and a surplus of mycobacterial RNA for downstream sequencing. This contrasts with our study, where a theoretical maximum number of ~2 million Mtb CFU could potentially be sequenced. However, this is under the improbable assumption that 100% of all engulfed Mtb are phagocytosed. This observation is emphasised by the disparity observed between the total host RNA and pathogen RNA yield (Fig. 40). Similar findings were observed in the monocyte-like THP-1 BCG infection model. In that study, the authors found that mycobacterial RNA was underrepresented in their samples approximately 1000-fold relative to THP-1 RNA [284]. Further, we show that a significant number of reads in the bacterial samples contain transcripts which align to the human genome, constituting sequence noise and in the pathogen samples. Despite using reagents specifically designed for the analysis of low yield prokaryotic RNA yields, the analysis of mycobacterial RNA quality via the RNA integrity number (RIN) becomes progressively less robust with decreasing RNA quantity in the sample (Fig. 41). This observation is further emphasised by the validatory sequence data which could be extrapolated from the "low quality" Mtb RNA samples (Fig. 46). Together, these lines of data imply that whilst the Mtb RNA is of low yield and seems to be below the limit of detection for the RNA quality analysis, the dual-GTC method and subsequent *in silico* analysis were successfully able to enrich Mtb transcripts and annotate sufficient mycobacterial reads from these separated samples for robust statistical analysis.

In this study, the dual RNA-seq methodology provided a mean total of 25.5M host and 57.4M Mtb reads; of which 22M and 25.5M mapped uniquely to the human and Mtb genomes, respectively. (Table 7 and Fig. 42). Within the *Mtb* samples, 9.4M reads aligned to the human genome (artefactual contamination) and contained ~84.7% rRNA which is similar to that of other dual-RNA-seq Mtb studies [249]. Correcting for this, approximately 2.8M unique Mtb reads (3.5 - 5.7 %) were found to available for downstream analysis (Table 7). This is in line with early bacterial sequencing studies which postulated that a minimum of 2-5 million sequence reads are required comprehensive transcriptomic coverage [231-233]. Whilst the reads acquired using this method in its current form are adequate, reducing the depth required during sequencing is economically beneficial. There are several aspects of this methodology which we are still working to improve upon. For instance, the contamination of host nucleic acid within our pathogen samples significantly increases the sequencing depth to which we must go to to achieve an adequate amount of Mtb-specific reads. Additional washing steps of the mycobacterial pellet may be beneficial in removing contaminating host nucleic acid.

In the following study, we describe a high-throughput method for the generation of MDMs, their subsequent infection with Mtb, and the extraction of host RNA, DNA and nuclei as well as internalised pathogenic RNA within those same macrophages on a per donor basis without the need for fluorescent cell sorting. This optimised enrichment methodology, in combination with additional epigenetic sequencing experiments, will allow for the identification and targeting of novel gene lncRNA interactions important to understanding the biology of TB pathogenesis. Such hypothesis-generating data will allow for the targeted investigation of subsequent follow-up epigenetic studies.

Conclusions and Future Work

TB is an ancient disease which has successfully affected humanity for millennia. Further, the modern emergence of multidrug resistance has highlighted the need for new anti-TB therapeutics. Understanding the biology of Mtb, particularly the homeostatic regulation of its cell wall, are crucial for the development of novel compounds. In this study, I have assessed the immunological effects of the Mtb deficient for two cell wall hydrolytic enzymes, Ami1 and Ami4, in the aim of both understanding the consequences of these deletions in the context of the host immune response, as well as potentially assessing the potential of these genes for novel drug development. In non-pathogenic mycobacterial species, amidase deficiency has been shown to confer deleterious cell wall remodelling phenomena such as atypical septation and the formation of long strings of filamentous mycobacterial. Further, these mutants have been shown to elicit heightened sensitivity to existing first-line anti-TB drugs. In this study, we show that amidase deficiency in Mtb alters the host immune response during acute infection, however, the single deletion of Ami1 or Ami4 was unable to elicit the clearance of Mtb in the acute or chronic phase of the infection relative to wild-type controls. Further, amidases probably act in synergy with other cell wall remodelling enzymes, thus, any sensitivity to antibiotic or immune pressures may be compensated for by additional genes. Interestingly we also found that the Δ*ami1* mutant was sensitive to meropenem *in vitro* and tolerant to isoniazid *in vivo*. In contrast, Δ*ami4* is dispensable for the host immune repose and antibiotic sensitivity. Taking this project further, we plan to further explore the phenomenon of antibiotic sensitivity and the host immune response in Ami1 deficient Mtb infection. This will be done both *in vitro* using NOD1/2 cell lines and culture supernatants from Δ*ami1* axenic cultures relative to complemented and wild type strains. Further, we plan to elaborate on our *in vivo* antibiotic data by examining the relationship of BCG vaccination and subsequent infection with Δ*ami1* Mtb.

Mtb infection and the subsequent host immune response involve complex interactions at the transcriptomic and epigenetic levels. There is increasing evidence for the ability of Mtb to subvert the host immune response through numerous strategies, such as DNA methylation, histone modification and the induction of ncRNAs. Understanding these changing landscapes during infection is key to adding to the knowledge of TB pathogenesis and for the elucidation of novel targets for anti-TB drug design. In this study, I report an optimised protocol for the high throughput generation of MDMs as well as a method for the enrichment of Mtb transcripts from bacilli engulfed by the primary MDMs. Therefore, this protocol will allow for the in-depth analysis of the host-pathogen interactions in response to epigenetic changes during infection. Not only will this add to the knowledge of TB, but it can also be applied to other Mtb mutant models of infection to elucidate novel drug targets. Further, this protocol can be readily adapted to other bacterial species which possess a thick outer capsule or cell wall.

Utilising this protocol, the next steps in the project will be the assessment of primary macrophages infected with Mtb deficient for Rv2966c, a 5-methylcytosine-specific DNA methyltransferase, which is secreted by Mtb and is translocated to the host nucleus, as well as Rv1988, an Mtb methyltransferase. Both Mtb proteins have been shown to play a role in the reprogramming of the host immune system to confer persistence within the host. Using dual RNA-seq in combination with ChIP-seq and BS-seq we hope to reconstruct the host-pathogen transcriptional and epigenetic dynamics to better elucidate the biology of Mtb infection.

Supplementary Figures

Supplementary Table 1: **List of primers used in the construction of amidase deficient M. tuberculosis strains.**

Primer	Sequence	Amplicon
H37*ami1*KOUSF	GTGAAGCTTGCCGCATTACCAGCTATGAC	1577 bp amplicon the 5' region of the *ami1* gene and 96 bp of the *ami1* gene
H37*ami1*KOUSR	GTGTCTAGAGTCGATGAAGACGACCATGC	
H37*ami1*KODSF	GTGTCTAGACGAGGGCAGGCAAAAATAC	1579 bp amplicon the 3' region of the *ami1* gene including 78 bp of the *ami1* gene
H37*ami1*KODSR	GTGGGTACCGCCATCAACCTCCAGTAGACA	
H37*ami4*KOUSF	GTGAAGCTTACCGGCAAGACTGCATAAC	1557 bp amplicon the 5' region of the *ami4* gene and 39 bp of the *ami4* gene
H37*ami4*KOUSR	GTGTCTAGACACCTCCTCGAGCCAAATC	
H37*ami4*KODSF	GTGTCTAGACGAGCTCGGCAATAAGGTC	1530 bp amplicon the 3' region of the *ami1* gene including 82 bp of the *ami1* gene
H37*ami4*KODSR	GTGGGTACCCGATCCGCTGTGACAATAGA	
H37*ami1*pMVF	GCGCGCGCAAGCTTGCCATCTTCGTCACCTGC	1126 bp *ami1* amplicon including 400 bp upstream the *ami1* start codon
H37*ami1*pMVR	GCCGCCGCGTTAACCTAACGCGCCTGGCCCTG	
H37*ami4*pMVF	GCGCGCGCAAGCTTCGGCCTCGCCCGTCCGAC	1311 bp *ami4* amplicon including 400 bp upstream the *ami4* start codon
H37*ami4*pMVR	GCCGCCGCGTTAACCCGGTTGACATCGTTGCA	

*red: restriction endonuclease site

Supplementary Table 2: **Bacterial strains and plasmids created/used in this study**

Strain	Genotype	Reference
H37RvS	Virulent laboratory isolate ATCC 25618	Laboratory Stock
H37Δ*ami1*S	A derivative of H37RvS carrying an unmarked, in-frame deletion in *ami1,* containing 96 bp of the 5' and 78 bp 3' regions, lacking 551 bp of the *ami1* gene	This study
H37Δ*ami4*S	A derivative of H37RvS carrying an unmarked, in-frame deletion in *ami4,* containing 39 bp of the 5' and 82 bp 3' regions, lacking 707 bp of the *ami4* gene	This study
Plasmids	**Genotype**	**Reference**
p2H37ΔAmi1G17	A derivative of p2NIL carrying a truncated derivative of the H37RvS *ami1* gene and the *lacZ* and *sacB* genes from pGOAL17, Kan^R	This study

p2H37ΔAmi4G17	A derivative of p2NIL carrying a truncated derivative of the H37RvS *ami4* gene and the *lacZ* and *sacB* genes from pGOAL17, Kan^R	This study

Kan^R: Kanamycin Resistance, Hyg^R: Hygromycin Resistance

Construction of amidase deficient strains in *M. tuberculosis*

To generate the *ami1* and *ami4* deletion mutants, H37*ami1*KO and H37*ami4*KO primers listed in Table S1 were designed to amplify the upstream and downstream regions of homology for both the *ami1* and *ami4* gene. The resulting upstream and downstream products were fused together to yield *ami1* and *ami4* in-frame deletion alleles. These were then cloned into p2NIL [288] respectively, followed by insertion of a marker cassette from pGOAL17 [288] into the resulting vectors to create the final amidase deletion constructs, p2H37ΔAmi1G17 and p2H37ΔAmi4G17. These suicide vectors were then transformed into electro-competent *M. tuberculosis* H37RvS which were then subjected to two-step allelic exchange mutagenesis yielding the Δ*ami1* and Δ*ami4* mutant strains. The resulting mutants were screened by PCR using the H37*ami1*pMV and H37*ami4*pMV then further validated using southern hybridization.

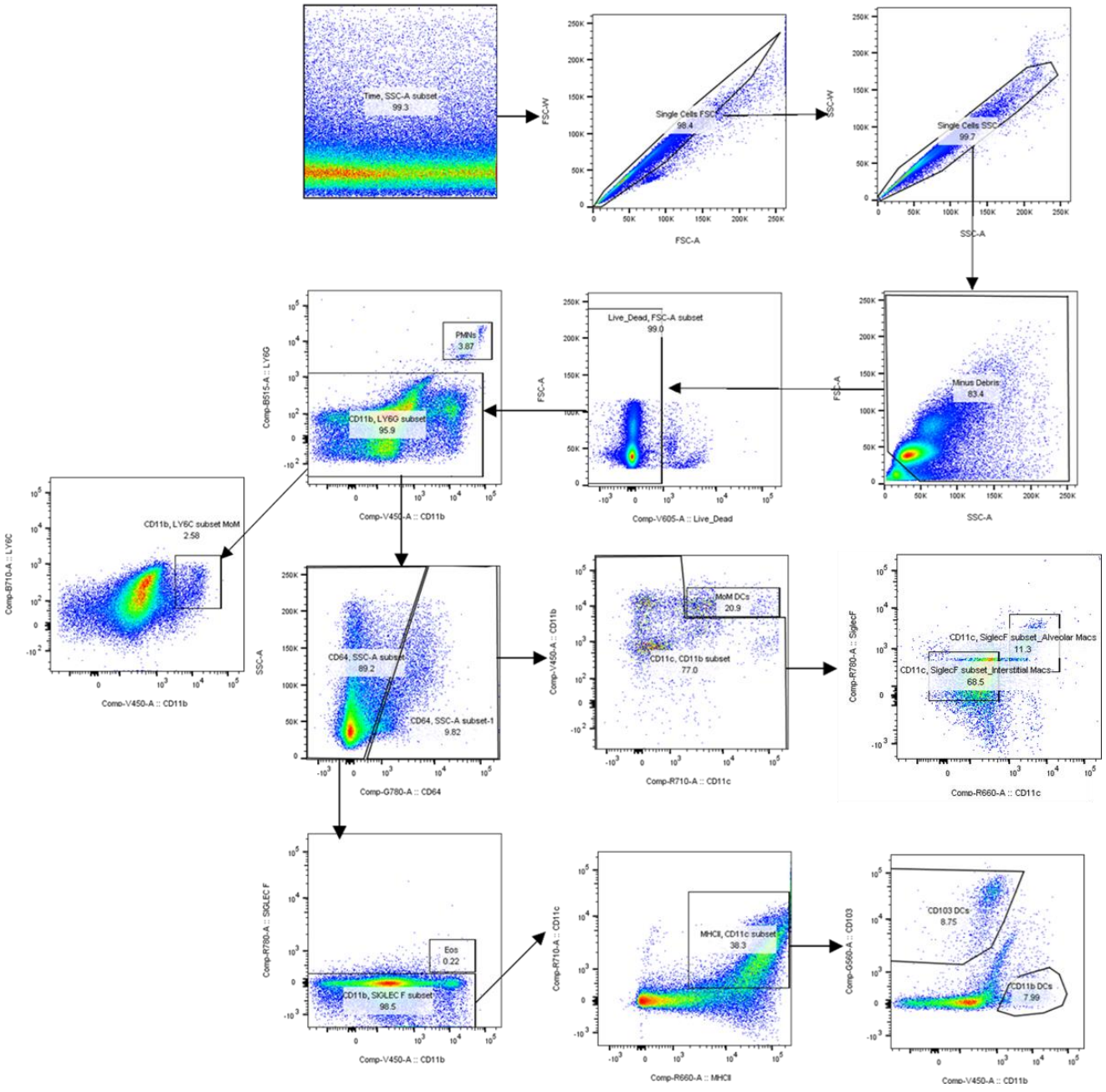

Supplementary Figure 1: **Gating strategy for myeloid cells isolated from Mtb infected mouse lungs**

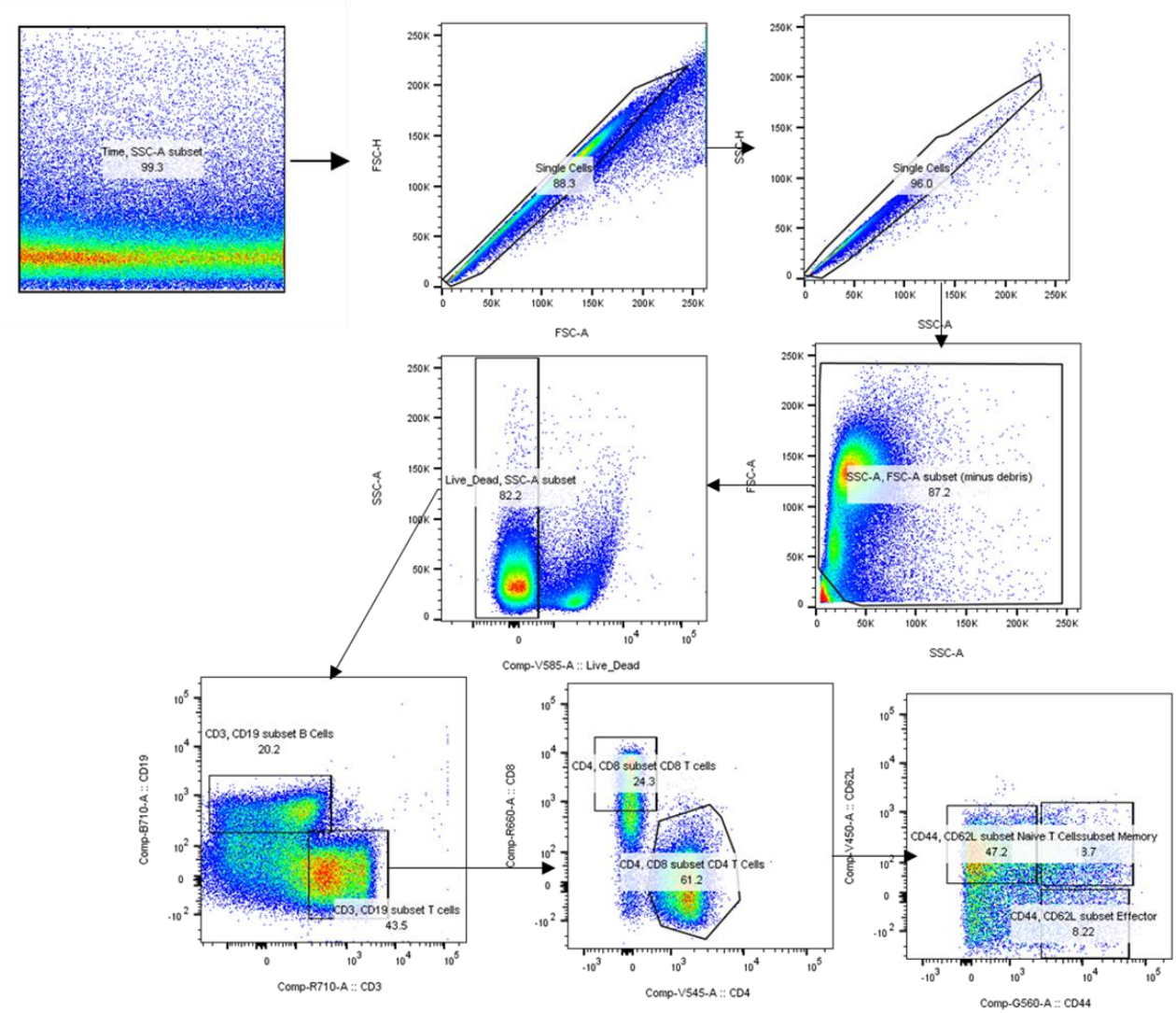

Supplementary Figure 2: **Gating strategy for lymphoid cells isolated from Mtb infected mouse lungs and lymph nodes**

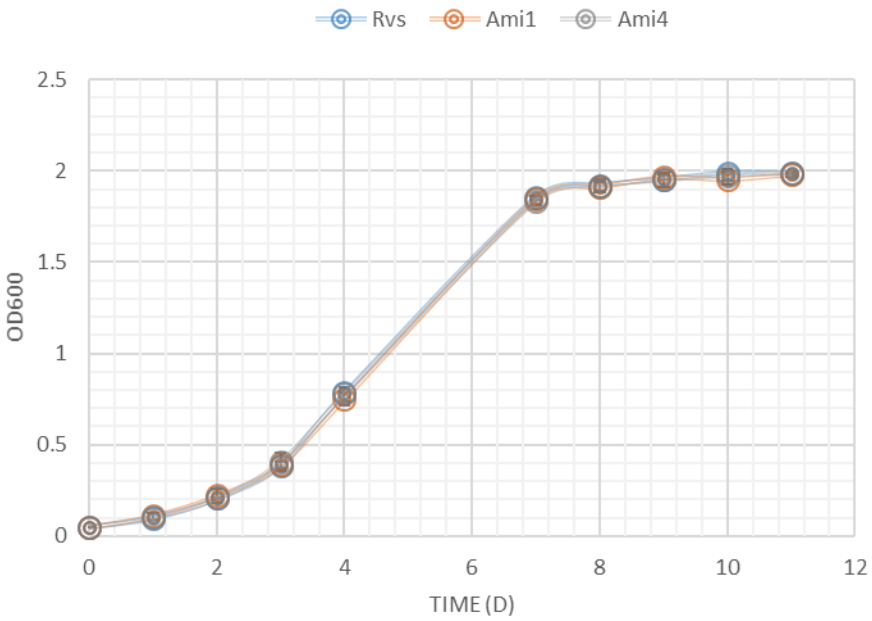

Supplementary Figure 3: **No difference in growth was observed per strain used in this study**. This was assessed Dr Sibusiso Senzani and Dr Melissa Dalcina Chengalroyen, DST/NRF Centre of Excellence for Biomedical TB Research, Faculty of Health Sciences, University of the Witwatersrand, National Health Laboratory Service, Johannesburg, 2001, South Africa, who developed the strains.

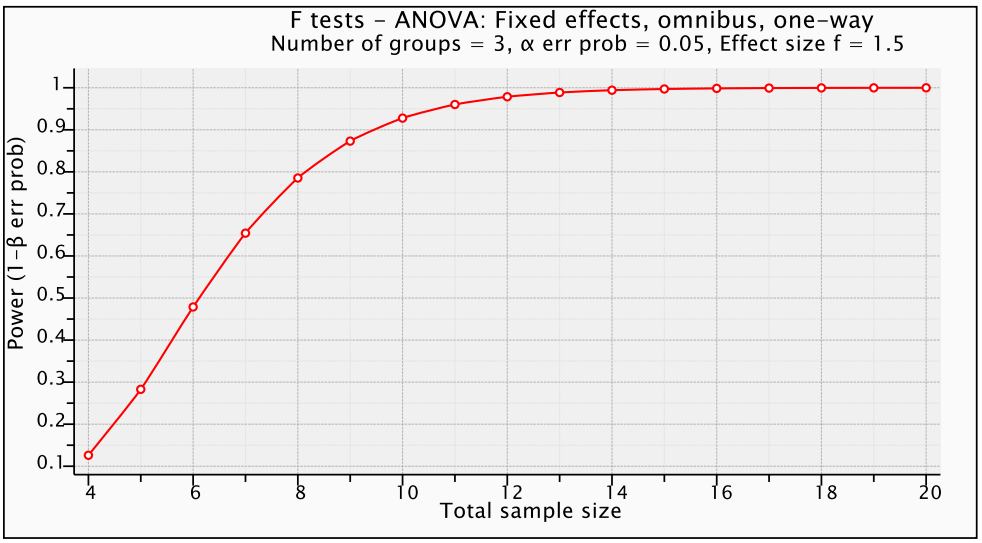

Supplementary Figure 4: **Plot of power (1-β error probability) vs. total sample size for determination of appropriate numbers of experimental mice per group.** A minimum of 9 samples (3 mice per group) was calculated to be sufficient to observe experimental differences with sufficient power (80%)

Bibliography

1. Donoghue, H.D., M. Spigelman, C.L. Greenblatt, G. Lev-Maor, G.K. Bar-Gal, C. Matheson, K. Vernon, A.G. Nerlich, and A.R. Zink, *Tuberculosis: from prehistory to Robert Koch, as revealed by ancient DNA.* The Lancet infectious diseases, 2004. **4**(9): p. 584-592.
2. Gutierrez, M.C., S. Brisse, R. Brosch, M. Fabre, B. Omais, M. Marmiesse, P. Supply, and V. Vincent, *Ancient origin and gene mosaicism of the progenitor of Mycobacterium tuberculosis.* PLoS Pathog, 2005. **1**(1): p. e5.
3. Sreevatsan, S., X. Pan, K.E. Stockbauer, N.D. Connell, B.N. Kreiswirth, T.S. Whittam, and J.M. Musser, *Restricted structural gene polymorphism in the Mycobacterium tuberculosis complex indicates evolutionarily recent global dissemination.* Proc Natl Acad Sci U S A, 1997. **94**(18): p. 9869-74.
4. Kapur, V., T.S. Whittam, and J.M. Musser, *Is Mycobacterium tuberculosis 15,000 years old?* Journal of Infectious Diseases, 1994. **170**(5): p. 1348-1349.
5. Gagneux, S., K. DeRiemer, T. Van, M. Kato-Maeda, B.C. de Jong, S. Narayanan, M. Nicol, S. Niemann, K. Kremer, M.C. Gutierrez, M. Hilty, P.C. Hopewell, and P.M. Small, *Variable host-pathogen compatibility in Mycobacterium tuberculosis.* Proc Natl Acad Sci U S A, 2006. **103**(8): p. 2869-73.
6. Zimmerman, M.R., *Pulmonary and osseous tuberculosis in an Egyptian mummy.* Bull N Y Acad Med, 1979. **55**(6): p. 604-8.
7. Cave, A. and A. Demonstrator, *The evidence for the incidence of tuberculosis in ancient Egypt.* British Journal of Tuberculosis, 1939. **33**(3): p. 142-152.
8. Crubezy, E., B. Ludes, J.D. Poveda, J. Clayton, B. Crouau-Roy, and D. Montagnon, *Identification of Mycobacterium DNA in an Egyptian Pott's disease of 5,400 years old.* C R Acad Sci III, 1998. **321**(11): p. 941-51.
9. Coar, T., *The aphorisms of Hippocrates: with a translation into latin, and english*. 1982: Classics of Medicine Library.
10. Barberis, I., N. Bragazzi, L. Galluzzo, and M. Martini, *The history of tuberculosis: from the first historical records to the isolation of Koch's bacillus.* Journal of preventive medicine and hygiene, 2017. **58**(1): p. E9.
11. Major, R.H., *Classic descriptions of disease: with biographical sketches of the authors*. 1945: Charles C. Thomas Publisher.
12. Koch, R., *Die aetiologie der tuberkulose.* Journal of Molecular Medicine, 1882. **11**(12): p. 490-492.
13. Koch, R., *Ueber bakteriologische Forschung. Verhandlungen des X Internationalen Medichinischen Congresses, Berlin, 1890, 1, 35.* August Hirschwald, Berlin, 1891.
14. von Pirquet, C., *Frequency of tuberculosis in childhood.* Journal of the American Medical Association, 1909. **52**(9): p. 675-678.
15. Long, E.R. and F.B. Seibert, *Further Studies on Purified Protein Derivative of Tuberculin,(PPD) Its Diagnostic Value and Keeping Qualities in Dilutions.* American Review of Tuberculosis, 1937. **35**(3): p. 281-295.
16. Calmette, A., *L'infection bacillaire et la tuberculose chez l'homme et chez les animaux: processus d'infection, et de defense, étude biologique et expérimentale*. 1922: Masson, et cie.
17. Schatz, A., E. Bugie, and S.A. Waksman, *Streptomycin, a substance exhibiting antibiotic activity against gram-positive and gram-negative bacteria.* Clin Orthop Relat Res, 1944(437): p. 3-6.
18. Hinshaw, H. and W. Feldman. *Streptomycin in Treatment of Clinical Tuberculosis: a Preliminary Report*. in *Proceedings of Staff Meetings of the Mayo Clinic*. 1945.
19. Fox, H.H., *The chemical approach to the control of tuberculosis.* Science, 1952. **116**(3006): p. 129-134.

20. Harvard University Library Open Collections Program. *Tuberculosis in Europe and North America, 1800–1922*. 2017 June 2017]; Available from: http://ocp.hul.harvard.edu/contagion/tuberculosis.html.
21. World Health Organization, *Global tuberculosis report 2019.* 2019.
22. Rappuoli, R. and A. Aderem, *A 2020 vision for vaccines against HIV, tuberculosis and malaria.* Nature, 2011. **473**(7348): p. 463-469.
23. Barry, C.E., H.I. Boshoff, V. Dartois, T. Dick, S. Ehrt, J. Flynn, D. Schnappinger, R.J. Wilkinson, and D. Young, *The spectrum of latent tuberculosis: rethinking the biology and intervention strategies.* Nature Reviews Microbiology, 2009. **7**(12): p. 845-855.
24. Narasimhan, P., J. Wood, C.R. MacIntyre, and D. Mathai, *Risk factors for tuberculosis.* Pulmonary medicine, 2013. **2013**.
25. National Institute of Allergy and Infectious Disease. *Tuberculosis (TB)*. 2012 [cited 2017 June 2017]; Available from: http://www.niaid.nih.gov/topics/tuberculosis/Pages/Default.aspx
26. Nunes-Alves, C., M.G. Booty, S.M. Carpenter, P. Jayaraman, A.C. Rothchild, and S.M. Behar, *In search of a new paradigm for protective immunity to TB.* Nature Reviews Microbiology, 2014. **12**(4): p. 289-299.
27. Cohen, S.B., B.H. Gern, J.L. Delahaye, K.N. Adams, C.R. Plumlee, J.K. Winkler, D.R. Sherman, M.Y. Gerner, and K.B. Urdahl, *Alveolar macrophages provide an early Mycobacterium tuberculosis niche and initiate dissemination.* Cell host & microbe, 2018. **24**(3): p. 439-446. e4.
28. Henderson, R.A., S.C. Watkins, and J. Flynn, *Activation of human dendritic cells following infection with Mycobacterium tuberculosis.* The Journal of Immunology, 1997. **159**(2): p. 635-643.
29. Tailleux, L., O. Schwartz, J.-L. Herrmann, E. Pivert, M. Jackson, A. Amara, L. Legres, D. Dreher, L.P. Nicod, and J.C. Gluckman, *DC-SIGN is the major Mycobacterium tuberculosis receptor on human dendritic cells.* The Journal of experimental medicine, 2003. **197**(1): p. 121-127.
30. Sköld, M. and S.M. Behar, *Tuberculosis triggers a tissue-dependent program of differentiation and acquisition of effector functions by circulating monocytes.* The Journal of Immunology, 2008. **181**(9): p. 6349-6360.
31. Samstein, M., H.A. Schreiber, I.M. Leiner, B. Sušac, M.S. Glickman, and E.G. Pamer, *Essential yet limited role for CCR2+ inflammatory monocytes during Mycobacterium tuberculosis-specific T cell priming.* Elife, 2013. **2**: p. e01086.
32. Chackerian, A.A., J.M. Alt, T.V. Perera, C.C. Dascher, and S.M. Behar, *Dissemination of Mycobacterium tuberculosis is influenced by host factors and precedes the initiation of T-cell immunity.* Infection and immunity, 2002. **70**(8): p. 4501-4509.
33. Peters, W. and J.D. Ernst, *Mechanisms of cell recruitment in the immune response to Mycobacterium tuberculosis.* Microbes and infection, 2003. **5**(2): p. 151-158.
34. Khader, S.A., L. Guglani, J. Rangel-Moreno, R. Gopal, B.A.F. Junecko, J.J. Fountain, C. Martino, J.E. Pearl, M. Tighe, and Y.-y. Lin, *IL-23 is required for long-term control of Mycobacterium tuberculosis and B cell follicle formation in the infected lung.* The Journal of Immunology, 2011. **187**(10): p. 5402-5407.
35. Cavalcanti, Y.V.N., M.C.A. Brelaz, J.K.d.A.L. Neves, J.C. Ferraz, and V.R.A. Pereira, *Role of TNF-alpha, IFN-gamma, and IL-10 in the development of pulmonary tuberculosis.* Pulmonary medicine, 2012. **2012**.
36. Cooper, A.M., D.K. Dalton, T.A. Stewart, J.P. Griffin, D.G. Russell, and I.M. Orme, *Disseminated tuberculosis in interferon gamma gene-disrupted mice.* Journal of Experimental Medicine, 1993. **178**(6): p. 2243-2247.
37. Pearl, J.E., B. Saunders, S. Ehlers, I.M. Orme, and A.M. Cooper, *Inflammation and lymphocyte activation during mycobacterial infection in the interferon-γ-deficient mouse.* Cellular immunology, 2001. **211**(1): p. 43-50.
38. Casanova, J.-L. and L. Abel, *The human model: a genetic dissection of immunity to infection in natural conditions.* Nature Reviews Immunology, 2004. **4**(1): p. 55.

39. Szabo, S.J., S.T. Kim, G.L. Costa, X. Zhang, C.G. Fathman, and L.H. Glimcher, *A novel transcription factor, T-bet, directs Th1 lineage commitment.* Cell, 2000. **100**(6): p. 655-669.
40. Sullivan, B.M., O. Jobe, V. Lazarevic, K. Vasquez, R. Bronson, L.H. Glimcher, and I. Kramnik, *Increased susceptibility of mice lacking T-bet to infection with Mycobacterium tuberculosis correlates with increased IL-10 and decreased IFN-γ production.* The Journal of Immunology, 2005. **175**(7): p. 4593-4602.
41. Remus, N., J. Reichenbach, C. Picard, C. Rietschel, P. Wood, D. Lammas, D.S. Kumararatne, and J.-L. Casanova, *Impaired interferon gamma-mediated immunity and susceptibility to mycobacterial infection in childhood.* Pediatric research, 2001. **50**(1): p. 8.
42. Demangel, C., P. Bertolino, and W.J. Britton, *Autocrine IL-10 impairs dendritic cell (DC)-derived immune responses to mycobacterial infection by suppressing DC trafficking to draining lymph nodes and local IL-12 production.* European journal of immunology, 2002. **32**(4): p. 994-1002.
43. Mahamed, D., M. Boulle, Y. Ganga, C. Mc Arthur, S. Skroch, L. Oom, O. Catinas, K. Pillay, M. Naicker, and S. Rampersad, *Intracellular growth of Mycobacterium tuberculosis after macrophage cell death leads to serial killing of host cells.* Elife, 2017. **6**: p. e22028.
44. Huang, L., E.V. Nazarova, S. Tan, Y. Liu, and D.G. Russell, *Growth of Mycobacterium tuberculosis in vivo segregates with host macrophage metabolism and ontogeny.* Journal of Experimental Medicine, 2018. **215**(4): p. 1135-1152.
45. MacMicking, J.D., R.J. North, R. LaCourse, J.S. Mudgett, S.K. Shah, and C.F. Nathan, *Identification of nitric oxide synthase as a protective locus against tuberculosis.* Proceedings of the National Academy of Sciences, 1997. **94**(10): p. 5243-5248.
46. Russell, D.G., P.-J. Cardona, M.-J. Kim, S. Allain, and F. Altare, *Foamy macrophages and the progression of the human tuberculosis granuloma.* Nature immunology, 2009. **10**(9): p. 943-948.
47. Gharun, K., J. Senges, M. Seidl, A. Lösslein, J. Kolter, F. Lohrmann, M. Fliegauf, M. Elgizouli, M. Vavra, and K. Schachtrup, *Mycobacteria exploit nitric oxide-induced transformation of macrophages into permissive giant cells.* EMBO reports, 2017. **18**(12): p. 2144-2159.
48. Ramakrishnan, L., *Revisiting the role of the granuloma in tuberculosis.* Nature Reviews Immunology, 2012. **12**(5): p. 352-366.
49. Carrol, E., J. Clark, and A. Cant, *Non-pulmonary tuberculosis.* Paediatric Respiratory Reviews, 2001. **2**(2): p. 113-119.
50. Marimani, M., A. Ahmad, and A. Duse, *The role of epigenetics, bacterial and host factors in progression of Mycobacterium tuberculosis infection.* Tuberculosis, 2018. **113**: p. 200-214.
51. World Health Organization, *Global tuberculosis report 2016.* 2016.
52. Andersen, P. and T.M. Doherty, *The success and failure of BCG—implications for a novel tuberculosis vaccine.* Nature Reviews Microbiology, 2005. **3**(8): p. 656-662.
53. Ndiaye, B.P., F. Thienemann, M. Ota, B.S. Landry, M. Camara, S. Dièye, T.N. Dieye, H. Esmail, R. Goliath, and K. Huygen, *Safety, immunogenicity, and efficacy of the candidate tuberculosis vaccine MVA85A in healthy adults infected with HIV-1: a randomised, placebo-controlled, phase 2 trial.* The Lancet Respiratory Medicine, 2015. **3**(3): p. 190-200.
54. Tameris, M.D., M. Hatherill, B.S. Landry, T.J. Scriba, M.A. Snowden, S. Lockhart, J.E. Shea, J.B. McClain, G.D. Hussey, and W.A. Hanekom, *Safety and efficacy of MVA85A, a new tuberculosis vaccine, in infants previously vaccinated with BCG: a randomised, placebo-controlled phase 2b trial.* The Lancet, 2013. **381**(9871): p. 1021-1028.
55. Tait, D.R., M. Hatherill, O. Van Der Meeren, A.M. Ginsberg, E. Van Brakel, B. Salaun, T.J. Scriba, E.J. Akite, H.M. Ayles, A. Bollaerts, M.A. Demoitie, A. Diacon, T.G. Evans, P. Gillard, E. Hellstrom, J.C. Innes, M. Lempicki, M. Malahleha, N. Martinson, D. Mesia Vela, M. Muyoyeta, V. Nduba, T.G. Pascal, M. Tameris, F. Thienemann, R.J. Wilkinson, and F. Roman, *Final Analysis of a Trial of M72/AS01E Vaccine to Prevent Tuberculosis.* N Engl J Med, 2019.
56. Pyle, M.M. *Relative numbers of resistant tubercle bacilli in sputa of patients before and during treatment with streptomycin*. in *Proceedings of the staff meetings. Mayo Clinic*. 1947.

57. Seung, K.J., S. Keshavjee, and M.L. Rich, *Multidrug-resistant tuberculosis and extensively drug-resistant tuberculosis.* Cold Spring Harbor perspectives in medicine, 2015. **5**(9): p. a017863.
58. Alderwick, L.J., J. Harrison, G.S. Lloyd, and H.L. Birch, *The mycobacterial cell wall—peptidoglycan and arabinogalactan.* Cold Spring Harbor perspectives in medicine, 2015. **5**(8): p. a021113.
59. Gupta, R., M. Lavollay, J.-L. Mainardi, M. Arthur, W.R. Bishai, and G. Lamichhane, *The Mycobacterium tuberculosis protein Ldt Mt2 is a nonclassical transpeptidase required for virulence and resistance to amoxicillin.* Nature medicine, 2010. **16**(4): p. 466-469.
60. Jankute, M., J.A. Cox, J. Harrison, and G.S. Besra, *Assembly of the mycobacterial cell wall.* Annual review of microbiology, 2015. **69**: p. 405-423.
61. Jackson, M., C. Raynaud, M.A. Lanéelle, C. Guilhot, C. Laurent-Winter, D. Ensergueix, B. Gicquel, and M. Daffé, *Inactivation of the antigen 85C gene profoundly affects the mycolate content and alters the permeability of the Mycobacterium tuberculosis cell envelope.* Molecular microbiology, 1999. **31**(5): p. 1573-1587.
62. Ronning, D.R., T. Klabunde, G.S. Besra, V.D. Vissa, J.T. Belisle, and J.C. Sacchettini, *Crystal structure of the secreted form of antigen 85C reveals potential targets for mycobacterial drugs and vaccines.* Nature structural biology, 2000. **7**(2): p. 141-146.
63. Nguyen, L., S. Chinnapapagari, and C.J. Thompson, *FbpA-dependent biosynthesis of trehalose dimycolate is required for the intrinsic multidrug resistance, cell wall structure, and colonial morphology of Mycobacterium smegmatis.* Journal of bacteriology, 2005. **187**(19): p. 6603-6611.
64. Lingaraju, S., L. Rigouts, A. Gupta, J. Lee, A.N. Umubyeyi, A.L. Davidow, S. German, E. Cho, S.-N. Cho, and C.T. Kim, *Geographic differences in the contribution of ubiA mutations to high-level ethambutol resistance in Mycobacterium tuberculosis.* Antimicrobial agents and chemotherapy, 2016. **60**(7): p. 4101-4105.
65. Brossier, F., W. Sougakoff, C. Bernard, M. Petrou, K. Adeyema, A. Pham, D.A. de La Brete que, M. Vallet, V. Jarlier, and C. Sola, *Molecular analysis of the embCAB locus and embR gene involved in ethambutol resistance in clinical isolates of Mycobacterium tuberculosis in France.* Antimicrobial agents and chemotherapy, 2015. **59**(8): p. 4800-4808.
66. Faller, M., M. Niederweis, and G.E. Schulz, *The structure of a mycobacterial outer-membrane channel.* Science, 2004. **303**(5661): p. 1189-1192.
67. Stahl, C., S. Kubetzko, I. Kaps, S. Seeber, H. Engelhardt, and M. Niederweis, *MspA provides the main hydrophilic pathway through the cell wall of Mycobacterium smegmatis.* Molecular microbiology, 2001. **40**(2): p. 451-464.
68. Mailaender, C., N. Reiling, H. Engelhardt, S. Bossmann, S. Ehlers, and M. Niederweis, *The MspA porin promotes growth and increases antibiotic susceptibility of both Mycobacterium bovis BCG and Mycobacterium tuberculosis.* Microbiology, 2004. **150**(4): p. 853-864.
69. Gupta, A.K., V.P. Reddy, M. Lavania, D. Chauhan, K. Venkatesan, V. Sharma, A. Tyagi, and V. Katoch, *jefA (Rv2459), a drug efflux gene in Mycobacterium tuberculosis confers resistance to isoniazid & ethambutol.* Indian J Med Res, 2010. **132**(2): p. 176-188.
70. Almeida Da Silva, P.E. and J.C. Palomino, *Molecular basis and mechanisms of drug resistance in Mycobacterium tuberculosis: classical and new drugs.* Journal of antimicrobial chemotherapy, 2011. **66**(7): p. 1417-1430.
71. Cohen, K.A., W.R. Bishai, and A.S. Pym, *Molecular basis of drug resistance in Mycobacterium tuberculosis.* Molecular Genetics of Mycobacteria, 2014: p. 411-429.
72. Torres, J.N., L.V. Paul, T.C. Rodwell, T.C. Victor, A.M. Amallraja, A. Elghraoui, A.P. Goodmanson, S.M. Ramirez-Busby, A. Chawla, and V. Zadorozhny, *Novel katG mutations causing isoniazid resistance in clinical M. tuberculosis isolates.* Emerging microbes & infections, 2015. **4**(1): p. 1-9.

73. Nasiri, M.J., H. Dabiri, D. Darban-Sarokhalil, and A.H. Shahraki, *Prevalence of non-tuberculosis mycobacterial infections among tuberculosis suspects in Iran: systematic review and meta-analysis.* PloS one, 2015. **10**(6): p. e0129073.
74. Gu, Y., X. Yu, G. Jiang, X. Wang, Y. Ma, Y. Li, and H. Huang, *Pyrazinamide resistance among multidrug-resistant tuberculosis clinical isolates in a national referral center of China and its correlations with pncA, rpsA, and panD gene mutations.* Diagnostic microbiology and infectious disease, 2016. **84**(3): p. 207-211.
75. Shi, W., J. Chen, J. Feng, P. Cui, S. Zhang, X. Weng, W. Zhang, and Y. Zhang, *Aspartate decarboxylase (PanD) as a new target of pyrazinamide in Mycobacterium tuberculosis.* Emerging microbes & infections, 2014. **3**(1): p. 1-8.
76. Shi, W., X. Zhang, X. Jiang, H. Yuan, J.S. Lee, C.E. Barry, H. Wang, W. Zhang, and Y. Zhang, *Pyrazinamide inhibits trans-translation in Mycobacterium tuberculosis.* Science, 2011. **333**(6049): p. 1630-1632.
77. Zhang, S., J. Chen, W. Shi, P. Cui, J. Zhang, S. Cho, W. Zhang, and Y. Zhang, *Mutation in clpC1 encoding an ATP-dependent ATPase involved in protein degradation is associated with pyrazinamide resistance in Mycobacterium tuberculosis.* Emerging Microbes & Infections, 2017. **6**(1): p. 1-2.
78. Zhang, S., J. Chen, W. Shi, W. Liu, W. Zhang, and Y. Zhang, *Mutations in panD encoding aspartate decarboxylase are associated with pyrazinamide resistance in Mycobacterium tuberculosis.* Emerging microbes & infections, 2013. **2**(1): p. 1-5.
79. Safi, H., S. Lingaraju, A. Amin, S. Kim, M. Jones, M. Holmes, M. McNeil, S.N. Peterson, D. Chatterjee, and R. Fleischmann, *Evolution of high-level ethambutol-resistant tuberculosis through interacting mutations in decaprenylphosphoryl-β-D-arabinose biosynthetic and utilization pathway genes.* Nature genetics, 2013. **45**(10): p. 1190-1197.
80. He, L., X. Wang, P. Cui, J. Jin, J. Chen, W. Zhang, and Y. Zhang, *ubiA (Rv3806c) encoding DPPR synthase involved in cell wall synthesis is associated with ethambutol resistance in Mycobacterium tuberculosis.* Tuberculosis, 2015. **95**(2): p. 149-154.
81. Nasiri, M.J., M. Haeili, M. Ghazi, H. Goudarzi, A. Pormohammad, A.A. Imani Fooladi, and M.M. Feizabadi, *New insights in to the intrinsic and acquired drug resistance mechanisms in mycobacteria.* Frontiers in microbiology, 2017. **8**: p. 681.
82. Guler, R. and F. Brombacher, *Host-directed drug therapy for tuberculosis.* Nature chemical biology, 2015. **11**(10): p. 748.
83. Doerks, T., V. Van Noort, P. Minguez, and P. Bork, *Annotation of the M. tuberculosis hypothetical orfeome: adding functional information to more than half of the uncharacterized proteins.* PloS one, 2012. **7**(4): p. e34302.
84. Kieser, K.J. and E.J. Rubin, *How sisters grow apart: mycobacterial growth and division.* Nature Reviews Microbiology, 2014. **12**(8): p. 550-562.
85. Aldridge, B.B., M. Fernandez-Suarez, D. Heller, V. Ambravaneswaran, D. Irimia, M. Toner, and S.M. Fortune, *Asymmetry and aging of mycobacterial cells lead to variable growth and antibiotic susceptibility.* Science, 2012. **335**(6064): p. 100-104.
86. Santi, I., N. Dhar, D. Bousbaine, Y. Wakamoto, and J.D. McKinney, *Single-cell dynamics of the chromosome replication and cell division cycles in mycobacteria.* Nature communications, 2013. **4**(1): p. 1-11.
87. Van der Ploeg, R., J. Verheul, N.O. Vischer, S. Alexeeva, E. Hoogendoorn, M. Postma, M. Banzhaf, W. Vollmer, and T. Den Blaauwen, *Colocalization and interaction between elongasome and divisome during a preparative cell division phase in E scherichia coli.* Molecular microbiology, 2013. **87**(5): p. 1074-1087.
88. Typas, A., M. Banzhaf, C.A. Gross, and W. Vollmer, *From the regulation of peptidoglycan synthesis to bacterial growth and morphology.* Nature Reviews Microbiology, 2012. **10**(2): p. 123-136.

89. Hett, E.C. and E.J. Rubin, *Bacterial growth and cell division: a mycobacterial perspective.* Microbiology and Molecular Biology Reviews, 2008. **72**(1): p. 126-156.
90. Adams, D.W. and J. Errington, *Bacterial cell division: assembly, maintenance and disassembly of the Z ring.* Nature Reviews Microbiology, 2009. **7**(9): p. 642-653.
91. Li, Y., J. Hsin, L. Zhao, Y. Cheng, W. Shang, K.C. Huang, H.-W. Wang, and S. Ye, *FtsZ protofilaments use a hinge-opening mechanism for constrictive force generation.* Science, 2013. **341**(6144): p. 392-395.
92. England, K., R. Crew, and R.A. Slayden, *Mycobacterium tuberculosis septum site determining protein, Ssd encoded by rv3660c, promotes filamentation and elicits an alternative metabolic and dormancy stress response.* BMC microbiology, 2011. **11**(1): p. 79.
93. Thakur, M. and P.K. Chakraborti, *GTPase activity of mycobacterial FtsZ is impaired due to its transphosphorylation by the eukaryotic-type Ser/Thr kinase, PknA.* Journal of Biological Chemistry, 2006. **281**(52): p. 40107-40113.
94. Hett, E.C., M.C. Chao, L.L. Deng, and E.J. Rubin, *A mycobacterial enzyme essential for cell division synergizes with resuscitation-promoting factor.* PLoS Pathog, 2008. **4**(2): p. e1000001.
95. Hett, E.C., M.C. Chao, A.J. Steyn, S.M. Fortune, L.L. Deng, and E.J. Rubin, *A partner for the resuscitation-promoting factors of Mycobacterium tuberculosis.* Molecular microbiology, 2007. **66**(3): p. 658-668.
96. Hett, E.C., M.C. Chao, and E.J. Rubin, *Interaction and modulation of two antagonistic cell wall enzymes of mycobacteria.* PLoS Pathog, 2010. **6**(7): p. e1001020.
97. Deng, L.L., D.E. Humphries, R.D. Arbeit, L.E. Carlton, S.C. Smole, and J.D. Carroll, *Identification of a novel peptidoglycan hydrolase CwlM in Mycobacterium tuberculosis.* Biochimica Et Biophysica Acta (BBA)-Proteins and Proteomics, 2005. **1747**(1): p. 57-66.
98. Machowski, E.E., S. Senzani, C. Ealand, and B.D. Kana, *Comparative genomics for mycobacterial peptidoglycan remodelling enzymes reveals extensive genetic multiplicity.* BMC microbiology, 2014. **14**(1): p. 75.
99. Healy, C., A. Gouzy, and S. Ehrt, *Peptidoglycan Hydrolases RipA and Ami1 Are Critical for Replication and Persistence of Mycobacterium tuberculosis in the Host.* Mbio, 2020. **11**(2).
100. Barry, C.E., D.C. Crick, and M.R. McNeil, *Targeting the formation of the cell wall core of M. tuberculosis.* Infect Disord Drug Targets, 2007. **7**(2): p. 182-202.
101. Kaur, D., M.E. Guerin, H. Skovierova, P.J. Brennan, and M. Jackson, *Chapter 2: Biogenesis of the cell wall and other glycoconjugates of Mycobacterium tuberculosis.* Adv Appl Microbiol, 2009. **69**: p. 23-78.
102. Heijenoort, J.v., *Formation of the glycan chains in the synthesis of bacterial peptidoglycan.* Glycobiology, 2001. **11**(3): p. 25R-36R.
103. Heidrich, C., A. Ursinus, J. Berger, H. Schwarz, and J.-V. Höltje, *Effects of multiple deletions of murein hydrolases on viability, septum cleavage, and sensitivity to large toxic molecules in Escherichia coli.* Journal of bacteriology, 2002. **184**(22): p. 6093-6099.
104. Sarkar, P., V. Yarlagadda, C. Ghosh, and J. Haldar, *A review on cell wall synthesis inhibitors with an emphasis on glycopeptide antibiotics.* MedChemComm, 2017. **8**(3): p. 516-533.
105. Koch, A.L., *Bacterial wall as target for attack: past, present, and future research.* Clinical microbiology reviews, 2003. **16**(4): p. 673-687.
106. Chambers, H.F., D. Moreau, D. Yajko, C. Miick, C. Wagner, C. Hackbarth, S. Kocagöz, E. Rosenberg, W. Hadley, and H. Nikaido, *Can penicillins and other beta-lactam antibiotics be used to treat tuberculosis?* Antimicrobial agents and chemotherapy, 1995. **39**(12): p. 2620-2624.
107. Bouhss, A., A.E. Trunkfield, T.D. Bugg, and D. Mengin-Lecreulx, *The biosynthesis of peptidoglycan lipid-linked intermediates.* FEMS microbiology reviews, 2007. **32**(2): p. 208-233.
108. Gee, C.L., K.G. Papavinasasundaram, S.R. Blair, C.E. Baer, A.M. Falick, D.S. King, J.E. Griffin, H. Venghatakrishnan, A. Zukauskas, and J.-R. Wei, *A phosphorylated pseudokinase complex controls cell wall synthesis in mycobacteria.* Science signaling, 2012. **5**(208): p. ra7.

109. Meniche, X., R. Otten, M.S. Siegrist, C.E. Baer, K.C. Murphy, C.R. Bertozzi, and C.M. Sassetti, *Subpolar addition of new cell wall is directed by DivIVA in mycobacteria.* Proceedings of the National Academy of Sciences, 2014. **111**(31): p. E3243-E3251.
110. Plocinski, P., N. Arora, K. Sarva, E. Blaszczyk, H. Qin, N. Das, R. Plocinska, M. Ziolkiewicz, J. Dziadek, and M. Kiran, *Mycobacterium tuberculosis CwsA interacts with CrgA and Wag31, and the CrgA-CwsA complex is involved in peptidoglycan synthesis and cell shape determination.* Journal of bacteriology, 2012. **194**(23): p. 6398-6409.
111. Plocinski, P., L. Martinez, K. Sarva, R. Plocinska, M. Madiraju, and M. Rajagopalan, *Mycobacterium tuberculosis CwsA overproduction modulates cell division and cell wall synthesis.* Tuberculosis, 2013. **93**: p. S21-S27.
112. Egan, A.J., J. Biboy, I. van't Veer, E. Breukink, and W. Vollmer, *Activities and regulation of peptidoglycan synthases.* Philosophical Transactions of the Royal Society B: Biological Sciences, 2015. **370**(1679): p. 20150031.
113. Lavollay, M., M. Arthur, M. Fourgeaud, L. Dubost, A. Marie, N. Veziris, D. Blanot, L. Gutmann, and J.-L. Mainardi, *The peptidoglycan of stationary-phase Mycobacterium tuberculosis predominantly contains cross-links generated by L, D-transpeptidation.* Journal of bacteriology, 2008. **190**(12): p. 4360-4366.
114. Mahapatra, S., H. Scherman, P.J. Brennan, and D.C. Crick, *N Glycolylation of the nucleotide precursors of peptidoglycan biosynthesis of Mycobacterium spp. is altered by drug treatment.* Journal of bacteriology, 2005. **187**(7): p. 2341-2347.
115. Raymond, J.B., S. Mahapatra, D.C. Crick, and M.S. Pavelka, *Identification of the namH gene, encoding the hydroxylase responsible for the N-glycolylation of the mycobacterial peptidoglycan.* Journal of Biological Chemistry, 2005. **280**(1): p. 326-333.
116. Bisicchia, P., D. Noone, E. Lioliou, A. Howell, S. Quigley, T. Jensen, H. Jarmer, and K.M. Devine, *The essential YycFG two-component system controls cell wall metabolism in Bacillus subtilis.* Molecular microbiology, 2007. **65**(1): p. 180-200.
117. Ohnishi, R., S. Ishikawa, and J. Sekiguchi, *Peptidoglycan hydrolase LytF plays a role in cell separation with CwlF during vegetative growth of Bacillus subtilis.* Journal of bacteriology, 1999. **181**(10): p. 3178-3184.
118. Vollmer, W. and J.-V. Höltje, *The architecture of the murein (peptidoglycan) in gram-negative bacteria: vertical scaffold or horizontal layer (s)?* Journal of bacteriology, 2004. **186**(18): p. 5978-5987.
119. Irazoki, O., S.B. Hernandez, and F. Cava, *Peptidoglycan muropeptides: release, perception, and functions as signaling molecules.* Frontiers in microbiology, 2019. **10**: p. 500.
120. Goodell, E., *Recycling of murein by Escherichia coli.* Journal of bacteriology, 1985. **163**(1): p. 305-310.
121. Johnson, J.W., J.F. Fisher, and S. Mobashery, *Bacterial cell-wall recycling.* Annals of the New York Academy of Sciences, 2013. **1277**(1): p. 54.
122. Park, J.T. and T. Uehara, *How bacteria consume their own exoskeletons (turnover and recycling of cell wall peptidoglycan).* Microbiol. Mol. Biol. Rev., 2008. **72**(2): p. 211-227.
123. Mauck, J., L. Chan, and L. Glaser, *Turnover of the cell wall of Gram-positive bacteria.* Journal of Biological Chemistry, 1971. **246**(6): p. 1820-1827.
124. Boothby, D., L. Daneo-Moore, M.L. Higgins, J. Coyette, and G.D. Shockman, *Turnover of bacterial cell wall peptidoglycans.* Journal of Biological Chemistry, 1973. **248**(6): p. 2161-2169.
125. Chaloupka, J. and M. Strnadová, *Turnover of murein in a diaminopimelic acid dependent mutant ofEscherichia coli.* Folia microbiologica, 1972. **17**(6): p. 446-455.
126. Reith, J. and C. Mayer, *Peptidoglycan turnover and recycling in Gram-positive bacteria.* Applied microbiology and biotechnology, 2011. **92**(1): p. 1.
127. Girardin, S.E., L.H. Travassos, M. Hervé, D. Blanot, I.G. Boneca, D.J. Philpott, P.J. Sansonetti, and D. Mengin-Lecreulx, *Peptidoglycan molecular requirements allowing detection by Nod1 and Nod2.* Journal of Biological Chemistry, 2003. **278**(43): p. 41702-41708.

128. Höltje, J.-V., *From growth to autolysis: the murein hydrolases inEscherichia coli.* Archives of microbiology, 1995. **164**(4): p. 243-254.
129. Vollmer, W., B. Joris, P. Charlier, and S. Foster, *Bacterial peptidoglycan (murein) hydrolases.* FEMS Microbiol Rev, 2008. **32**(2): p. 259-86.
130. Herlihey, F.A. and A.J. Clarke, *Controlling autolysis during flagella insertion in Gram-negative bacteria*, in *Protein Reviews*. 2016, Springer. p. 41-56.
131. Callewaert, L., J.M. Van Herreweghe, L. Vanderkelen, S. Leysen, A. Voet, and C.W. Michiels, *Guards of the great wall: bacterial lysozyme inhibitors.* Trends in microbiology, 2012. **20**(10): p. 501-510.
132. Vermassen, A., S. Leroy, R. Talon, C. Provot, M. Popowska, and M. Desvaux, *Cell wall hydrolases in bacteria: insight on the diversity of cell wall amidases, glycosidases and peptidases towards peptidoglycan.* Frontiers in microbiology, 2019. **10**: p. 331.
133. Smith, T.J., S.A. Blackman, and S.J. Foster, *Autolysins of Bacillus subtilis: multiple enzymes with multiple functions.* Microbiology, 2000. **146**(2): p. 249-262.
134. Loessner, M.J., *Bacteriophage endolysins—current state of research and applications.* Current opinion in microbiology, 2005. **8**(4): p. 480-487.
135. Young, R., *Bacteriophage lysis: mechanism and regulation.* Microbiology and Molecular Biology Reviews, 1992. **56**(3): p. 430-481.
136. Kerff, F., S. Petrella, F. Mercier, E. Sauvage, R. Herman, A. Pennartz, A. Zervosen, A. Luxen, J.-M. Frère, and B. Joris, *Specific structural features of the N-acetylmuramoyl-L-alanine amidase AmiD from Escherichia coli and mechanistic implications for enzymes of this family.* Journal of molecular biology, 2010. **397**(1): p. 249-259.
137. Heidrich, C., M.F. Templin, A. Ursinus, M. Merdanovic, J. Berger, H. Schwarz, M.A. De Pedro, and J.V. Höltje, *Involvement of N-acetylmuramyl-L-alanine amidases in cell separation and antibiotic-induced autolysis of Escherichia coli.* Molecular microbiology, 2001. **41**(1): p. 167-178.
138. Bernhardt, T.G. and P.A. De Boer, *The Escherichia coli amidase AmiC is a periplasmic septal ring component exported via the twin-arginine transport pathway.* Molecular microbiology, 2003. **48**(5): p. 1171-1182.
139. Korndörfer, I.P., J. Danzer, M. Schmelcher, M. Zimmer, A. Skerra, and M.J. Loessner, *The crystal structure of the bacteriophage PSA endolysin reveals a unique fold responsible for specific recognition of Listeria cell walls.* Journal of molecular biology, 2006. **364**(4): p. 678-689.
140. Weidel, W. and H. Pelzer, *Bagshaped Macromolecules--a New Outlook on Bacterial Cell Walls.* Adv Enzymol Relat Areas Mol Biol, 1964. **26**: p. 193-232.
141. Höltje, J.-V., *"Three for one"—a Simple Growth Mechanism that Guarantees a Precise Copy of the Thin, Rod-Shaped Murein Sacculus of Escherichia coli*, in *Bacterial Growth and Lysis*. 1993, Springer. p. 419-426.
142. Vollmer, W. and U. Bertsche, *Murein (peptidoglycan) structure, architecture and biosynthesis in Escherichia coli.* Biochimica et Biophysica Acta (BBA)-Biomembranes, 2008. **1778**(9): p. 1714-1734.
143. Goodell, E.W. and U. Schwarz, *Release of cell wall peptides into culture medium by exponentially growing Escherichia coli.* Journal of bacteriology, 1985. **162**(1): p. 391-397.
144. Korsak, D., S. Liebscher, and W. Vollmer, *Susceptibility to antibiotics and β-lactamase induction in murein hydrolase mutants of Escherichia coli.* Antimicrobial agents and chemotherapy, 2005. **49**(4): p. 1404-1409.
145. Steiner, H., *Peptidoglycan recognition proteins: on and off switches for innate immunity.* Immunological reviews, 2004. **198**(1): p. 83-96.
146. Mellroth, P. and H. Steiner, *PGRP-SB1: an N-acetylmuramoyl L-alanine amidase with antibacterial activity.* Biochemical and biophysical research communications, 2006. **350**(4): p. 994-999.

147. Zaidman-Rémy, A., M. Hervé, M. Poidevin, S. Pili-Floury, M.-S. Kim, D. Blanot, B.-H. Oh, R. Ueda, D. Mengin-Lecreulx, and B. Lemaitre, *The Drosophila amidase PGRP-LB modulates the immune response to bacterial infection*. Immunity, 2006. **24**(4): p. 463-473.
148. Yoshimura, A., E. Lien, R.R. Ingalls, E. Tuomanen, R. Dziarski, and D. Golenbock, *Cutting edge: recognition of Gram-positive bacterial cell wall components by the innate immune system occurs via Toll-like receptor 2.* The Journal of Immunology, 1999. **163**(1): p. 1-5.
149. Takeuchi, O., K. Hoshino, T. Kawai, H. Sanjo, H. Takada, T. Ogawa, K. Takeda, and S. Akira, *Differential roles of TLR2 and TLR4 in recognition of gram-negative and gram-positive bacterial cell wall components.* Immunity, 1999. **11**(4): p. 443-451.
150. Ozinsky, A., D.M. Underhill, J.D. Fontenot, A.M. Hajjar, K.D. Smith, C.B. Wilson, L. Schroeder, and A. Aderem, *The repertoire for pattern recognition of pathogens by the innate immune system is defined by cooperation between toll-like receptors.* Proceedings of the National Academy of Sciences, 2000. **97**(25): p. 13766-13771.
151. Travassos, L.H., S.E. Girardin, D.J. Philpott, D. Blanot, M.A. Nahori, C. Werts, and I.G. Boneca, *Toll-like receptor 2-dependent bacterial sensing does not occur via peptidoglycan recognition.* EMBO reports, 2004. **5**(10): p. 1000-1006.
152. Dziarski, R. and D. Gupta, *Staphylococcus aureus peptidoglycan is a toll-like receptor 2 activator: a reevaluation.* Infection and immunity, 2005. **73**(8): p. 5212-5216.
153. Wolf, A.J. and D.M. Underhill, *Peptidoglycan recognition by the innate immune system.* Nature Reviews Immunology, 2018. **18**(4): p. 243.
154. Royet, J., D. Gupta, and R. Dziarski, *Peptidoglycan recognition proteins: modulators of the microbiome and inflammation.* Nature Reviews Immunology, 2011. **11**(12): p. 837-851.
155. Chamaillard, M., M. Hashimoto, Y. Horie, J. Masumoto, S. Qiu, L. Saab, Y. Ogura, A. Kawasaki, K. Fukase, and S. Kusumoto, *An essential role for NOD1 in host recognition of bacterial peptidoglycan containing diaminopimelic acid.* Nature immunology, 2003. **4**(7): p. 702-707.
156. Girardin, S.E., I.G. Boneca, L.A. Carneiro, A. Antignac, M. Jéhanno, J. Viala, K. Tedin, M.-K. Taha, A. Labigne, and U. Zähringer, *Nod1 detects a unique muropeptide from gram-negative bacterial peptidoglycan.* Science, 2003. **300**(5625): p. 1584-1587.
157. Melnyk, J.E., V. Mohanan, A.K. Schaefer, C.-W. Hou, and C.L. Grimes, *Peptidoglycan modifications tune the stability and function of the innate immune receptor Nod2.* Journal of the American Chemical Society, 2015. **137**(22): p. 6987-6990.
158. Girardin, S.E., I.G. Boneca, J. Viala, M. Chamaillard, A. Labigne, G. Thomas, D.J. Philpott, and P.J. Sansonetti, *Nod2 is a general sensor of peptidoglycan through muramyl dipeptide (MDP) detection.* Journal of Biological Chemistry, 2003. **278**(11): p. 8869-8872.
159. Lee, J., I. Tattoli, K.A. Wojtal, S.R. Vavricka, D.J. Philpott, and S.E. Girardin, *pH-dependent internalization of muramyl peptides from early endosomes enables Nod1 and Nod2 signaling.* Journal of Biological Chemistry, 2009. **284**(35): p. 23818-23829.
160. Caruso, R., N. Warner, N. Inohara, and G. Núñez, *NOD1 and NOD2: signaling, host defense, and inflammatory disease.* Immunity, 2014. **41**(6): p. 898-908.
161. Vollmer, W. and A. Tomasz, *The pgdA gene encodes for a peptidoglycanN-acetylglucosamine deacetylase in Streptococcus pneumoniae.* Journal of Biological Chemistry, 2000. **275**(27): p. 20496-20501.
162. Boneca, I.G., O. Dussurget, D. Cabanes, M.-A. Nahori, S. Sousa, M. Lecuit, E. Psylinakis, V. Bouriotis, J.-P. Hugot, and M. Giovannini, *A critical role for peptidoglycan N-deacetylation in Listeria evasion from the host innate immune system.* Proceedings of the National Academy of Sciences, 2007. **104**(3): p. 997-1002.
163. Bera, A., S. Herbert, A. Jakob, W. Vollmer, and F. Götz, *Why are pathogenic staphylococci so lysozyme resistant? The peptidoglycan O-acetyltransferase OatA is the major determinant for lysozyme resistance of Staphylococcus aureus.* Molecular microbiology, 2005. **55**(3): p. 778-787.

164. Wolf, A.J., C.N. Reyes, W. Liang, C. Becker, K. Shimada, M.L. Wheeler, H.C. Cho, N.I. Popescu, K.M. Coggeshall, and M. Arditi, *Hexokinase is an innate immune receptor for the detection of bacterial peptidoglycan.* Cell, 2016. **166**(3): p. 624-636.
165. Vijayrajratnam, S., A.C. Pushkaran, A. Balakrishnan, A.K. Vasudevan, R. Biswas, and C.G. Mohan, *Bacterial peptidoglycan with amidated meso-diaminopimelic acid evades NOD1 recognition: an insight into NOD1 structure–recognition.* Biochemical Journal, 2016. **473**(24): p. 4573-4592.
166. Coulombe, F., M. Divangahi, F. Veyrier, L. de Léséleuc, J.L. Gleason, Y. Yang, M.A. Kelliher, A.K. Pandey, C.M. Sassetti, and M.B. Reed, *Increased NOD2-mediated recognition of N-glycolyl muramyl dipeptide.* Journal of Experimental Medicine, 2009. **206**(8): p. 1709-1716.
167. Hansen, J.M., S.A. Golchin, F.J. Veyrier, P. Domenech, I.G. Boneca, A.K. Azad, M.V. Rajaram, L.S. Schlesinger, M. Divangahi, and M.B. Reed, *N-glycolylated peptidoglycan contributes to the immunogenicity but not pathogenicity of Mycobacterium tuberculosis.* Journal of Infectious Diseases, 2013: p. jit622.
168. Emori, K., S. Nagao, N. Shigematsu, S. Kotani, M. Tsujimoto, T. Shiba, S. Kusumoto, and A. Tanaka, *Granuloma formation by muramyl dipeptide associated with branched fatty acids, a structure probably essential for tubercle formation by Mycobacterium tuberculosis.* Infection and immunity, 1985. **49**(1): p. 244-249.
169. Tanaka, A. and K. Emori, *Epithelioid granuloma formation by a synthetic bacterial cell wall component, muramyl dipeptide (MDP).* The American journal of pathology, 1980. **98**(3): p. 733.
170. Emori, K. and A. Tanaka, *Granuloma formation by synthetic bacterial cell wall fragment: muramyl dipeptide.* Infection and immunity, 1978. **19**(2): p. 613-620.
171. Kumar, A., S. Kumar, D. Kumar, A. Mishra, R.P. Dewangan, P. Shrivastava, S. Ramachandran, and B. Taneja, *The structure of Rv3717 reveals a novel amidase from Mycobacterium tuberculosis.* Acta Crystallographica Section D: Biological Crystallography, 2013. **69**(12): p. 2543-2554.
172. Prigozhin, D.M., D. Mavrici, J.P. Huizar, H.J. Vansell, and T. Alber, *Structural and biochemical analyses of Mycobacterium tuberculosis N-acetylmuramyl-L-alanine amidase Rv3717 point to a role in peptidoglycan fragment recycling*. Journal of Biological Chemistry, 2013. **288**(44): p. 31549-31555.
173. Höltje, J.-V. and E.I. Tuomanen, *The murein hydrolases of Escherichia coli: properties, functions and impact on the course of infections in vivo.* Microbiology, 1991. **137**(3): p. 441-454.
174. Senzani, S., D. Li, A. Bhaskar, C. Ealand, J. Chang, B. Rimal, C. Liu, S. Joon Kim, N. Dhar, and B. Kana, *An Amidase_3 domain-containing N-acetylmuramyl-L-alanine amidase is required for mycobacterial cell division.* Sci Rep, 2017. **7**(1): p. 1140.
175. Kana, B.D., B.G. Gordhan, K.J. Downing, N. Sung, G. Vostroktunova, E.E. Machowski, L. Tsenova, M. Young, A. Kaprelyants, and G. Kaplan, *The resuscitation-promoting factors of Mycobacterium tuberculosis are required for virulence and resuscitation from dormancy but are collectively dispensable for growth in vitro.* Molecular microbiology, 2008. **67**(3): p. 672-684.
176. Jenuwein, T. and C.D. Allis, *Translating the histone code.* Science, 2001. **293**(5532): p. 1074-1080.
177. Kouzarides, T., *Chromatin modifications and their function.* Cell, 2007. **128**(4): p. 693-705.
178. Bhavsar, A.P., J.A. Guttman, and B.B. Finlay, *Manipulation of host-cell pathways by bacterial pathogens.* Nature, 2007. **449**(7164): p. 827-834.
179. Bártová, E., J. Krejčí, A. Harničarová, G. Galiová, and S. Kozubek, *Histone modifications and nuclear architecture: a review.* Journal of Histochemistry & Cytochemistry, 2008. **56**(8): p. 711-721.

180. Bannister, A.J., P. Zegerman, J.F. Partridge, E.A. Miska, J.O. Thomas, R.C. Allshire, and T. Kouzarides, *Selective recognition of methylated lysine 9 on histone H3 by the HP1 chromo domain.* Nature, 2001. **410**(6824): p. 120-124.
181. Pennini, M.E., R.K. Pai, D.C. Schultz, W.H. Boom, and C.V. Harding, *Mycobacterium tuberculosis 19-kDa lipoprotein inhibits IFN-γ-induced chromatin remodeling of MHC2TA by TLR2 and MAPK signaling.* The Journal of Immunology, 2006. **176**(7): p. 4323-4330.
182. Kleinnijenhuis, J., J. Quintin, F. Preijers, L.A. Joosten, D.C. Ifrim, S. Saeed, C. Jacobs, J. van Loenhout, D. de Jong, and H.G. Stunnenberg, *Bacille Calmette-Guerin induces NOD2-dependent nonspecific protection from reinfection via epigenetic reprogramming of monocytes.* Proceedings of the National Academy of Sciences, 2012. **109**(43): p. 17537-17542.
183. Kumar, P., R. Agarwal, I. Siddiqui, H. Vora, G. Das, and P. Sharma, *ESAT6 differentially inhibits IFN-γ-inducible class II transactivator isoforms in both a TLR2-dependent and-independent manner.* Immunology and cell biology, 2012. **90**(4): p. 411-420.
184. Duan, L., M. Yi, J. Chen, S. Li, and W. Chen, *Mycobacterium tuberculosis EIS gene inhibits macrophage autophagy through up-regulation of IL-10 by increasing the acetylation of histone H3.* Biochemical and biophysical research communications, 2016. **473**(4): p. 1229-1234.
185. Jose, L., R. Ramachandran, R. Bhagavat, R.L. Gomez, A. Chandran, S. Raghunandanan, R.V. Omkumar, N. Chandra, S. Mundayoor, and R.A. Kumar, *Hypothetical protein Rv3423. 1 of Mycobacterium tuberculosis is a histone acetyltransferase.* The FEBS journal, 2016. **283**(2): p. 265-281.
186. Koo, M.-S., S. Subbian, and G. Kaplan, *Strain specific transcriptional response in Mycobacterium tuberculosis infected macrophages.* Cell Communication and Signaling, 2012. **10**(1): p. 2.
187. Bouttier, M., D. Laperriere, B. Memari, J. Mangiapane, A. Fiore, E. Mitchell, M. Verway, M.A. Behr, R. Sladek, and L.B. Barreiro, *Alu repeats as transcriptional regulatory platforms in macrophage responses to M. tuberculosis infection.* Nucleic acids research, 2016. **44**(22): p. 10571-10587.
188. Deaton, A.M. and A. Bird, *CpG islands and the regulation of transcription.* Genes & development, 2011. **25**(10): p. 1010-1022.
189. Zheng, L., E.T. Leung, H. Wong, G. Lui, N. Lee, K.-F. To, K. Choy, R.C. Chan, and M. Ip, *Unraveling methylation changes of host macrophages in Mycobacterium tuberculosis infection.* Tuberculosis, 2016. **98**: p. 139-148.
190. Shell, S.S., E.G. Prestwich, S.-H. Baek, R.R. Shah, C.M. Sassetti, P.C. Dedon, and S.M. Fortune, *DNA methylation impacts gene expression and ensures hypoxic survival of Mycobacterium tuberculosis.* PLoS pathogens, 2013. **9**(7).
191. Sharma, G., S. Upadhyay, M. Srilalitha, V.K. Nandicoori, and S. Khosla, *The interaction of mycobacterial protein Rv2966c with host chromatin is mediated through non-CpG methylation and histone H3/H4 binding.* Nucleic acids research, 2015. **43**(8): p. 3922-3937.
192. Yaseen, I., P. Kaur, V.K. Nandicoori, and S. Khosla, *Mycobacteria modulate host epigenetic machinery by Rv1988 methylation of a non-tail arginine of histone H3.* Nat Commun, 2015. **6**: p. 8922.
193. DiNardo, A.R., K. Rajapakshe, T. Nishiguchi, S.L. Grimm, G. Mtetwa, Q. Dlamini, J. Kahari, S. Mahapatra, A. Kay, and G. Maphalala, *DNA hypermethylation during tuberculosis dampens host immune responsiveness.* The Journal of Clinical Investigation, 2020. **130**(6): p. 3113-3123.
194. Esterhuyse, M.M., J. Weiner, E. Caron, A.G. Loxton, M. Iannaccone, C. Wagman, P. Saikali, K. Stanley, W.E. Wolski, and H.-J. Mollenkopf, *Epigenetics and proteomics join transcriptomics in the quest for tuberculosis biomarkers.* MBio, 2015. **6**(5).
195. Ambros, V., *The functions of animal microRNAs.* Nature, 2004. **431**(7006): p. 350-355.
196. Bushati, N. and S.M. Cohen, *microRNA functions.* Annu. Rev. Cell Dev. Biol., 2007. **23**: p. 175-205.

197. Siddle, K.J., M. Deschamps, L. Tailleux, Y. Nédélec, J. Pothlichet, G. Lugo-Villarino, V. Libri, B. Gicquel, O. Neyrolles, and G. Laval, *A genomic portrait of the genetic architecture and regulatory impact of microRNA expression in response to infection.* Genome research, 2014. **24**(5): p. 850-859.
198. Furci, L., E. Schena, P. Miotto, and D.M. Cirillo, *Alteration of human macrophages microRNA expression profile upon infection with Mycobacterium tuberculosis.* International Journal of Mycobacteriology, 2013. **2**(3): p. 128-134.
199. Zheng, L., E. Leung, N. Lee, G. Lui, K.-F. To, R.C. Chan, and M. Ip, *Differential microRNA expression in human macrophages with Mycobacterium tuberculosis infection of Beijing/W and non-Beijing/W strain types.* PLoS One, 2015. **10**(6).
200. Das, K., S. Saikolappan, and S. Dhandayuthapani, *Differential expression of miRNAs by macrophages infected with virulent and avirulent Mycobacterium tuberculosis.* Tuberculosis, 2013. **93**: p. S47-S50.
201. Ma, F., S. Xu, X. Liu, Q. Zhang, X. Xu, M. Liu, M. Hua, N. Li, H. Yao, and X. Cao, *The microRNA miR-29 controls innate and adaptive immune responses to intracellular bacterial infection by targeting interferon-γ.* Nature immunology, 2011. **12**(9): p. 861-869.
202. Iwai, H., K. Funatogawa, K. Matsumura, M. Kato-Miyazawa, F. Kirikae, K. Kiga, C. Sasakawa, T. Miyoshi-Akiyama, and T. Kirikae, *MicroRNA-155 knockout mice are susceptible to Mycobacterium tuberculosis infection.* Tuberculosis, 2015. **95**(3): p. 246-250.
203. Etna, M.P., A. Sinigaglia, A. Grassi, E. Giacomini, A. Romagnoli, M. Pardini, M. Severa, M. Cruciani, F. Rizzo, and E. Anastasiadou, *Mycobacterium tuberculosis-induced miR-155 subverts autophagy by targeting ATG3 in human dendritic cells.* PLoS pathogens, 2018. **14**(1): p. e1006790.
204. Rothchild, A.C., J.R. Sissons, S. Shafiani, C. Plaisier, D. Min, D. Mai, M. Gilchrist, J. Peschon, R.P. Larson, and A. Bergthaler, *MiR-155–regulated molecular network orchestrates cell fate in the innate and adaptive immune response to Mycobacterium tuberculosis.* Proceedings of the National Academy of Sciences, 2016. **113**(41): p. E6172-E6181.
205. Rajaram, M.V., B. Ni, J.D. Morris, M.N. Brooks, T.K. Carlson, B. Bakthavachalu, D.R. Schoenberg, J.B. Torrelles, and L.S. Schlesinger, *Mycobacterium tuberculosis lipomannan blocks TNF biosynthesis by regulating macrophage MAPK-activated protein kinase 2 (MK2) and microRNA miR-125b.* Proceedings of the national academy of sciences, 2011. **108**(42): p. 17408-17413.
206. Tamgue, O., L. Gcanga, M. Ozturk, L. Whitehead, S. Pillay, R. Jacobs, S. Roy, S. Schmeier, M. Davids, and Y.A. Medvedeva, *Differential targeting of c-Maf, Bach-1, and Elmo-1 by microRNA-143 and microRNA-365 promotes the intracellular growth of mycobacterium tuberculosis in alternatively IL-4/IL-13 activated macrophages.* Frontiers in immunology, 2019. **10**: p. 421.
207. Singh, Y., V. Kaul, A. Mehra, S. Chatterjee, S. Tousif, V.P. Dwivedi, M. Suar, L. Van Kaer, W.R. Bishai, and G. Das, *Mycobacterium tuberculosis controls microRNA-99b (miR-99b) expression in infected murine dendritic cells to modulate host immunity.* Journal of Biological Chemistry, 2013. **288**(7): p. 5056-5061.
208. Kim, J.K., J.-M. Yuk, S.Y. Kim, T.S. Kim, H.S. Jin, C.-S. Yang, and E.-K. Jo, *MicroRNA-125a inhibits autophagy activation and antimicrobial responses during mycobacterial infection.* The Journal of Immunology, 2015. **194**(11): p. 5355-5365.
209. Ouimet, M., S. Koster, E. Sakowski, B. Ramkhelawon, C. Van Solingen, S. Oldebeken, D. Karunakaran, C. Portal-Celhay, F.J. Sheedy, and T.D. Ray, *Mycobacterium tuberculosis induces the miR-33 locus to reprogram autophagy and host lipid metabolism.* Nature immunology, 2016. **17**(6): p. 677-686.
210. Ni, B., M.V. Rajaram, W.P. Lafuse, M.B. Landes, and L.S. Schlesinger, *Mycobacterium tuberculosis decreases human macrophage IFN-γ responsiveness through miR-132 and miR-26a.* The Journal of Immunology, 2014. **193**(9): p. 4537-4547.

211. Sahu, S.K., M. Kumar, S. Chakraborty, S.K. Banerjee, R. Kumar, P. Gupta, K. Jana, U.D. Gupta, Z. Ghosh, and M. Kundu, *MicroRNA 26a (miR-26a)/KLF4 and CREB-C/EBPβ regulate innate immune signaling, the polarization of macrophages and the trafficking of Mycobacterium tuberculosis to lysosomes during infection.* PLoS pathogens, 2017. **13**(5): p. e1006410.
212. Lou, J., Y. Wang, Z. Zhang, and W. Qiu, *MiR-20b inhibits mycobacterium tuberculosis induced inflammation in the lung of mice through targeting NLRP3.* Experimental Cell Research, 2017. **358**(2): p. 120-128.
213. Liu, Y., X. Wang, J. Jiang, Z. Cao, B. Yang, and X. Cheng, *Modulation of T cell cytokine production by miR-144* with elevated expression in patients with pulmonary tuberculosis.* Molecular immunology, 2011. **48**(9-10): p. 1084-1090.
214. Arnvig, K. and D. Young, *Non-coding RNA and its potential role in Mycobacterium tuberculosis pathogenesis.* RNA biology, 2012. **9**(4): p. 427-436.
215. Li, M., J. Cui, W. Niu, J. Huang, T. Feng, B. Sun, and H. Yao, *Long non-coding PCED1B-AS1 regulates macrophage apoptosis and autophagy by sponging miR-155 in active tuberculosis.* Biochemical and biophysical research communications, 2019. **509**(3): p. 803-809.
216. Fathizadeh, H., S.M.G. Hayat, S. Dao, K. Ganbarov, A. Tanomand, M. Asgharzadeh, and H.S. Kafil, *Long non-coding RNA molecules in tuberculosis.* International Journal of Biological Macromolecules, 2020.
217. Chen, Z.-l., L.-L. Wei, L.-Y. Shi, M. Li, T.-T. Jiang, J. Chen, C.-M. Liu, S. Yang, H.-h. Tu, and Y.-t. Hu, *Screening and identification of lncRNAs as potential biomarkers for pulmonary tuberculosis.* Scientific reports, 2017. **7**(1): p. 1-10.
218. Bai, H., Q. Wu, X. Hu, T. Wu, J. Song, T. Liu, Z. Meng, M. Lv, X. Lu, and X. Chen, *Clinical significance of lnc-AC145676. 2.1-6 and lnc-TGS1-1 and their variants in western Chinese tuberculosis patients.* International Journal of Infectious Diseases, 2019. **84**: p. 8-14.
219. Fu, Y., K. Gao, E. Tao, R. Li, and Z. Yi, *Aberrantly expressed long non-coding RNAs in CD8+ T cells response to active tuberculosis.* Journal of Cellular Biochemistry, 2017. **118**(12): p. 4275-4284.
220. He, J., Q. Ou, C. Liu, L. Shi, C. Zhao, Y. Xu, S.K. Kong, J.F.C. Loo, B. Li, and D. Gu, *Differential expression of long non-coding RNAs in patients with tuberculosis infection.* Tuberculosis, 2017. **107**: p. 73-79.
221. Huang, S., Z. Huang, Q. Luo, and C. Qing, *The expression of lncRNA NEAT1 in human tuberculosis and its antituberculosis effect.* BioMed Research International, 2018. **2018**.
222. Wang, Y., H. Zhong, X. Xie, C.Y. Chen, D. Huang, L. Shen, H. Zhang, Z.W. Chen, and G. Zeng, *Long noncoding RNA derived from CD244 signaling epigenetically controls CD8+ T-cell immune responses in tuberculosis infection.* Proceedings of the National Academy of Sciences, 2015. **112**(29): p. E3883-E3892.
223. Yang, X., J. Yang, J. Wang, Q. Wen, H. Wang, J. He, S. Hu, W. He, X. Du, and S. Liu, *Microarray analysis of long noncoding RNA and mRNA expression profiles in human macrophages infected with Mycobacterium tuberculosis.* Scientific reports, 2016. **6**: p. 38963.
224. Wang, L., B. Xie, P. Zhang, Y. Ge, Y. Wang, and D. Zhang, *LOC152742 as a biomarker in the diagnosis of pulmonary tuberculosis infection.* Journal of cellular biochemistry, 2019. **120**(6): p. 8949-8955.
225. Kubista, M., J.M. Andrade, M. Bengtsson, A. Forootan, J. Jonak, K. Lind, R. Sindelka, R. Sjoback, B. Sjogreen, L. Strombom, A. Stahlberg, and N. Zoric, *The real-time polymerase chain reaction.* Mol Aspects Med, 2006. **27**(2-3): p. 95-125.
226. Kozera, B. and M. Rapacz, *Reference genes in real-time PCR.* J Appl Genet, 2013. **54**(4): p. 391-406.
227. Heid, C.A., J. Stevens, K.J. Livak, and P.M. Williams, *Real time quantitative PCR.* Genome research, 1996. **6**(10): p. 986-994.
228. Westermann, A.J., S.A. Gorski, and J. Vogel, *Dual RNA-seq of pathogen and host.* Nature Reviews Microbiology, 2012. **10**(9): p. 618-630.

229. Sultan, M., M.H. Schulz, H. Richard, A. Magen, A. Klingenhoff, M. Scherf, M. Seifert, T. Borodina, A. Soldatov, and D. Parkhomchuk, *A global view of gene activity and alternative splicing by deep sequencing of the human transcriptome.* Science, 2008. **321**(5891): p. 956-960.
230. Marioni, J.C., C.E. Mason, S.M. Mane, M. Stephens, and Y. Gilad, *RNA-seq: an assessment of technical reproducibility and comparison with gene expression arrays.* Genome research, 2008. **18**(9): p. 1509-1517.
231. Perkins, T.T., R.A. Kingsley, M.C. Fookes, P.P. Gardner, K.D. James, L. Yu, S.A. Assefa, M. He, N.J. Croucher, and D.J. Pickard, *A strand-specific RNA–Seq analysis of the transcriptome of the typhoid bacillus salmonella typhi.* PLoS genet, 2009. **5**(7): p. e1000569.
232. Yoder-Himes, D., P. Chain, Y. Zhu, O. Wurtzel, E. Rubin, J.M. Tiedje, and R. Sorek, *Mapping the Burkholderia cenocepacia niche response via high-throughput sequencing.* Proceedings of the National Academy of Sciences, 2009. **106**(10): p. 3976-3981.
233. Oliver, H.F., R.H. Orsi, L. Ponnala, U. Keich, W. Wang, Q. Sun, S.W. Cartinhour, M.J. Filiatrault, M. Wiedmann, and K.J. Boor, *Deep RNA sequencing of L. monocytogenes reveals overlapping and extensive stationary phase and sigma B-dependent transcriptomes, including multiple highly transcribed noncoding RNAs.* BMC genomics, 2009. **10**(1): p. 641.
234. Sharma, C.M., S. Hoffmann, F. Darfeuille, J. Reignier, S. Findeiß, A. Sittka, S. Chabas, K. Reiche, J. Hackermüller, and R. Reinhardt, *The primary transcriptome of the major human pathogen Helicobacter pylori.* Nature, 2010. **464**(7286): p. 250-255.
235. Stark, R., M. Grzelak, and J. Hadfield, *RNA sequencing: the teenage years.* Nature Reviews Genetics, 2019. **20**(11): p. 631-656.
236. Morris, K.V. and J.S. Mattick, *The rise of regulatory RNA.* Nature Reviews Genetics, 2014. **15**(6): p. 423-437.
237. Djebali, S., C.A. Davis, A. Merkel, A. Dobin, T. Lassmann, A. Mortazavi, A. Tanzer, J. Lagarde, W. Lin, and F. Schlesinger, *Landscape of transcription in human cells.* Nature, 2012. **489**(7414): p. 101-108.
238. Li, W., D. Notani, and M.G. Rosenfeld, *Enhancers as non-coding RNA transcription units: recent insights and future perspectives.* Nature Reviews Genetics, 2016. **17**(4): p. 207.
239. Wang, E.T., R. Sandberg, S. Luo, I. Khrebtukova, L. Zhang, C. Mayr, S.F. Kingsmore, G.P. Schroth, and C.B. Burge, *Alternative isoform regulation in human tissue transcriptomes.* Nature, 2008. **456**(7221): p. 470-476.
240. Westermann, A.J., L. Barquist, and J. Vogel, *Resolving host–pathogen interactions by dual RNA-seq.* PLoS pathogens, 2017. **13**(2): p. e1006033.
241. Tierney, L., J. Linde, S. Müller, S. Brunke, J.C. Molina, B. Hube, U. Schöck, R. Guthke, and K. Kuchler, *An interspecies regulatory network inferred from simultaneous RNA-seq of Candida albicans invading innate immune cells.* Frontiers in microbiology, 2012. **3**: p. 85.
242. Strong, M.J., G. Xu, J. Coco, C. Baribault, D.S. Vinay, M.R. Lacey, A.L. Strong, T.A. Lehman, M.B. Seddon, and Z. Lin, *Differences in gastric carcinoma microenvironment stratify according to EBV infection intensity: implications for possible immune adjuvant therapy.* PLoS Pathog, 2013. **9**(5): p. e1003341.
243. Choi, Y.-J., M.T. Aliota, G.F. Mayhew, S.M. Erickson, and B.M. Christensen, *Dual RNA-seq of parasite and host reveals gene expression dynamics during filarial worm–mosquito interactions.* PLoS Negl Trop Dis, 2014. **8**(5): p. e2905.
244. Pittman, K.J., M.T. Aliota, and L.J. Knoll, *Dual transcriptional profiling of mice and Toxoplasma gondii during acute and chronic infection.* BMC genomics, 2014. **15**(1): p. 806.
245. Westermann, A.J., K.U. Förstner, F. Amman, L. Barquist, Y. Chao, L.N. Schulte, L. Müller, R. Reinhardt, P.F. Stadler, and J. Vogel, *Dual RNA-seq unveils noncoding RNA functions in host–pathogen interactions.* Nature, 2016. **529**(7587): p. 496-501.

246. Humphrys, M.S., T. Creasy, Y. Sun, A.C. Shetty, M.C. Chibucos, E.F. Drabek, C.M. Fraser, U. Farooq, N. Sengamalay, and S. Ott, *Simultaneous transcriptional profiling of bacteria and their host cells.* PloS one, 2013. **8**(12): p. e80597.
247. Mavromatis, C., N.J. Bokil, M. Totsika, A. Kakkanat, K. Schaale, C.V. Cannistraci, T. Ryu, S.A. Beatson, G.C. Ulett, and M.A. Schembri, *The co-transcriptome of uropathogenic E scherichia coli-infected mouse macrophages reveals new insights into host–pathogen interactions.* Cellular microbiology, 2015. **17**(5): p. 730-746.
248. Baddal, B., A. Muzzi, S. Censini, R.A. Calogero, G. Torricelli, S. Guidotti, A.R. Taddei, A. Covacci, M. Pizza, and R. Rappuoli, *Dual RNA-seq of nontypeable Haemophilus influenzae and host cell transcriptomes reveals novel insights into host-pathogen cross talk.* MBio, 2015. **6**(6).
249. Pisu, D., L. Huang, J.K. Grenier, and D.G. Russell, *Dual RNA-Seq of Mtb-infected macrophages in vivo reveals ontologically distinct host-pathogen interactions.* Cell reports, 2020. **30**(2): p. 335-350. e4.
250. Roy, S., R. Guler, S.P. Parihar, S. Schmeier, B. Kaczkowski, H. Nishimura, J.W. Shin, Y. Negishi, M. Ozturk, and R. Hurdayal, *Batf2/Irf1 induces inflammatory responses in classically activated macrophages, lipopolysaccharides, and mycobacterial infection.* The Journal of Immunology, 2015. **194**(12): p. 6035-6044.
251. Senzani, S., *Characterisation of mycobacterial amidases and their role in bacterial growth and physiology*, in *WIReDSpace*. 2018, University of Witwatersrand: WIReDSpace - Electronic Theses and Dissertations (ETD).
252. Guler, R., S.P. Parihar, S. Savvi, E. Logan, A. Schwegmann, S. Roy, N.E. Nieuwenhuizen, M. Ozturk, S. Schmeier, and H. Suzuki, *IL-4Rα-dependent alternative activation of macrophages is not decisive for mycobacterium tuberculosis pathology and bacterial burden in mice.* PLoS One, 2015. **10**(3).
253. Welsh, K.J., A.N. Abbott, S.-A. Hwang, J. Indrigo, L.Y. Armitige, M.R. Blackburn, R.L. Hunter Jr, and J.K. Actor, *A role for tumour necrosis factor-α, complement C5 and interleukin-6 in the initiation and development of the mycobacterial cord factor trehalose 6, 6'-dimycolate induced granulomatous response.* Microbiology (Reading, England), 2008. **154**(Pt 6): p. 1813.
254. Brennan, P.J. and D.C. Crick, *The cell-wall core of Mycobacterium tuberculosis in the context of drug discovery.* Current topics in medicinal chemistry, 2007. **7**(5): p. 475-488.
255. Wu, K.J., C.C. Boutte, T.R. Ioerger, and E.J. Rubin, *Mycobacterium smegmatis HtrA Blocks the Toxic Activity of a Putative Cell Wall Amidase.* Cell reports, 2019. **27**(8): p. 2468-2479. e3.
256. Epand, R.M., C. Walker, R.F. Epand, and N.A. Magarvey, *Molecular mechanisms of membrane targeting antibiotics.* Biochimica et Biophysica Acta (BBA)-Biomembranes, 2016. **1858**(5): p. 980-987.
257. Hett, E.C., M.C. Chao, L.L. Deng, and E.J. Rubin, *A mycobacterial enzyme essential for cell division synergizes with resuscitation-promoting factor.* PLoS pathogens, 2008. **4**(2): p. e1000001.
258. Boutte, C.C., C.E. Baer, K. Papavinasasundaram, W. Liu, M.R. Chase, X. Meniche, S.M. Fortune, C.M. Sassetti, T.R. Ioerger, and E.J. Rubin, *A cytoplasmic peptidoglycan amidase homologue controls mycobacterial cell wall synthesis.* Elife, 2016. **5**: p. e14590.
259. Turapov, O., F. Forti, B. Kadhim, D. Ghisotti, J. Sassine, A. Straatman-Iwanowska, A.R. Bottrill, P.J. Moynihan, R. Wallis, and P. Barthe, *Two faces of CwlM, an essential PknB substrate, in Mycobacterium tuberculosis.* Cell reports, 2018. **25**(1): p. 57-67. e5.
260. Guler, R., S.P. Parihar, G. Spohn, P. Johansen, F. Brombacher, and M.F. Bachmann, *Blocking IL-1alpha but not IL-1beta increases susceptibility to chronic Mycobacterium tuberculosis infection in mice.* Vaccine, 2011. **29**(6): p. 1339-46.
261. Hasan, Z., J.M. Cliff, H.M. Dockrell, B. Jamil, M. Irfan, M. Ashraf, and R. Hussain, *CCL2 responses to Mycobacterium tuberculosis are associated with disease severity in tuberculosis.* PloS one, 2009. **4**(12).

262. Li, X., J. He, W. Fu, P. Cao, S. Zhang, and T. Jiang, *Effect of Mycobacterium tuberculosis Rv3717 on cell division and cell adhesion.* Microbial pathogenesis, 2018. **117**: p. 184-190.
263. He, J., W. Fu, S. Zhao, C. Zhang, T. Sun, and T. Jiang, *Lack of MSMEG_6281, a peptidoglycan amidase, affects cell wall integrity and virulence of Mycobacterium smegmatis.* Microbial pathogenesis, 2019. **128**: p. 405-413.
264. Chauhan, A., M.V. Madiraju, M. Fol, H. Lofton, E. Maloney, R. Reynolds, and M. Rajagopalan, *Mycobacterium tuberculosis cells growing in macrophages are filamentous and deficient in FtsZ rings.* J Bacteriol, 2006. **188**(5): p. 1856-65.
265. Ferwerda, G., S.E. Girardin, B.-J. Kullberg, L. Le Bourhis, D.J. De Jong, D.M. Langenberg, R. Van Crevel, G.J. Adema, T.H. Ottenhoff, and J.W. Van der Meer, *NOD2 and toll-like receptors are nonredundant recognition systems of Mycobacterium tuberculosis.* PLoS pathogens, 2005. **1**(3): p. e34.
266. Kang, T.J. and G.-T. Chae, *The role of intracellular receptor NODs for cytokine production by macrophages infected with Mycobacterium leprae.* Immune network, 2011. **11**(6): p. 424-427.
267. Liu, Y., S. Tan, L. Huang, R.B. Abramovitch, K.H. Rohde, M.D. Zimmerman, C. Chen, V. Dartois, B.C. VanderVen, and D.G. Russell, *Immune activation of the host cell induces drug tolerance in Mycobacterium tuberculosis both in vitro and in vivo.* Journal of Experimental Medicine, 2016: p. jem. 20151248.
268. Schnappinger, D., S. Ehrt, M.I. Voskuil, Y. Liu, J.A. Mangan, I.M. Monahan, G. Dolganov, B. Efron, P.D. Butcher, C. Nathan, and G.K. Schoolnik, *Transcriptional Adaptation of Mycobacterium tuberculosis within Macrophages: Insights into the Phagosomal Environment.* J Exp Med, 2003. **198**(5): p. 693-704.
269. Dibbern, J., L. Eggers, and B.E. Schneider, *Sex differences in the C57BL/6 model of Mycobacterium tuberculosis infection.* Scientific Reports, 2017. **7**(1): p. 1-8.
270. Hertz, D., J. Dibbern, L. Eggers, L. von Borstel, and B.E. Schneider, *increased male susceptibility to Mycobacterium tuberculosis infection is associated with smaller B cell follicles in the lungs.* Scientific Reports, 2020. **10**(1): p. 1-9.
271. Kim, K.H., D.R. An, J. Song, J.Y. Yoon, H.S. Kim, H.J. Yoon, H.N. Im, J. Kim, S.J. Lee, and K.-H. Kim, *Mycobacterium tuberculosis Eis protein initiates suppression of host immune responses by acetylation of DUSP16/MKP-7.* Proceedings of the National Academy of Sciences, 2012. **109**(20): p. 7729-7734.
272. Wang, J., B.-X. Li, P.-P. Ge, J. Li, Q. Wang, G.F. Gao, X.-B. Qiu, and C.H. Liu, *Mycobacterium tuberculosis suppresses innate immunity by coopting the host ubiquitin system.* Nature immunology, 2015. **16**(3): p. 237.
273. Li, J., Q.-Y. Chai, Y. Zhang, B.-X. Li, J. Wang, X.-B. Qiu, and C.H. Liu, *Mycobacterium tuberculosis Mce3E suppresses host innate immune responses by targeting ERK1/2 signaling.* The Journal of Immunology, 2015. **194**(8): p. 3756-3767.
274. Ng, V.H., J.S. Cox, A.O. Sousa, J.D. MacMicking, and J.D. McKinney, *Role of KatG catalase-peroxidase in mycobacterial pathogenesis: countering the phagocyte oxidative burst.* Molecular microbiology, 2004. **52**(5): p. 1291-1302.
275. Liu, C.H., H. Liu, and B. Ge, *Innate immunity in tuberculosis: host defense vs pathogen evasion.* Cellular & molecular immunology, 2017. **14**(12): p. 963-975.
276. Houben, D., C. Demangel, J. Van Ingen, J. Perez, L. Baldeón, A.M. Abdallah, L. Caleechurn, D. Bottai, M. Van Zon, and K. De Punder, *ESX-1-mediated translocation to the cytosol controls virulence of mycobacteria.* Cellular microbiology, 2012. **14**(8): p. 1287-1298.
277. Maloney, E., D. Stankowska, J. Zhang, M. Fol, Q.-J. Cheng, S. Lun, W.R. Bishai, M. Rajagopalan, D. Chatterjee, and M.V. Madiraju, *The two-domain LysX protein of Mycobacterium tuberculosis is required for production of lysinylated phosphatidylglycerol and resistance to cationic antimicrobial peptides.* PLoS pathogens, 2009. **5**(7): p. e1000534.
278. Wang, Z., M. Gerstein, and M. Snyder, *RNA-Seq: a revolutionary tool for transcriptomics.* Nature reviews genetics, 2009. **10**(1): p. 57-63.

279. Jobe, O., J. Kim, E. Tycksen, S. Onkar, N.L. Michael, C.R. Alving, and M. Rao, *Human primary macrophages derived in vitro from circulating monocytes comprise adherent and non-adherent subsets with differential expression of Siglec-1 and CD4 and permissiveness to HIV-1 infection.* Frontiers in immunology, 2017. **8**: p. 1352.
280. Wang, J., S.A. Rieder, J. Wu, S. Hayes, R.A. Halpin, M. de Los Reyes, Y. Shrestha, R. Kolbeck, and R. Raja, *Evaluation of ultra-low input RNA sequencing for the study of human T cell transcriptome.* Scientific reports, 2019. **9**(1): p. 1-13.
281. Zhang, L.Q., D. Cheranova, M. Gibson, S. Ding, D.P. Heruth, D. Fang, and S.Q. Ye, *RNA-seq reveals novel transcriptome of genes and their isoforms in human pulmonary microvascular endothelial cells treated with thrombin.* PloS one, 2012. **7**(2): p. e31229.
282. Westermann, A.J. and J. Vogel, *Host-Pathogen Transcriptomics by Dual RNA-Seq.* Methods Mol Biol, 2018. **1737**: p. 59-75.
283. Zimmermann, M., M. Kogadeeva, M. Gengenbacher, G. McEwen, H.-J. Mollenkopf, N. Zamboni, S.H.E. Kaufmann, and U. Sauer, *Integration of metabolomics and transcriptomics reveals a complex diet of Mycobacterium tuberculosis during early macrophage infection.* MSystems, 2017. **2**(4): p. e00057-17.
284. Rienksma, R.A., M. Suarez-Diez, H.-J. Mollenkopf, G.M. Dolganov, A. Dorhoi, G.K. Schoolnik, V.A.M. dos Santos, S.H. Kaufmann, P.J. Schaap, and M. Gengenbacher, *Comprehensive insights into transcriptional adaptation of intracellular mycobacteria by microbe-enriched dual RNA sequencing.* BMC genomics, 2015. **16**(1): p. 1-15.
285. Montoya, D.J., P. Andrade, B.J. Silva, R.M. Teles, F. Ma, B. Bryson, S. Sadanand, T. Noel, J. Lu, and E. Sarno, *Dual RNA-seq of human leprosy lesions identifies bacterial determinants linked to host immune response.* Cell reports, 2019. **26**(13): p. 3574-3585. e3.
286. Gordon, S. and P.R. Taylor, *Monocyte and macrophage heterogeneity.* Nature reviews immunology, 2005. **5**(12): p. 953-964.
287. Arnvig, K.B., I. Comas, N.R. Thomson, J. Houghton, H.I. Boshoff, N.J. Croucher, G. Rose, T.T. Perkins, J. Parkhill, and G. Dougan, *Sequence-based analysis uncovers an abundance of non-coding RNA in the total transcriptome of Mycobacterium tuberculosis.* PLoS Pathog, 2011. **7**(11): p. e1002342.
288. Parish, T. and N.G. Stoker, *Use of a flexible cassette method to generate a double unmarked Mycobacterium tuberculosis tlyA plcABC mutant by gene replacement.* Microbiology, 2000. **146**(8): p. 1969-1975.